THE STRUCTURE OF SOUTHERN EXTRAGALACTIC RADIO SOURCES

PAUL A. JONES AND W. BRUCE MCADAM

Department of Astrophysics, School of Physics, University of Sydney, NSW 2006 Australia
Received 1991 July 16; accepted 1991 October 9

ABSTRACT

We report the structure of extragalactic radio sources south of declination -30° that have been imaged with the Molonglo Observatory Synthesis Telescope (MOST) at 843 MHz with a resolution of 44". Our sample includes those sources noted in the Molonglo Reference Catalogue (MRC) as extended (larger than $\sim 1'$), as well as those noted as multiple—that is, within 8' of a neighbor and possibly related. The sample is representative of the strong extended extragalactic radio sources of the southern sky, but is not statistically complete.

We observed 339 sources with either time-shared or full 12 hr aperture-synthesis observations. The results are given as radio images and a table of flux densities, positions and, sizes for 383 sources. Most of the groups of multiple sources are found to be separate, unrelated sources, as expected, but some are components of larger sources. Some of the sources flagged as extended in the MRC are also groups of unrelated sources, confused in the MRC beam. After excluding such random associations we then determine a *confirmed MRC extended sample* of 193 sources with flux density greater than 0.4 Jy (at 843 MHz) and size greater than 0.5. The selection effects and completeness for this sample are discussed.

The UK Schmidt southern sky survey was used to make 117 new optical identifications, and to reexamine previous identifications. The positions and IIIaJ magnitudes are presented for all sources that now have an identification, together with their redshifts when known. We present new redshifts for 14 galaxies from observations with the Anglo-Australian Telescope.

Subject headings: galaxies: distances and redshifts — galaxies: photometry — radio continuum: galaxies — surveys — techniques: interferometric

1. INTRODUCTION

The identification in 1949 of the first radio galaxies, Centaurus A and Virgo A (Bolton, Stanley, & Slee 1949), stimulated surveys of the sky for other extragalactic radio sources and measurements of the size and structure of the individual sources found. In the earliest all-sky catalog (Pawsey 1955) there were notes on the angular size or extended structure for nine out of the 38 sources. Following publication of the 3C catalog (Edge et al. 1959; Bennett 1962), the structures of its 471 sources were studied using the Cambridge One-Mile radio telescope, and images published for 142 sources (Macdonald, Kenderline, & Neville 1968; Mackay 1969). Subsequently, these 3C northern sources have been studied in considerable detail by the many radio telescopes available in the northern hemisphere.

In the southern sky, there have been four major radio surveys:

- 1. MSH 85.5 MHz (Mills, Slee, & Hill 1960, 1961),
- 2. Parkes 408 MHz (Bolton, Gardner, & Mackey 1964; Price & Milne 1965),
- 3. Parkes 2700 MHz (e.g., Bolton, Savage, & Wright 1979), and
- 4. the Molonglo Reference Catalogue 408 MHz (Large et al. 1981, 1991).

The MSH and Parkes 408 MHz surveys were followed by both interferometer and pencil beam studies of the broadened or unusual sources. For example, Ekers (1969) observed 123 sources with the Parkes Interferometer at 468 MHz and 1403 MHz and fitted two-dimensional models to the brightness dis-

tribution although images were not made. The equivalent resolution was $\sim 2'$ with baselines out to 1950 λ . The larger sources were mapped at 5 GHz using the Parkes Telescope with a resolution of 4'1 (Wall & Schilizzi 1979).

A comprehensive survey of Parkes 408 MHz sources considered likely to be extended was made at 408 MHz with the Molonglo Cross Radio Telescope by Schilizzi & McAdam (1975; SM), who presented images for 116 sources. Their pencil beam had a resolution of 2.86×2.86 sec Z arcmin² (where Z = zenith distance). Selected sources studied by SM were also observed with the Fleurs Synthesis Telescope (FST) at 1415 MHz, initially with a resolution of 50" (e.g., Christiansen et al. 1977) and later 25". The Culgoora Radioheliograph was used to image 163 extended sources at 160 MHz with beamwidth 1'9 (Slee 1977) selected after an examination of 2045 sources north of declination -45° from the MSH, Parkes 408 MHz, and 4C surveys. (Although Culgoora is at latitude 30°S the array was designed primarily for solar observations and the antennas could not point further south than -45°.) Sources north of declination -40° are also accessible to the Very Large Array (VLA), and high-resolution VLA images are now available for a complete sample of 91 radio galaxies from the Parkes 2.7 GHz survey (Ekers et al. 1989).

This paper presents observations of sources selected from the fourth major survey of the southern sky. Between 1967 and 1978, this independent survey of the sky south of declination $\delta = +18^{\circ}$ was made at 408 MHz with the Molonglo Cross Radio Telescope. The results were published as the Molonglo Reference Catalogue (MRC; Large et al. 1981). The catalog is now available on a computer floppy disk (Large et al. 1991)

with the addition of J2000 positions, references to this study, and access programs.

In the MRC flags were placed on sources that had evidence of significant beam broadening or multiplicity at its angular resolution of 2.62×2.86 sec Z arcmin². This paper describes an exhaustive survey of these extended or multiple sources in the MRC south of -30° , made using the Molonglo Observatory Synthesis Telescope. This telescope—the MOST—which was created from the EW arm of the Molonglo Cross Radio Telescope (Mills 1981; Durdin, Large, & Little 1984), operates at a frequency of 843 MHz with a resolution of 44×44 cosec $|\delta|$ arcsec².

The present survey represents the most extensive exploration of extended radio sources in the southern sky to date. The following two sections outline the selection of the sources, the observing procedures and their uncertainties for the radio measurements. Section 4 discusses a careful search for optical identifications for all sources, using the radio images to narrow the search area and distinguish between alternative candidates. Redshifts for some of the new identifications were also obtained (§ 5). The major results are contained in the comments on individual sources in § 6, in the parameter lists of Table 1 and in the contour images of the fields shown in Figure 1. Section 7 defines a confirmed MRC extended sample of 193 sources and considers the completeness of this sample. Section 8 discusses classification generalisations for the radio morphologies of all sources in the confirmed sample.

2. MRC EXTENDED SOURCES

The sources in this study were selected from the Molonglo Reference Catalogue of radio sources which lists 12,141 sources stronger than 0.7 Jy at 408 MHz with declination $-85^{\circ} \leq \delta \leq +18.5^{\circ}$ and Galactic latitude $|b| > 3^{\circ}$ from a uniform survey of the southern sky (Large et al. 1981) with the 1.6 km Molonglo Cross. The survey was undertaken as a series of transit observations by the pencil beams of the 408 MHz Molonglo Cross. The program used to analyze the 408 MHz survey data provided two measures of source morphology: beam broadening and apparent position angle. These parameters were used to classify each source, according to the following descriptions:

- 1. unresolved sources which have no flag;
- 2. extended sources, flag E, recognized by beam-broadening, with one peak of emission;
- 3. complex sources, flag C, beam-broadened and with more than one peak of emission;
- 4. slightly extended sources, flag A, recognized by apparent position angle (Hunstead 1972).
- 5. There is also a flag M, for multiple MRC sources, within 8' of each other.
- 6. The entries for the strongest sources were modified (as explained by Large et al. 1981) and given flag T.

These flagged sources are the subject of the present study with the Molonglo Observatory Synthesis Telescope (MOST).

The MOST is an east-west synthesis telescope, with a limit to the steering in meridian distance that gives a full synthesis only for those sources lying south of -30° . The present sample thus includes all the extended (E, C, and A) and multiple (M) MRC sources with $\delta \leq -30^{\circ}$, with the exception of the multi-

ple 1450–685/1451–685 (since 1451–685 is a pulsar) and 17 known supernova remnants and H II regions in the Magellanic Clouds (from Clarke, Little, & Mills 1976). Two sources, Fornax A (0320–373) and Centaurus A (1322–427), flagged in the MRC as T sources are added since they satisfy all selection criteria for the sample. The multiple M sources from the MRC are included since it is known that some double sources have their radio lobes separated enough to be cataloged as separate sources (e.g., 0211–479 and 0211–480).

The sample is drawn from extended sources listed in the MRC, with a limiting flux density of 0.7 Jy at 408 MHz and a size greater than $\sim 1'$. However, the sample is not complete to these limits. The MRC is known to be complete for point sources only above a fitted flux density of 1.0 Jy. For extended sources, the computer fit used to produce the MRC underestimates flux densities, and the ratio of the fitted to the integrated flux density depends on both the angular size and the structure of the source. More specifically, the two tests used to assign flags for extended sources are subject to selection effects (Large et al. 1981). The test of beam-broadening (E, C sources) depends on the source flux density, in the sense that extension of a weaker source is more difficult to detect, giving a larger cutoff in angular size. On the other hand, the test for apparent position angle (A sources) is useful for sources of angular size less than 1', but is only effective for position angles away from the north-south or east-west directions. We discuss the effect of these selections in § 7.

3. RADIO OBSERVATIONS

The criteria described above yielded a sample of 339 sources. These were observed with the MOST at 843 MHz, mainly using a time-shared or "cuts" mode (Mills 1985) wherein several sources are observed in sequence with the fanbeams at, typically eight, evenly spaced hour angles during a 12 hr period. Although the dynamic range is reduced in this mode (primarily due to confusion in the large radial sidelobes) the images are satisfactory for sources having simple structure. More complex sources required complete hour-angle coverage and were observed with a full 12 hr synthesis observation. Many of these fields included more than one source so that 264 fields covering the whole sample are shown in Figure 1.

Calibration sources were included in the sequence for timeshared observations, or observed with the fan-beams immediately before and after a full 12 hr synthesis.

All images were CLEANed using standard procedures (Högbom 1974) and restored with a Gaussian of HPBW 44 \times 44 cosec $|\delta|$ arcsec². The results are displayed (Fig. 1) as contour images to a common angular scale, except for eleven sources of large angular size, which have a smaller scale. The standard contour levels are at 90, 70, 50, 30, 20, 10, 5, and in some cases 2%, 1%, or 0.5% of the peak brightness. The lowest contour plotted is set at approximately 4 times the limit of the dynamic range and is generally 2% for the full-synthesis observations and 5% for the time-shared observations. The peak brightness (in Jy beam⁻¹) and percentage value associated with the lowest level contour are given in the captions. The HPBW ellipse is plotted in the lower right corner and the positions of optical identifications (§ 4) are marked with crosses.

The flux densities of the sources were obtained from the

 $\label{eq:TABLE 1} \textbf{RADIO PARAMETERS OBTAINED FROM THE MOST OBSERVATIONS}$

·								
MOST		RA (B1950)	Dec (B1950)	Size	PA		RA (B1950)	Dec (B1950) Size PA
Source	Jу	h m s				Source Jy	h m s	
¶0003–833	3.40	00 03 53.3	-83 22 42	d 1.0	156	0248-600Ac 1.29	02 48 17.8	$-60\ 01\ 21$ } s 2.5 101
0014–311	0.41	00 14 47.2	-31 11 19	s 6.9	49	0248-600Bc 0.155	02 48 37.4	-60 01 50 J
0015-311	0.42	00 15 11.7		{		0250-682Ac 0.62	02 50 30.5	-68 14 23 } s 2.1 118
0016-770 0017-769	$0.59 \\ 0.72$	00 16 09.5 00 17 26.3	-77 01 17 -76 56 59	s 6.1	45	0250–682Bc 0.30 ¶0251–677 1.28	02 50 50.4 02 51 19.0	-68 15 21 \ \ -67 45 37 \ d 0.9 165
0017-769	0.72	00 17 26.3	-10 30 39	,		1.28	02 31 19.0	-07 45 57 Q 0.9 105
¶0020–747	1.26	00 20 01.3	-74 44 36	d 1.5	125	0254-484 1.15	02 54 19.7	-48 27 44 <0.3 -
0021 - 742c	0.40	00 21 25.2	-74 12 05	s 2.9	126	¶0258–520 0.67	02 58 51.7	-52 02 57 d 2.0 134
0022-742c	0.32	00 22 00.1	-74 13 49	∫ 0.7	122	0305-417Bc 0.121	03 05 39.2	-41 46 12
0023-588	0.61	00 23 29.9	-58 50 54	s 6.8	126	0305-417Ac 0.265	03 05 48.0	-41 47 06
0024-589	0.49	00 24 12.2	-58 54 53	,		0305-418 c 0.253	03 05 54.6	-41 49 11 J
$0028505\mathrm{Ac}$	1.30	00 28 15.0		s 2.6	68	¶0319–453* 4.82	03 19 26.1	-45 23 34 e 25.6 49
0028-505Bc	0.186		-50 34 20	J		¶0320–373 169	03 20 48.5	-37 22 19 ℓ 48 99
¶0030485	0.83	00 30 53.8	-48 35 51	d 2.3	87	¶0332–391* 2.41	03 32 17.0	-39 10 02 <i>l</i> 7 -
¶0032–738	0.67	00 32 15.8		d 1.8	154	¶0336–356 0.92	03 36 33.6	$-35\ 36\ 30$ } e 2.5 173
0033–513	0.34	00 33 42.8	-51 22 14	s 5.1	38	¶0336–355 2.92	03 36 51.0	$-35 \ 32 \ 22 \int d \ 1.5 41$
0034–513	0.36	00 34 02.8	-51 18 10	J		#0244 24F # 10	02 44 25 5	24 21 55 3 - 44 105
4 100.42 42.4	11.0	00.40.54.0	40.04.04	200	10-	¶0344–345 5.12 0345–345N 0.53	03 44 35.5	-34 31 55 } e 4.4 105
¶0043–424 0046–585Bc	11.8 0.35	00 43 54.8 00 46 31.0	-42 24 04 -58 33 30	d 2.0	135	0345-345N 0.53 ¶0357-506 0.79	03 45 28.9 03 57 42.5	-34 33 39 ∫ -50 41 06 d 1.9 23
0046-585Ac	0.52	00 46 36.2	-58 33 30 -58 31 32	s 2.1	19	¶0357-371 2.47	03 57 56.9	-37 08 53 m 1.3 150
¶0058-507	1.44	00 40 30.2	-50 47 27	, ℓ5	156	¶0408–479 0.99		-47 56 22 m 0.5 90
¶0101–649	0.77	01 01 37.7	-64 55 06	e 2.8	134			
#0101 010	0	01 01 01	01 00 00	0 2.0	101	0412-441Bc 0.31	04 12 34.4	-44 09 01 \ s 2.2 125
¶0103-453	4.04	01 03 05.7	-45 21 33	d 2.3	54	0412-441Ac 0.47	04 12 44.6	-44 10 17 } s 2.2 123
0107-371	1.37	01 07 47.4		} s 4.7	1	¶0423–687 0.79	04 23 04.8	-68 44 30 d 2.1 101
0107-370	0.34	01 07 47.8	-37 02 16	} * 4'		¶0424–728c 3.06	04 24 40.4	-72 52 45 \ d 3.6 163
0108-348A	0.88	01 08 39.4	-34 53 28	s 6.5	34	0425-728c 0.276	04 25 46.3	-725344 $\int s4.8101$
0108-348B	0.50	01 08 57.3	-34 48 04	}				
						¶0427–539* 8.41	04 27 50.0	-53 56 09 e 4.6 82
¶0110–692	3.10	01 10 02.2	-69 15 52	d 1.0	168	0429-615c 0.065	04 29 16.2	-61 35 10 s 4.6 151
¶0111–385	0.95	01 11 59.7		d 1.5	137	¶0429–616c 2.79	04 29 35.3	-61 39 13 d 1.9 14 -61 33 40 m 1.7 90
0113-808c	0.57	01 13 20.8	-80 51 09	s 3.4	137	0430-615c 0.13 0435-587A 0.58	04 30 05.6 04 35 06.9	E0 44 OF)
0114-808c	0.216		-80 53 37	, 05	150	0435-587B 0.39	04 35 52.4	> 5 0.2 109
¶0114–476*	3.79	01 14 11.7	-47 38 13	e 9.5	156	0400-001B 0.03	04 00 02.4	-30 40 00
¶0118–501	0.48	01 18 59.3	-50 11 52	Ì d 1.2	107	0437-662Ac 0.69	04 37 09.5	$-66\ 13\ 50$ $s\ 4.5$ 47
0119-501	0.74	01 19 00.3	-50 07 47	∫ s 4.1	2	0437–662Bc 0.079	04 37 42.3	-66 10 46 J
¶0130–620	1.36	01 30 42.0	-62 02 02	d 1.6	20	¶0450–387B 0.60	04 50 08.1	-38 44 18 } d 1.8 160
	10.3	01 31 42.3	-36 44 29	e 10.2	97	0450–387A 0.93 ¶0456–301 3.08	04 50 31.0	-38 46 08 ∫ s 4.8 112 -30 11 44 ℓ 5.8 2
¶0150–480	0.69	01 50 39.1	-48 03 22	d 2.1	82	¶0456–301 3.08	04 56 30.7	-30 11 44 2 5.6 2
¶0153–826	0.74	01 53 34.3		d 1.7	122	¶0456–470 0.64	04 56 37.9	
0156-483	0.51		-48 19 34	} s 3.8	35		05 07 24.1	
0156-482	0.47	01 56 33.9		Į		0511-484Cc 0.206	05 11 11.1	,
0208-418c	0.55	02 08 49.5	-41 48 44	$\left.\right\}$	20	¶0511-484Ac 4.28	05 11 30.4	4
0209–418c	0.162	02 09 06.2	-41 49 48	∫ s 3.3	109	¶0511-484Bc 1.13 ¶0511-305* 4.57	05 11 44.4 05 11 39.4	
0210-432Ac	0.58	02 10 19.5	-43 15 46) 0.5	160	10011-000 4.07	00 11 05.4	00 01 00 E 10.0 21
0210-432Bc	0.070			} s 2.2	73	¶0518-458* 85.7	05 18 19.9	-45 49 31 e 7.2 103
¶0211–479*	1.51	02 11 15.4		e 5.9	170	¶0521–478 0.95	05 21 12.2	
	0.60	02 13 23.2	-40 38 35	ໄ d 2.9	129	¶0523–327 1.63	05 23 35.3	-32 45 07 e 2.4 159
0213–406Bc	0.49	02 13 39.2	-40 41 18	∫ s 4.1	132	0534-613Ac 1.15	05 34 11.6	> 5 1.0 101
¶0214–480	3.12	02 14 53.8	-48 03 03	e 7.1	175	0534-613Bc 0.86	05 34 26.1	-61 23 56 J
¶0214-450	0.65		-45 17 16	e 3.3		¶0540–617 1.09	05 40 20.5	-61 43 55 d 1.2 49
0230–666Bc	0.256		-66 36 30	} s 3.5		¶0540–628 0.96	05 40 28.7	
	1.80	02 30 51.2	-66 40 01	ر ه ع	110	0543-479Bc 0.38	05 43 33.0	_
0231-383Bc	0.258		-38 20 28	$\frac{1}{3}$ s 3.6	155	0543-479Ac 0.73		-47 57 41 \\ 8 3.7 37
0231-383Ac	0.42	02 31 33.2	-38 23 45	\ \ \ \ \ \ \ \ \ \ \ \ \ \ \ \ \ \ \	100	¶0546–329* 1.85	05 46 39.5	-32 59 27 e 8.0 18

. =												
0	MOST	S843	RA (B1950)	Dec (B1950) Size	PA	MOST	S843	RA (B1950)	Dec (B1950)	Size	PA
: _	Source	Jу	h`m s´	0 `1 11	<u> </u>	•	Source	Jу	h`m s´	<u> </u>	· ·	۰
ο	¶0558–388	0.69	05 58 44.3	-38 53 48	d 1.0	76	¶0918-383	1.19	09 18 18.0	-38 22 27	d 3.3	130
r yyzapus	0559–389	0.55	05 59 10.4	-38 56 44	s 5.9	120	¶0930–399	1.17	09 30 39.0	-39 57 08	d 5.8	77
7	¶0608–658	1.81	06 08 46.1	-65 50 52	d 1.1	75	¶0932-372	1.37	09 32 02.6	-37 14 51	ℓ3	145
4	¶0609–585	0.68	06 09 10.4	-58 30 40	d 2.8	57	¶0936–622	1.10	09 36 17.7	-62 15 39	d 0.7	32
	0610–316Bc	0.203		-31 37 32	s 2.3	105	¶0945-370	0.90	09 45 44.2	-37 00 48	d 2.3	167
	0610–316Ac	0.85	06 10 37.4	-31 38 07	J		#00 * 0 000					~=
	0611-557Bc	0.224	06 11 00 9	EE 47 10	`	1	¶0952–306	0.93	09 52 20.9	-30 39 12	d 1.5	65
	0611-557Ac	0.224	06 11 20.8 06 11 24.0	-55 47 18 -55 43 27	s 3.9	7	¶1002–320 ¶1010–647	1.33 4.65	10 02 26.1 10 10 49.0	-32 02 06 -64 43 07	m 1.8 m 1.7	22 51
	0611-557AC 0616-487c	0.59	06 16 46.7	-33 43 27 -48 44 51) s 3.2	25	¶1010-047 ¶1011-316	2.31	10 10 49.0	-31 38 26	d 1.3	
	¶0616–486c	0.84	06 16 54.8	-48 41 57	m 1.8		¶1011-310	0.73	10 11 36.9	-32 04 49	d 2.4	
	¶0618–371	4.34	06 18 17.6		d 1.3	81	,					
							1015-385Bc	0.273	10 15 03.9	-38 32 59	} s 3.4	67
	¶0620-526	4.96	06 20 34.7	-52 39 34	ℓ 5.3	-	1015-385Ac	0.63	10 15 20.0	-38 31 40	} ° 0.4	01
	¶0625-545	5.61	06 25 46.8	-54 30 48	ℓ 5.5	176	¶1025–612	0.81	10 25 22.9	-61 15 06	e 5.2	68
	0629 - 729c	0.49	06 29 45.6	-72 54 16	} s 3.6	70	1033–660c	0.167		-66 03 13	} s 3.6	23
	0630–728c	0.147	06 30 31.7	-72 53 02	J		1034–659c	0.53	10 34 03.9	-65 59 53	J	
	¶0641-584	0.99	06 41 31.6	-58 27 05	d 1.7	42	1051 045	0.004	10 51 01 5	04.00.01	,	
	¶0645-729	0.67	06 45 06.6	-72 55 33	d 1.9	91	1051-345c	0.294		-34 30 31	s 2.9	72
	¶0649–557	1.65	06 49 23.9	-55 45 52	d 2.2		1051-344c ¶1056-360	0.98 2.40	10 51 15.2 10 56 31.0	-34 29 36 -36 03 40) 18	159
	¶0651–603	1.90	06 51 15.0	-60 18 22	ℓ 3.2		¶1030–360 ¶1112–545	1.37	11 12 31.8		d 2.0	61
	¶0655–486	0.68	06 55 03.3	-48 38 52	d 1.6		¶1112 040	4.11	11 23 28.5	-35 06 49	d 1.0	87
	¶0703–595	0.72	07 03 07.0	-59 34 37	d 2.1	1	#1120 001		11 20 20.0	00 00 10	u 1.0	٥.
							¶1136–678	4.55	11 36 07.1	-67 53 44	m 1.4	55
	0703–451c	0.077	07 03 40.4	-45 10 38	}	1	¶1136–320	3.87	11 36 47.3	-32 05 59	m 1.2	162
	¶0704–451c	1.16	07 04 00.3	-45 08 30	∫ d 4.3	69	¶1137–463c	1.17	11 37 26.7	-46 21 54	} e 4.5	40
	¶0707-359*	3.26	07 07 35.0	-35 57 16	e 8.1	123	1137-464c	0.039		-46 24 24	∫ s 3.0	
	0713-371Ac	0.71	07 13 39.6	-37 10 46	s 3.6	33	¶1141–391	0.62	11 41 40.7	-39 06 00	d 2.0	19
	0713–371Bc	0.278	07 13 49.5	-37 07 43	J		11.49 21.7	0.70	11 40 17 5	21 40 02	`	
	¶0715–362	3.78	07 15 18.5	-36 16 14	ℓ 7.5	74	1143-317 1143-316	$0.70 \\ 2.41$	11 43 17.5	-31 42 23 -31 40 33	s 7.0	75
	¶0713-302 ¶0718-340	2.99	07 18 16.3	-34 01 23	d 0.8	53	1143-316	1.78	11 43 49.4 11 44 30.7		{	
	¶0719–553	3.39	07 19 12.2	-55 19 36	m 0.9		1145-379	0.41	11 45 01.3	-37 58 15	s 6.6	114
	0724-375	0.94	07 24 32.1	-37 32 52	} s 7.9	33	¶1148–353	2.21	11 48 43.6		m 1.8	41
	0724-374	0.64	07 24 53.9	-37 26 13	} 8 1.9	33	,		11 10 1010	30 20 10	222 210	
							¶1152–694	2.54	11 52 04.9	-69 28 49	d 1.4	61
	0747–674c	0.130	07 47 31.0	-67 24 46	s 2.8	65	1153-807Ac	0.54	11 53 23.7	-80 44 33	$s_{2.7}$	27
	0747–673c	0.55	07 47 57.8	-67 23 35	J		1153-807Bc	0.119	11 53 54.7	-80 42 09	J	
	¶0807389	4.21	08 07 44.0	-38 56 38	d 2.2	70	¶1158–652	0.84	11 58 49.8		d 2.8	
	¶0809–492	3.29	08 09 14.3	-49 15 25 40 20 45	$\left.\right\} \begin{array}{c} \ell \ 2.4 \\ 0.6 \end{array}$	32	1225-816	0.39	12 25 11.7	-81 37 22	s 4.3	
	0809-493	0.86	08 09 40.8	-49 20 45	∫ s 6.9	141	1226-816c	0.080		-81 40 34	s 1.8	30
	¶0809–499	2.18	08 09 58.2	-49 58 51	d 1.4	36	1227–816c	0.69	12 27 00.9	-81 39 03	,	
	0815-675Ac			-67 30 13		1	¶1234–723	1 86	12 34 06.1	-72 18 25	<i>l</i> 14	5
	0815-675Bc	0.53	08 15 45.5		s 2.6	104		0.224)	
	¶0816-704	1.85	08 16 36.7		<i>l</i> 6	60	1234-490Ac	0.67	12 34 52.3		s 2.9	44
	¶0819–300*	6.41	08 19 23.8		d 5.1	128	¶1241–663*	1.15	12 41 37.9		e 5.0	116
							1242-664n	0.160		-66 24 35	e 3.1	
	0842-571	0.54	08 42 19.2		s 4.7	125						
	0842-572	0.61	08 42 47.1	-57 13 13	J		1256–331	0.81	12 56 36.7	-33 08 32	s 7.2	120
	¶0843–336	3.00	08 43 08.1	-33 36 51	ℓ8	165	1257-332	0.81	12 57 06.4		J _	
	¶0843–568	0.95	08 43 25.8	-56 53 44	d 1.5	54	¶1259–445	2.19	12 59 39.6		d 2.2	
	0851-314Ac		08 51 08.2 08 51 16.8	-31 29 39 -31 26 47	s 3.2	33	¶1259–367	1.38	12 59 54.3		m 2.0	
	0851-314Bc	0.262	00 01 10.8	-31 20 47	,		¶1302–325*	2.42	13 02 10.6	-32 34 08	e 5.7	32
	¶0905-353	1.82	09 05 44.7	-35 23 31	ℓ 6.5	101	¶1302–492	8.30	13 02 32.6	-49 12 02	ℓ 8.5	40
					m 0.7	1	¶1302–432 ¶1304–748	0.77	13 04 50.8			43
		3.05	09 09 25.5	-56 24 29	111 0.1							
	¶0909–564 0915–543Bc	3.05 0.234	09 09 25.5 09 15 48.7	-56 24 29 -54 21 32) s 2.1							
	¶0909–564	0.234				141	¶1308–441	1.76	13 08 29.6	-44 07 35	e 14.4	117
	¶0909–564 0915–543Bc	0.234 1.23	09 15 48.7	-54 21 32	} s 2.1	141 118	¶1308–441 ¶1312–593Ac	1.76				117 114

TABLE 1—Continued

											
MOST Source	S ₈₄₃ Jy	RA (B1950) h m s	Dec (B1950)	Size	PA •	MOST Source	S ₈₄₃ Jy	RA (B1950) h m s	Dec (B1950)	Size	P
¶1318–434*	7.16	13 18 14.9	-43 26 58	<i>l</i> 17	37	¶1758–473	0.93	17 58 20.9	-47 19 28	<i>l</i> 5	11
¶1322–427	392	13 22 35.8	-42 44 29	e 6.8	49	¶1815–546	1.31	18 15 59.5	-54 36 28	d 1.0	1
Cen A total	1790			e 300		1820–774c	0.35	18 20 32.0	-77 29 44	s 1.8	6
¶1324–300	1.76	13 24 56.2	-30 02 38	d 2.0	112	1821-774c	0.40	18 21 01.3	-77 28 51	5 2 2.0	
¶1333–337*	14.9	13 33 46.9	-33 43 45	<i>ℓ</i> 32	133	¶1821–583	2.16	18 21 21.4	-58 19 21	d 3.3	8
¶1343–377	1.29	13 43 20.3	-37 43 32	e 2.7	89						
						¶1829–778	0.69	18 29 01.8	-77 50 29	m 0.8	10
¶1355–416	6.53	13 55 57.1	-41 38 18	d 0.8	124	¶1837–365	0.59	18 37 33.3	-36 30 03	l d 0.7	10
¶1411–657	2.19	14 11 30.6	-65 43 21	d 1.5	10	1838-365	1.09	18 38 07.7	-36 31 57	∫ s 7.2	10
¶1413–364	3.66	14 13 32.4	-36 26 57	d 2.9	40	¶1840–404	3.44	18 40 59.0	-40 25 02	m 1.1	11
1416-516	1.36	14 16 13.7	-51 41 13	} s 4.3	1.45	1846-631 A	1.10	18 46 00.9	-63 08 00)	
1416-517	0.45	14 16 29.8	-51 44 46	\ \ \ \ \ \ \ \ \ \ \ \ \ \ \ \ \ \ \	1 10	1846-632 с	0.35	18 46 03.9	-63 13 59	s 6.0	17
						1846-631Bc	0.60	18 46 14.4	-63 11 35	0.6	16
¶1418–557	4.12	14 18 55.9	-55 46 26	d 0.6	73						
¶1421-382	3.65	14 21 12.1	-38 13 15	d 0.9	143	¶1849–397	0.90	18 49 57.7	-39 45 12	d 1.7	6
¶1425–479	1.46	14 25 38.8	-47 58 40	l 4.5	52	1902-579с	0.33	19 02 39.0	-57 54 10	} s 2.6	6
¶1437–368	1.55	14 37 27.7	-36 52 39	d 1.8	71	1902-578c	0.091	19 02 56.9	-57 53 03	} 8 2.0	U
¶1451–364	4.89	14 51 20.8	-36 27 53	d 2.0	157	1908-623	0.47	19 08 39.9	-62 23 40	s 7.5	13
						1909-624	0.43	19 09 29.7		~1.0	
¶1452-367	1.65	14 52 00.9	-36 43 29	ℓ 3.5	32					•	
¶1452–517	2.87	14 52 28.4	-51 47 39	<i>l</i> 19	24	¶1910–800	1.37	19 10 37.4	-80 04 26	e 4.9	16
¶1511–315	1.59	15 11 59.5	-31 33 27	d 2.1	55	1919-551Ac	0.45	19 19 16.9	-55 06 33	0.3	13
¶1516–477	1.04	15 16 28.9	-47 42 30	d 3.3	102	1919-551Bc	0.44	19 19 20.9		} s 2.7	16
¶1518–530	0.97	15 18 14.5	-53 03 03	d 1.6	117	¶1921-577	1.75	19 21 55.0	-57 46 19	ℓ 5.5	17
•						¶1922–627	2.68	19 22 53.0	-62 45 36	d 1.1	
1532-495Bc	0.125	15 32 22.3	-49 32 36	} s 3.1	1.41	-					
1532-495A	0.59	15 32 34.4	-49 35 01	} 8 3.1	141	1925-746	0.36	19 25 37.9	-74 40 37	} s 6.3	10
¶1541-383	0.98	15 41 01.4	-38 19 11	d 2.0	142	1926-747	0.76	19 26 49.9	-74 44 41	} 8 0.3	13
¶1545-321	2.50	15 45 50.0		e 7.0		¶1929–397	3.81	19 29 59.0		d 1.7	12
1600-445B	0.50	16 00 38.0	-44 34 35	} s 4.1	72	1936-357Bc	0.53	19 36 01.8		} s 2.9	
1600–445A	1.21	16 00 59.7	-44 33 21	} * 4.1	12	1936–357Ac	0.69	19 36 15.9	-35 47 58	} \$ 2.5	3
¶1602–633*	9.57	16 02 09.2	-63 21 49	e 7.3	114	1939–406	0.38	19 39 48.0	-40 36 38	\ s 7.3	9
1607-454	0.82	16 07 04.8	-45 26 54	} s 4.8	35	¶1940–406	2.29	19 40 26.1	-40 37 16	∫ d 2.2	17
1607-453	0.80	16 07 20.4	-45 23 01	}		1942-316	0.42	19 42 37.1	-31 39 47	} s 7.0	129
¶1610–605	6.01	16 10 31.3	-60 30 39	ℓ 25	112	1943-317	1.48	19 43 02.7	-31 44 08	}	
¶1610–608*	90.0	16 10 40.3	-60 48 28	<i>l</i> 16	88	¶1945–304	1.44	19 45 12.4	-30 27 37	d 2.1	10
¶1619–634	1.44	16 19 55.5	-63 28 49	ℓ 5.5	123	1951-310A	0.50	19 51 09.8	-31 05 07) s 5.2	6
¶1623–434	0.92	16 23 29.2	-43 29 52	d 1.6	45	¶1951-310B	0.64	19 51 32.5	-31 03 12	d 0.9	
¶1623–421*	1.86	16 23 26.8) d 4.2		¶1951-501	1.94	19 51 23.6	-50 10 16	m 0.8	
1623-420	0.58	16 23 47.4	-42 00 16	} s 7.3	32	1951-500	0.53	19 51 25.7	-50 05 44	s 4.5	
¶1637–771	8.18	16 37 07.7	-77 10 00	ℓ 5.5	170	¶1954–552	8.14	19 54 18.5	-55 17 43	<i>l</i> 6	3
¶1717–620	0.99	17 17 15.9	-62 05 34	d 1.6	155	¶1954–356	0.61	19 54 33.9	-35 39 08	d 2.8	4
1720-476Ac		17 20 08.5		} s 3.1		¶1955-470	1.25	19 55 21.3	-47 05 49	d 1.6	
1720-476Bc				\ \ \ \ \ \ \ \ \ \ \ \ \ \ \ \ \ \ \	100	¶1953–879	1.16	19 53 45.6	-87 55 51	\ d 1.4	
¶1721-568	0.76	17 21 56.6		<i>l</i> 4.5	124	2007-879	0.60	20 07 33.1	-87 58 31	∫ s 7.9	11
¶1733–565*	11.0	17 33 21.7		e 4.6		2007 408	0.54	00.05.00.0	40 51 54	`	
				,		2005-428	0.54	20 05 38.0		s 6.2	17
1733-712	0.72	17 33 29.0		s 4.8	160	2005-429	0.63	20 05 43.9	-42 58 01)) (
1733–713	0.88	17 33 49.3	-71 21 45	J		¶2006-565	1.89	20 06 19.7		ℓ^{28}	15
¶1737–608	3.91	17 37 28.2	-60 53 52	d 1.3	147	¶2007–568N	0.77	20 07 25.9	-56 52 31	$\int_{0}^{\infty} \frac{\ell}{2} \frac{2.3}{4}$	
1744–630c 1744–629c	0.47 0.193	17 44 33.0 17 44 39.4		} s 4.3	10	¶2013–308 2013–307	$0.97 \\ 1.25$	20 13 08.1 20 13 23.1		$\begin{cases} d 3.4 \\ s 7.0 \end{cases}$	
1/44-029C	0.193			,		_					
1749–508	0.39	17 49 54.5		s 8.0	85	¶2013–312c	0.70	20 13 58.7		d 1.1	
1750-508	0.89	17 50 45.1	-50 48 18	} - 5.0		2014-312c	0.38	20 14 08.2		0.3	
1750-433	0.39	17 50 01.8	-43 20 15) s 7.0	151	2014-311c	0.24	20 14 16.0		0.5	
			10.00.00	7		I #10014 FF0	9.49	20 14 05 0	EE 40 E1	/ 20	15
¶1750–434	0.79	17 50 20.7	-43 26 22	∫m 0.9	140	¶2014–558 ¶2020–575	2.43 4.43	20 14 05.9 20 20 21.5		ℓ 20 m 1.1	

TABLE 1—Continued

MOST Source	S ₈₄₃ Jy	RA (B1950) h m s	Dec (B1950)	Size	PA •	MOS Source		RA (B1950) h m s	Dec (B1950)	Size	PA •
¶2022–537	0.57	20 22 24.3	-53 42 19	m 1.2	7	2238-60	0.34	22 38 46.3	-60 58 23	s 3.4	115
2022-538	0.37	20 22 53.2	-53 48 19	\$ 7.4		2238-60			-60 56 06	s 4.5	
2026-413	0.45	20 26 04.5		s 8.0		¶2239–60		22 39 11.5	-60 59 48	d 1.4	
¶2026–414	1.51	20 26 14.2		} d 2.7		2243-52		22 43 12.4	-52 59 11	} s 7.9	
¶2028–732	1.98	20 28 22.2	-73 14 19	d 1.3	58	2243-53	30 0.45	22 43 46.9	-53 05 12	} * '.9	139
2030–378A	0.34	20 30 01.1	-37 52 23	s 6.8	52	2252-52	29 0.68	22 52 28.3	-52 57 21	۱	1.40
¶2030-378B	0.46	20 30 28.2	-37 48 10	d 0.9	159	2252-53		22 52 51.2	-53 01 41	s 5.5	142
["] 2036–612Bc	0.227	20 36 22.7	-61 17 08	s 3.9	22	¶2302-71) d 1.6	40
2036-612Ac	0.46	20 36 34.8	-61 13 32	J 8 0.5		2302-71			-71 17 35	}	
2040-631	0.33	20 40 34.1	-63 10 21	s 4.1	104	¶2315-42		23 15 11.5	-42 30 05	e 6.0	86
2041-631	0.64	20 41 09.2	-63 11 20	, ,	101						
						¶2316–42	23 1.61	23 16 27.1	-42 22 46	ℓ 5	60
¶2041–604	4.15	20 41 18.1	-60 29 56	m 0.5	64	¶2320–61	13 0.78	23 20 38.8	-61 20 34	d 2.4	37
2046-376	0.223	20 46 43.7	-37 41 02	d 0.9	78	2331-49	93 0.43	23 31 48.3	-49 23 08	s 8.0	11
$\P2047-572c$	0.87	20 47 43.9	-57 15 11	d 1.3	102	2331-49	0.51	23 31 57.7	-49 15 14	} ° 0.0	11
2048-572c	2.26	20 48 11.8	-57 15 22	∫ s 3.8	93	¶2340-58	36 0.74	23 40 46.0	-58 40 38	d 1.6	47
¶2052–736*	0.98	20 52 46.9	-73 39 54	e 5.3	96						
						¶2341-50	0.88	23 41 57.4	-50 57 22	d 1.8	135
2055–650	1.23	20 55 14.4	-65 01 36	s 7.6	92	¶2356–61	11* 29.0	23 56 25.8	-61 11 26	e 6.3	135
2056–650	0.30	20 56 26.7	-65 01 52	j		2356-83	31c 0.39	23 56 47.2	-83 07 22	s 3.8	35
2121-660c	0.42	21 21 50.3	-66 04 34	s 2.6	77	¶2357–83	30c 0.48	23 57 59.4		∫m 1.2	115
2122 - 660c	0.92	21 22 15.5	-66 03 58)		¶2359–69	90c 0.58	23 59 08.4		્રે d 1.7	100
¶2130–538	2.50	21 30 44.1	-53 49 52	ℓ 5	165	¶2359–69	91c 0.42	23 59 34.1	-69 08 35	∫ d 1.4	44
¶2132–554	0.75	21 32 38.6	-55 27 14	d 2.0	139						
2140-568	0.168		-56 51 09	d 1.6	53						
2143–556	0.64	21 43 52.9		s 4.7	133						
2144-556	0.59	21 44 17.4	-55 40 22	J							
2147–721Ac	0.40	21 47 15.2	-72 09 39 <u>]</u>								
2147–721Bc	0.099		-72 11 37	> s 3.8	111						
2148–721c	0.094	21 48 02.0	-72 11 01 J								
¶2148-555*	2.45	21 48 01.2	-55 34 37	<i>l</i> 13	26						
¶2151–461	1.29	21 51 11.2	-46 06 37	e 6.3	44						
2152-325Ac	0.71	21 52 09.3	–32 34 12								
2152-325Bc	0.246	21 52 18.8	-32 33 09	s 4.8	74						
2152–325Cc	0.208	21 52 31.4	-32 32 51 J								
¶2152–699	35.1	21 52 58.5	-69 55 39	d 1.0	24						
2153-699	4.73	21 53 40.5	-69 56 10	∫ s 3.6	98						
2154-325A	0.40	21 54 26.8	-32 34 50	s 3.3	70						
2154-325B	0.56	° 21 54 41.7	-32 33 43)							
¶2156–374	0.98	21 56 52.4	-37 24 59	d 1.5	119	1					
¶2158–380	2.14	21 58 15.4	-38 01 04	d 1.6	51	1					
2215-508	1.48	22 15 09.5	-50 53 45	<0.5	_						
¶2217-505	1.49	22 17 57.7	-50 33 29	d 1.2	71	1					
2218–505	0.56	22 18 19.3		∫ s 3.8	66						
¶2225–308	1.26	22 25 01.4	-30 49 01	d 1.7	142						
¶2225–619	0.45	22 25 55.1	-61 55 38	d 1.7	50						
2226-411	5.99	22 26 22.1	-41 06 53	s 6.1	52						
2226-410	0.56	22 26 47.5	-41 03 08	S 6.1	02						
¶2227–665	1.25	22 27 33.4	-66 34 19	d 1.1	62						
2232–488	1.15	22 32 11.6	-48 51 31	s 6.1							
2232-489	0.53	22 32 31.5	-48 56 38) S 0.1	7.71						
						d .					

Notes.—Columns give: radio source name; integrated flux density at 843 MHz; centroid position; angular size; and position angle. The source and size flags are described below.

Nearby sources in the same field; kept together in Table 1 though this gives minor discrepancies in the R.A. sequence.

Source flags: (¶) A member of the Confirmed MRC Extended Sample. (*) Single source which has multiple listings in the MRC. (c) Two or three sources that are combined in one MRC listing. (N) Nearby source, listed in MRC but not flagged. (n) Nearby source, not listed in MRC.

Size flags: (d) Separation of peaks in a double source. (e) Largest separation of peaks in a complex source. (l) Largest size of low-brightness emission in a complex source: PA is given for the central axis. (m) Deconvolved extent along axis of source. (s) largest separation of centroids of nearby sources.

CLEANed image by integration within decreasing contour levels and extrapolating the results to the local zero level. The integrated flux densities have an rms uncertainty of $\pm 9\%$, of which 6% arises from the calibration of the observations and 7% from the integration. The lowest reliable contour level defined the boundary used to calculate the centroid positions. These positions have an accuracy of 1.6 in right ascension and 2.2 cosec $|\delta|$ in declination. Changes in the lowest contour used for the centroid position may give shifts of up to 10% for more extended, asymmetrical sources. These uncertainty estimates were obtained from the consistency of repeated observations. The results were checked against previously published data, and systematic errors were estimated to be less than 5% in flux density (including uncertainty in the absolute flux density scale), and 0.5% in position for compact sources.

The flux densities and centroid positions are listed in Table 1, along with the angular size and position angle. The angular size listed is the distance between brightness maxima for double and complex sources (d or e flag), the largest size of low-brightness emission for diffuse complex sources (l flag), or the deconvolved major axis width for single peaks (m flag). The position angle (north through east) of the peak separation or deconvolved major axis is given except for a few curved sources where the quoted position angle refers to the axis of the central region.

4. OPTICAL IDENTIFICATIONS

Film copies of the UK Schmidt IIIaJ survey were searched for optical identifications of all sources. The optical fields were examined relative to the radio structure by using a transparent overlay of the radio positions. Polaroid photographic enlargements of each optical field were also taken. Optical positions were measured with a two-coordinate measuring machine, using nearby reference stars from the SAO and Cape star catalogs (Hunstead 1971). The plate parameters were determined by a least-squares six-parameter fit to the reference stars to give optical positions with an estimated accuracy of 0.5 in each coordinate.

The magnitudes (b_J) of the possible optical identifications were estimated to the nearest 0.5 mag by comparison of the Polaroid enlargements with reference images of galaxies and stars of known magnitude. The reference galaxies were from the lists of Carter (1980) and Dickens, Currie, & Lucey (1986), while the stars were from Hawkins (1979, 1981). The reference magnitudes were corrected to the survey color using the equation $b_J = B - 0.23(B - V)$ (Shanks et al. 1984).

For unresolved radio sources, the search radius for galaxies and stellar objects was 5".6, which is approximately twice the combined radio and optical position errors.

For the resolved sources, most of which do not have compact core components and are larger than 1', the area searched for optical counterparts must be large. In many sources there are offsets between the radio centroid and the optical object, arising from intrinsic asymmetry in the flux and size of the lobes, or from bending of the radio structure. The criteria for acceptance of identifications were developed by considering the properties of those sources in our sample already having reliable identifications—sources with core radio components or bright optical counterparts. The position of the optical nucleus was found to lie, on average, between the midpoint and

centroid of double sources, and slightly closer to the centroid. The rms scatter about the centroid was 10% of the lobe separation (6% normal and 7% parallel to the axis).

We considered, but rejected, a criterion based solely on a search out to a radius proportional to the lobe separation (as used by Laing, Riley, & Longair 1983 for 3CR sources) since, if the adopted radius were large enough to include most known identifications (e.g., 20% of lobe separation), it would lead to many spurious identifications with faint objects on the UK Schmidt Survey.

The criterion adopted was to use a fixed physical search radius from the radio centroid (similar to that used by Schilizzi 1975). The distribution of optical-radio centroid offsets, for 55 sources in the sample, with reliable identifications and known redshift, is given in Figure 2. There is a long tail to the distribution, extending to 140 kpc. This was considered excessive for a search radius, and to limit the proportion of spurious identifications, we chose a cutoff value of 50 kpc that includes $\sim 90\%$ of the offsets in the distribution.

Galaxies were accepted as identifications of the extended radio sources if the projected optical-radio centroid offset were less than 50 kpc. The distance was estimated by assuming an absolute magnitude M of -21.0 and making corrections to apparent magnitude for absorption and redshift. We used a Galactic extinction of A = 0.20 cosec |b|, and an approximate cosmological K-correction of $4 \times z$ (Pence 1976).

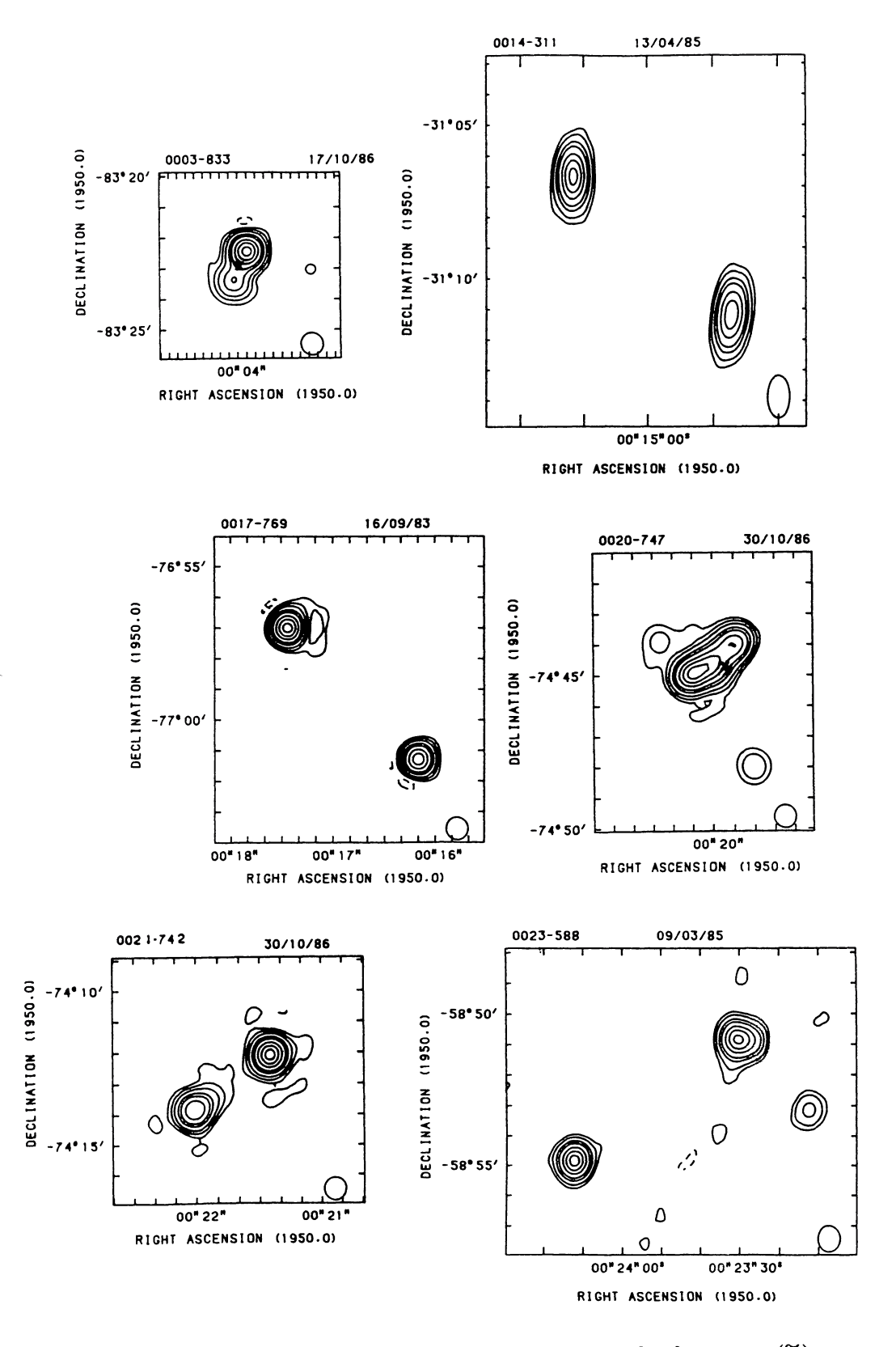
If more than one galaxy satisfied the 50 kpc criterion, the brightest galaxy was chosen. A few identifications were accepted for sources having offsets greater than 50 kpc when there was other evidence supporting the identification (for example, a radio core coincident with the optical object).

The adopted identifications are summarized in Table 2 and comments on the optical fields are included in § 6.

5. REDSHIFTS

Spectra of 14 galaxies were obtained using the Anglo-Australian Telescope, as service observations in 1986 October and December and by R. W. Hunstead as a backup program in 1989 February. The RGO Cassegrain spectrograph and Image Photon Counting System (IPCS) detector were used, and in addition the Faint Object Red Spectrograph (FORS) was used for the 1986 October observations (0319-453 and 1452-517). None of the galaxies had detectable emission lines in the (blue) wavelength range of the IPCS spectra so redshifts were obtained from the absorption features, by measuring the wavelengths of prominent absorption features, and by crosscorrelating the spectra with a high signal-to-noise template (the 1986 December observation of 1308-441). The two FORS spectra showed weak emission lines of H α in 0319-453, and H α and [S II] in 1452-517, at wavelengths consistent with the redshifts obtained from the absorption features.

All known redshifts are listed, for completeness, in § 6 and summarized in the data of Table 2. The redshifts have been obtained from the literature, largely from the compilations of Véron-Cetty & Véron (1983) and Palumbo, Tanzella-Nitti, & Vettolani (1983). The original references are quoted except for three objects with many redshift measurements where the weighted average from Palumbo et al. (1983) was used. The redshifts have not been corrected for Galactic rotation.



Maximum flux density per beam in each map and lowest-level contours (%): 0014-311 0.39 Jy $\pm~2~\%$ $2.59 \mathrm{Jy}$ 0003-833 2 % 0.43 Jy $0.72 \mathrm{~Jy}$ $\pm 2\%$ 0020-747 0017-769 $\pm 5\%$ 2 % 0023-588 0.45 Jy0021-742 0.40 Jy

FIG. 1.—MOST images of the extended and multiple sources in the Molonglo Reference Catalogue. The contour levels are at 0.5%, 1%, 2%, 5%, 10%, 20%, 30%, 50%, 70%, and 90% of the peak brightness, with the lowest level plotted dependent on the dynamic range. The peak brightness per beam (in Jy) and the low-level contours (in %) are given in the captions. The HPBW ellipse is plotted in the lower right corner and the positions of the optical identifications are marked with crosses.

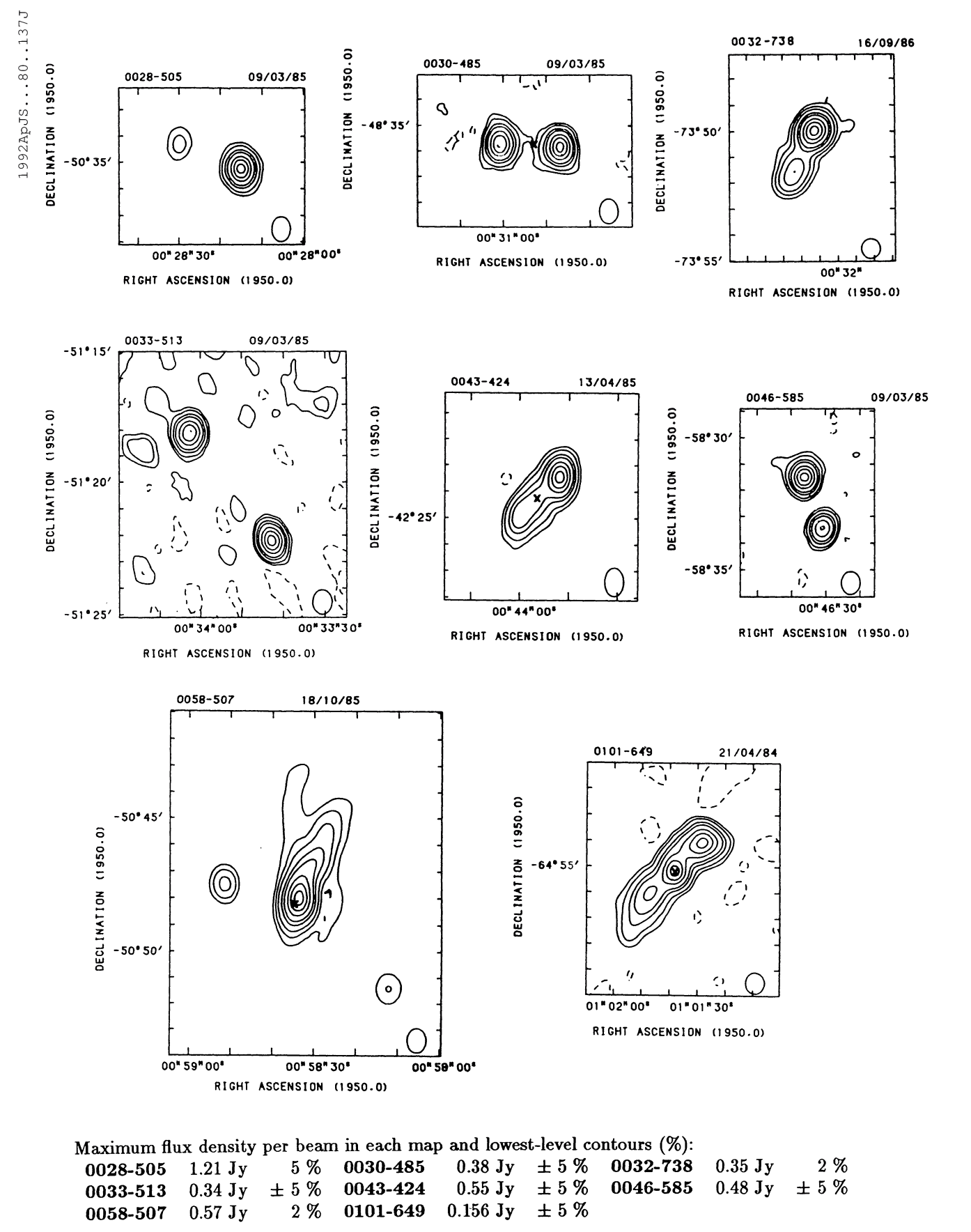
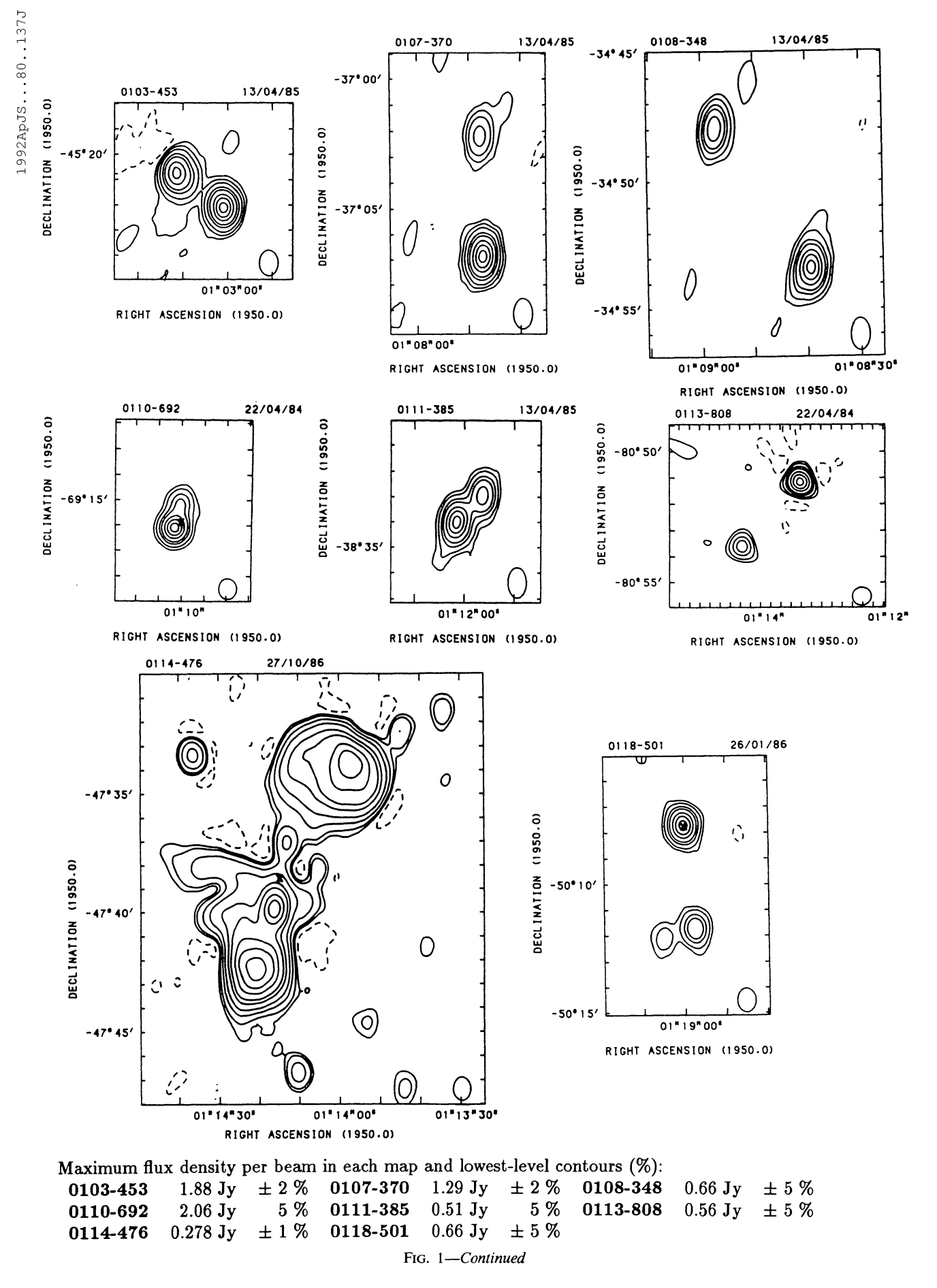
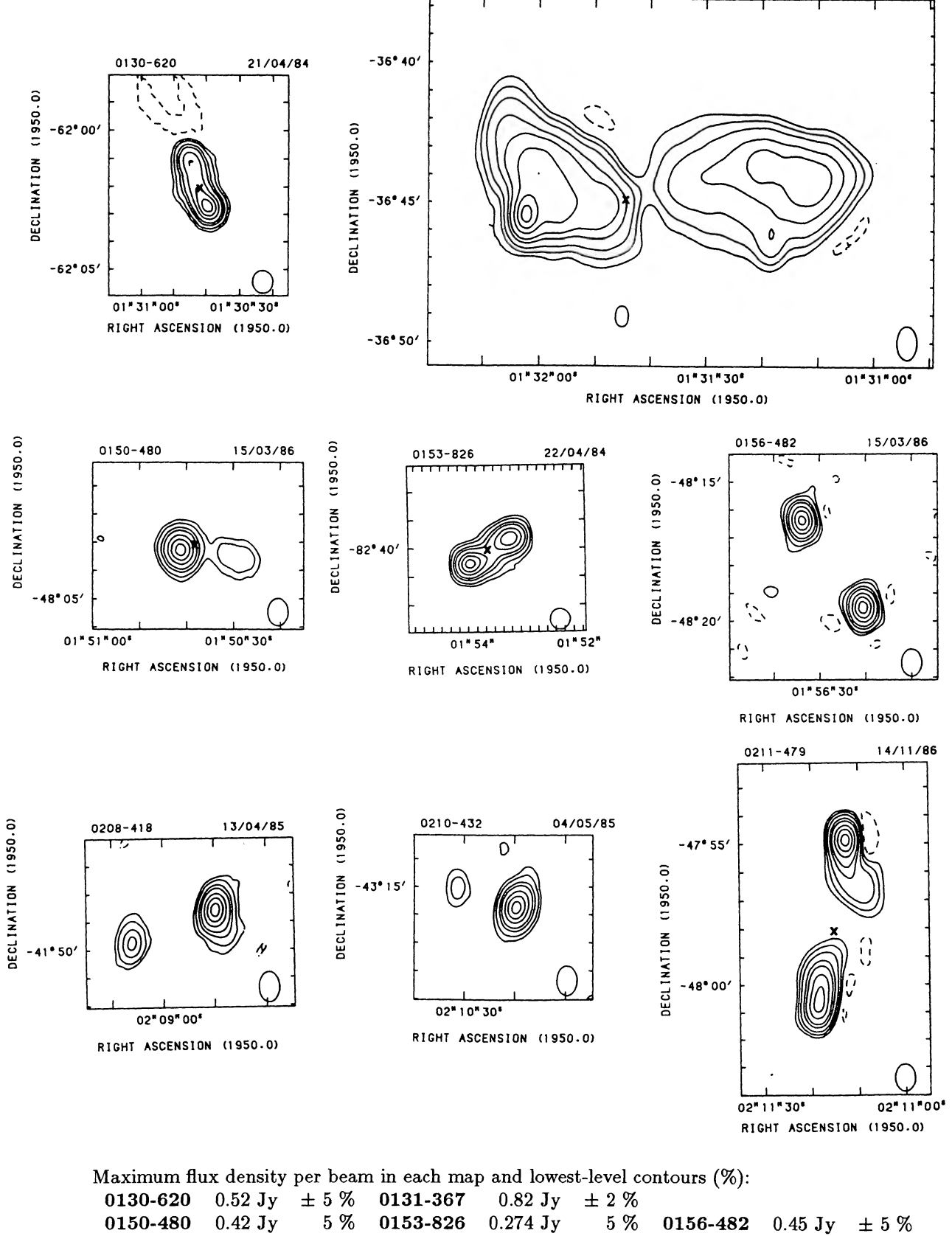


Fig. 1—Continued





0131-367

28/10/86

 $\pm~5~\%$ 5%0208-418 $0.44 \mathrm{~Jy}$ 0210-432 0.46 Jy0211 - 479 $0.56 \; \mathbf{Jy}$ \pm 2 %

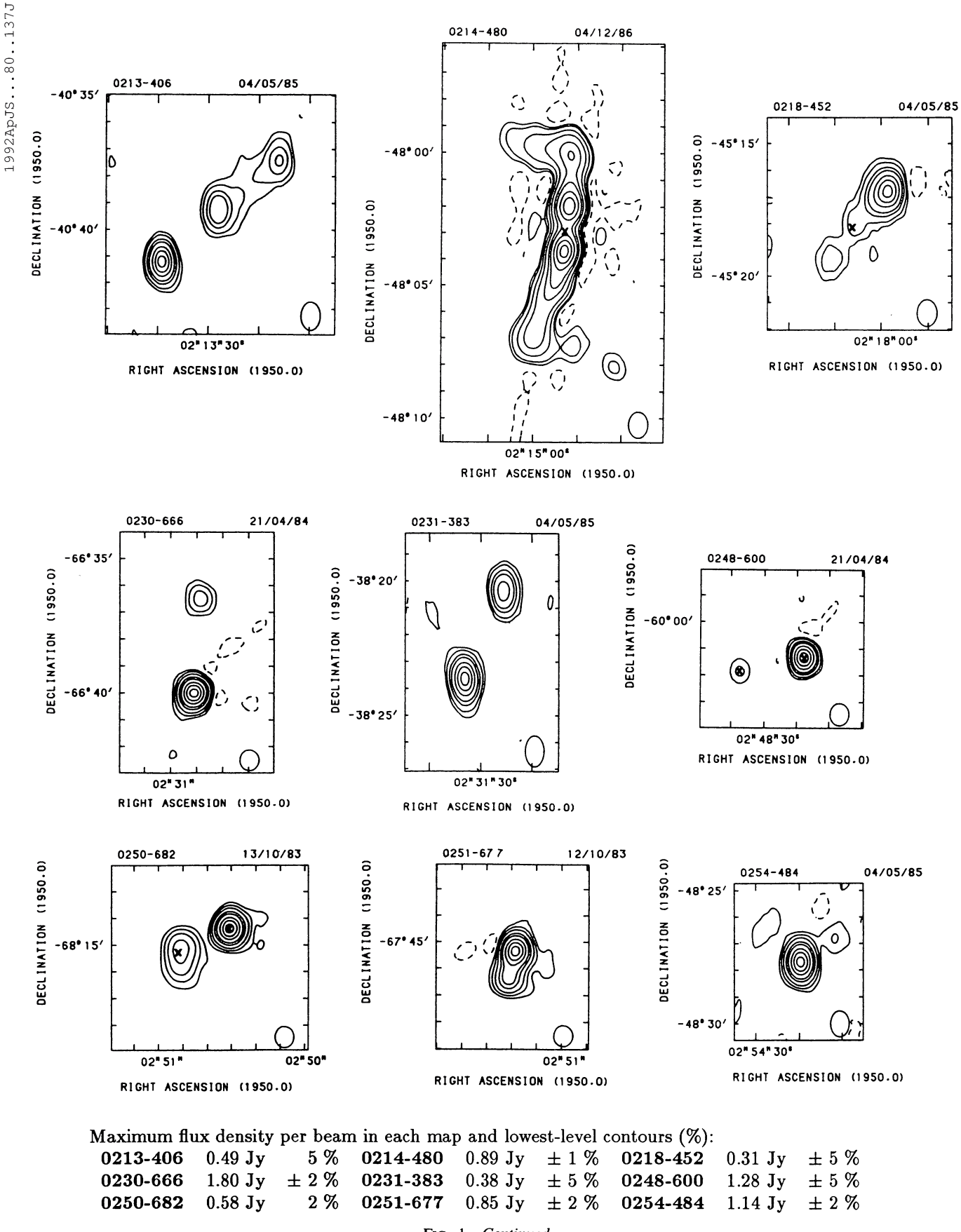
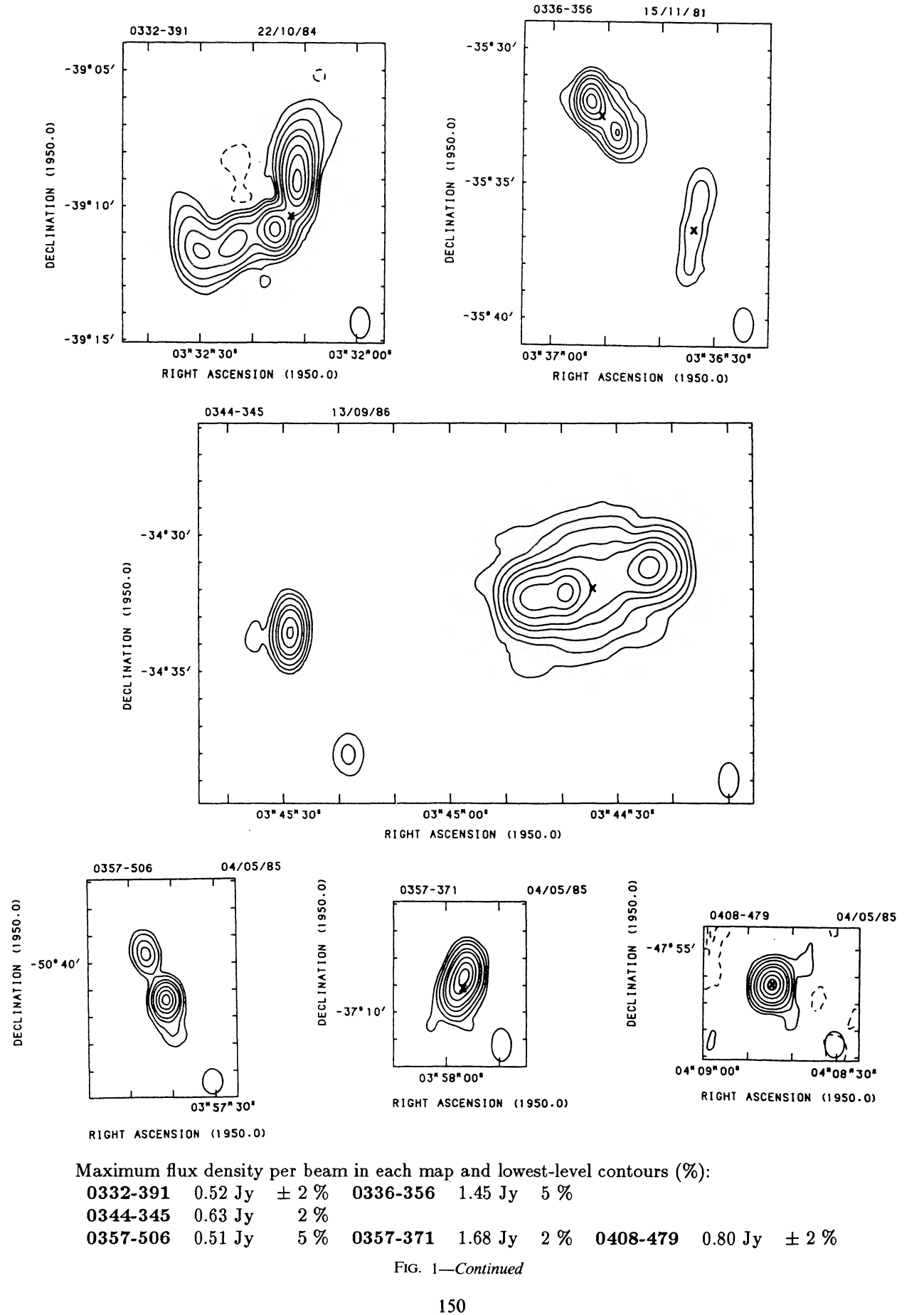
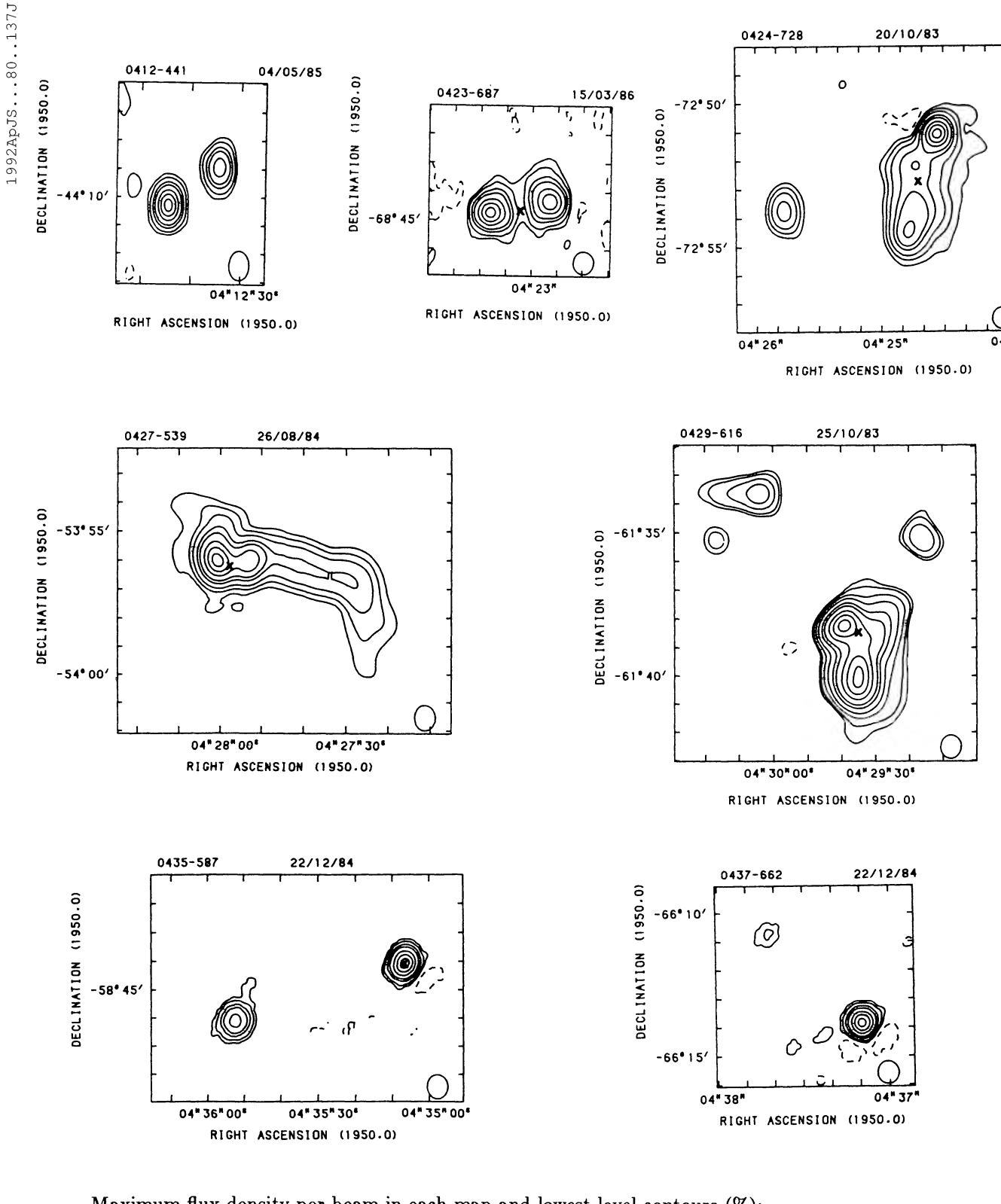


Fig. 1—Continued

149

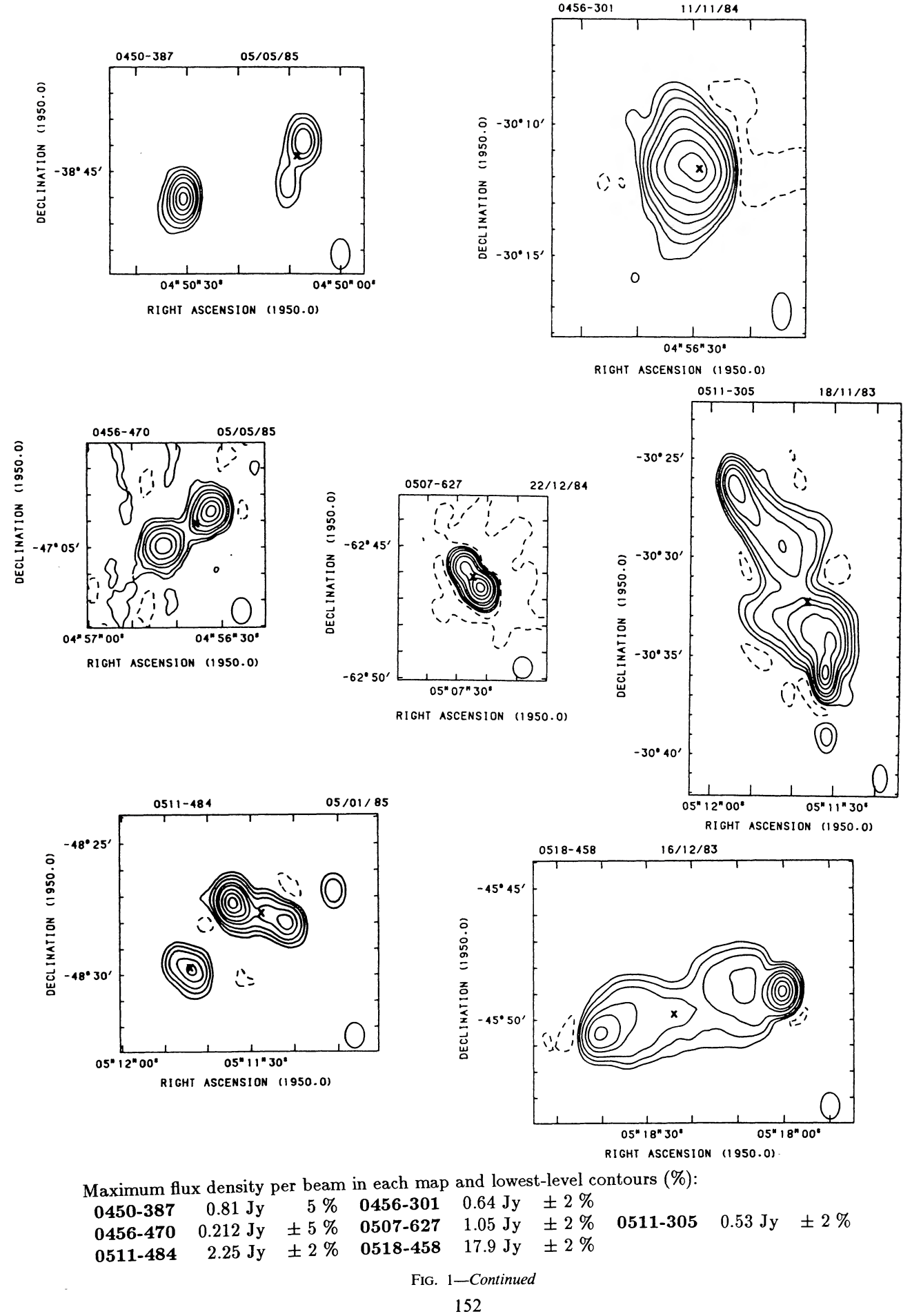




Maximum flux density per beam in each map and lowest-level contours (%):

 \pm 5 % 0412-441 $0.47 \mathrm{~Jy}$ 0423-687 $0.238 \mathrm{~Jy}$ \pm 5 % 0424 - 728 $0.78 \text{ Jy} \pm 2 \%$ 0427-539 2 % 1.89 Jy0429-616 0.53 Jy1, -2 % 0435-587 $0.57 \mathrm{~Jy}$ $\pm 5\%$ 0437-662 0.69 Jy $\pm 5\%$

Fig. 1—Continued



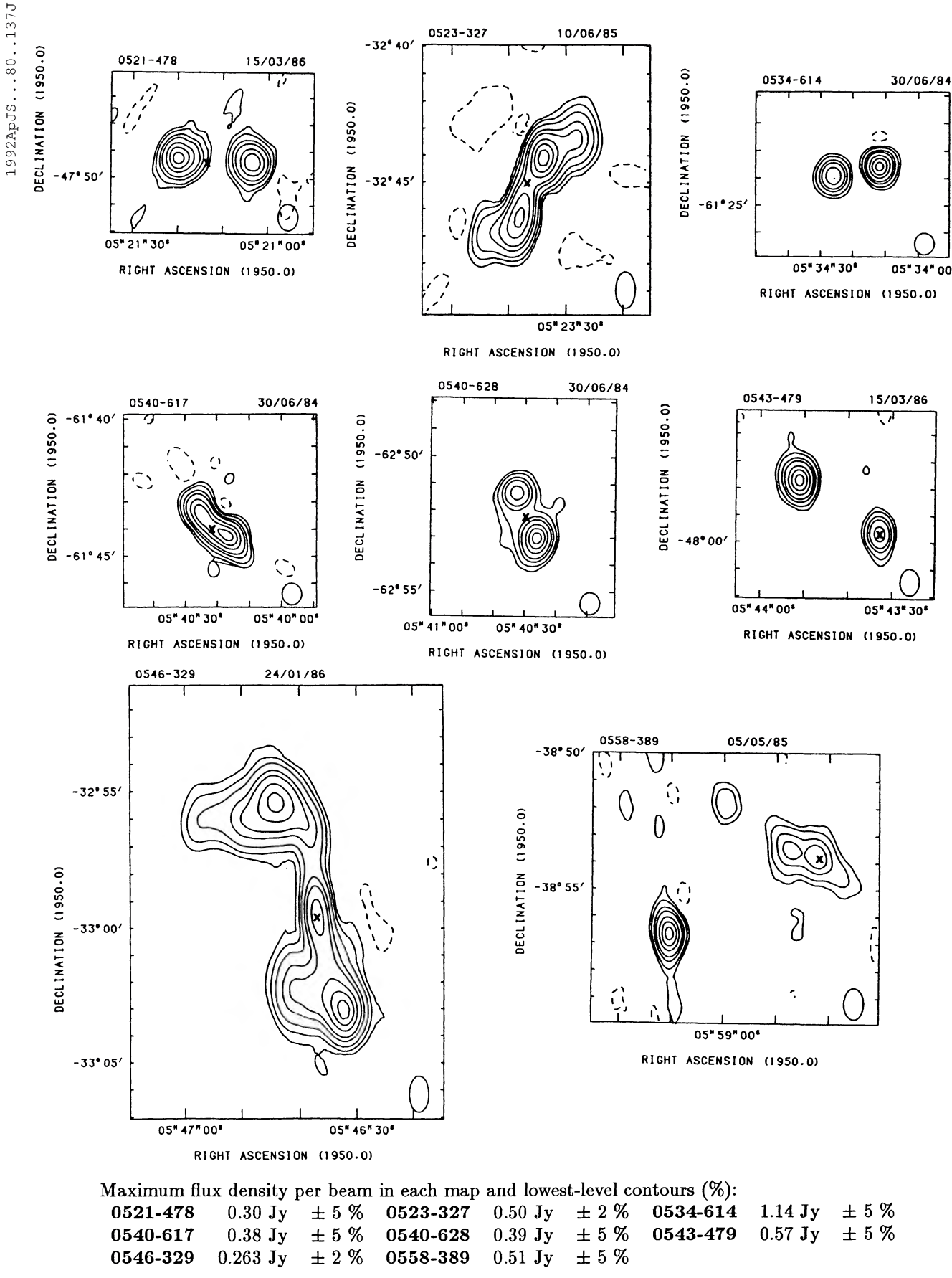


Fig. 1—Continued

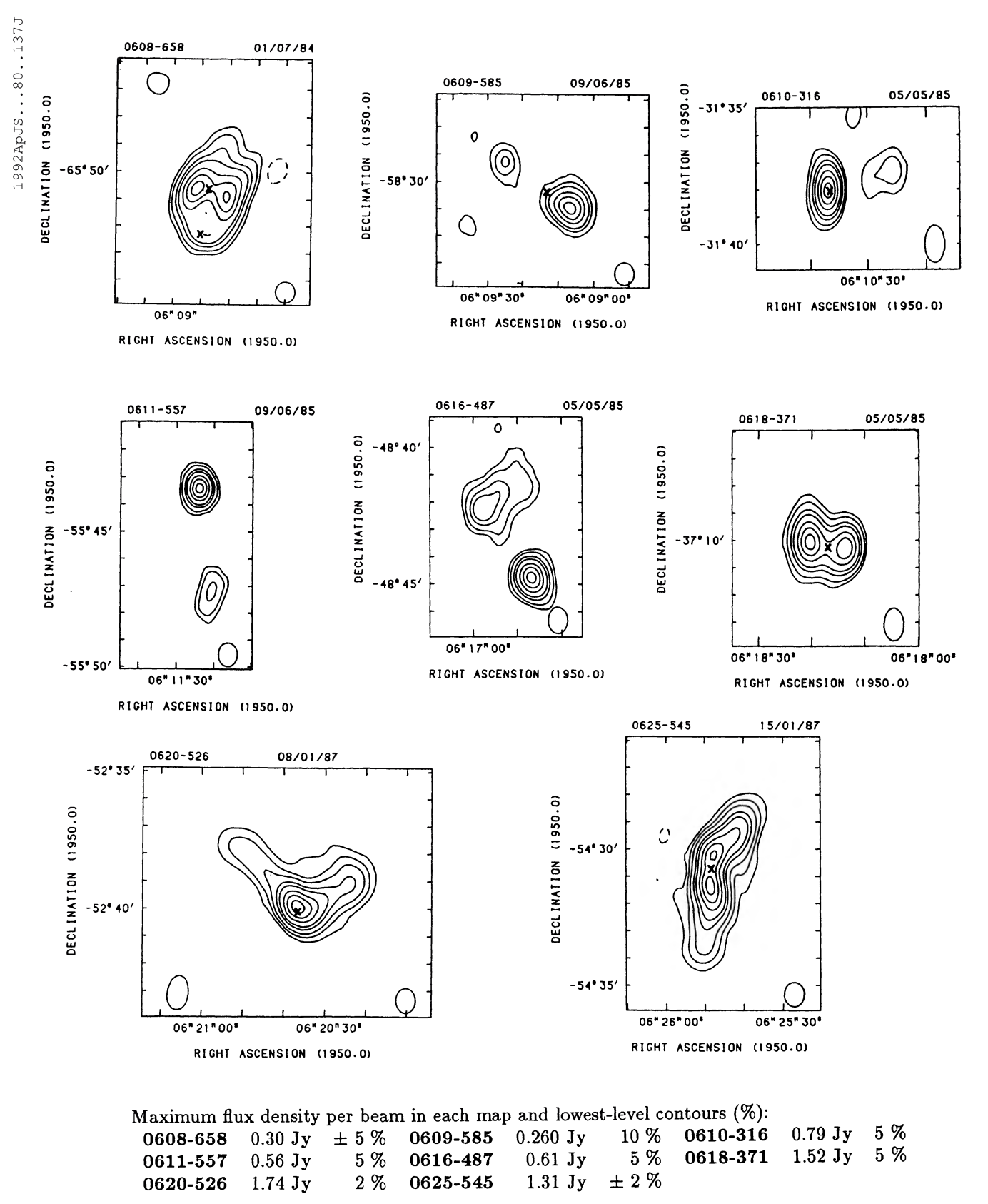


Fig. 1—Continued

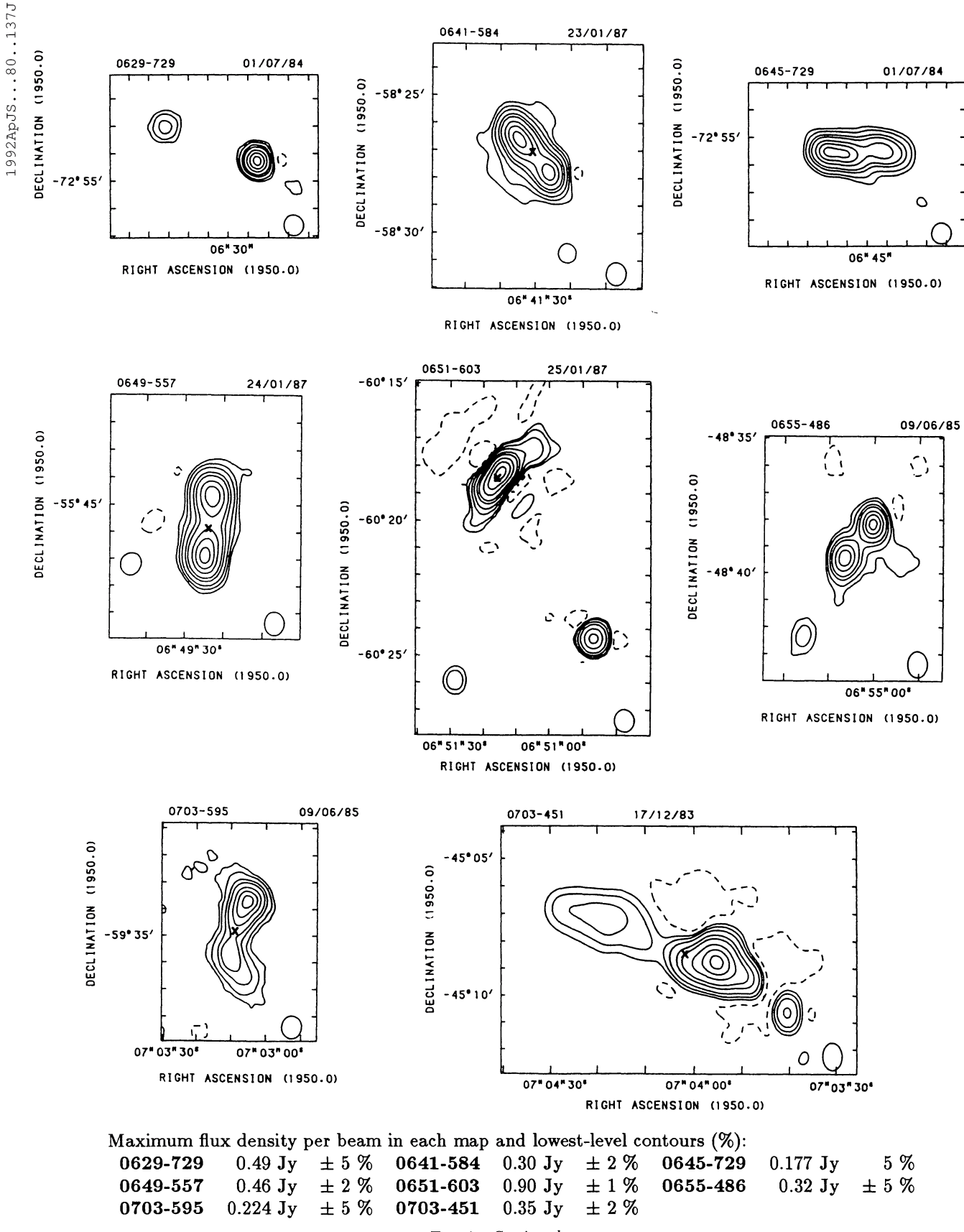
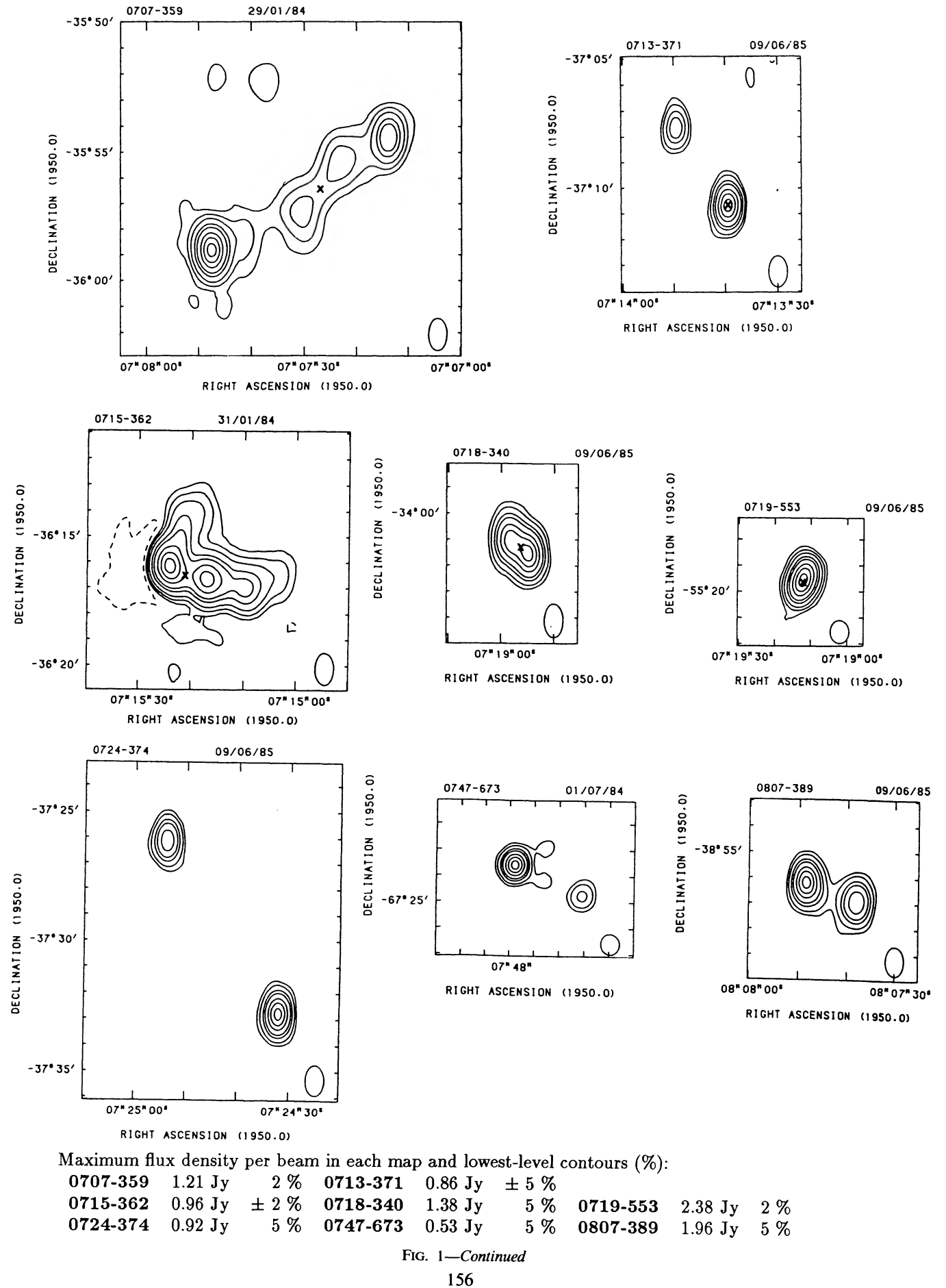
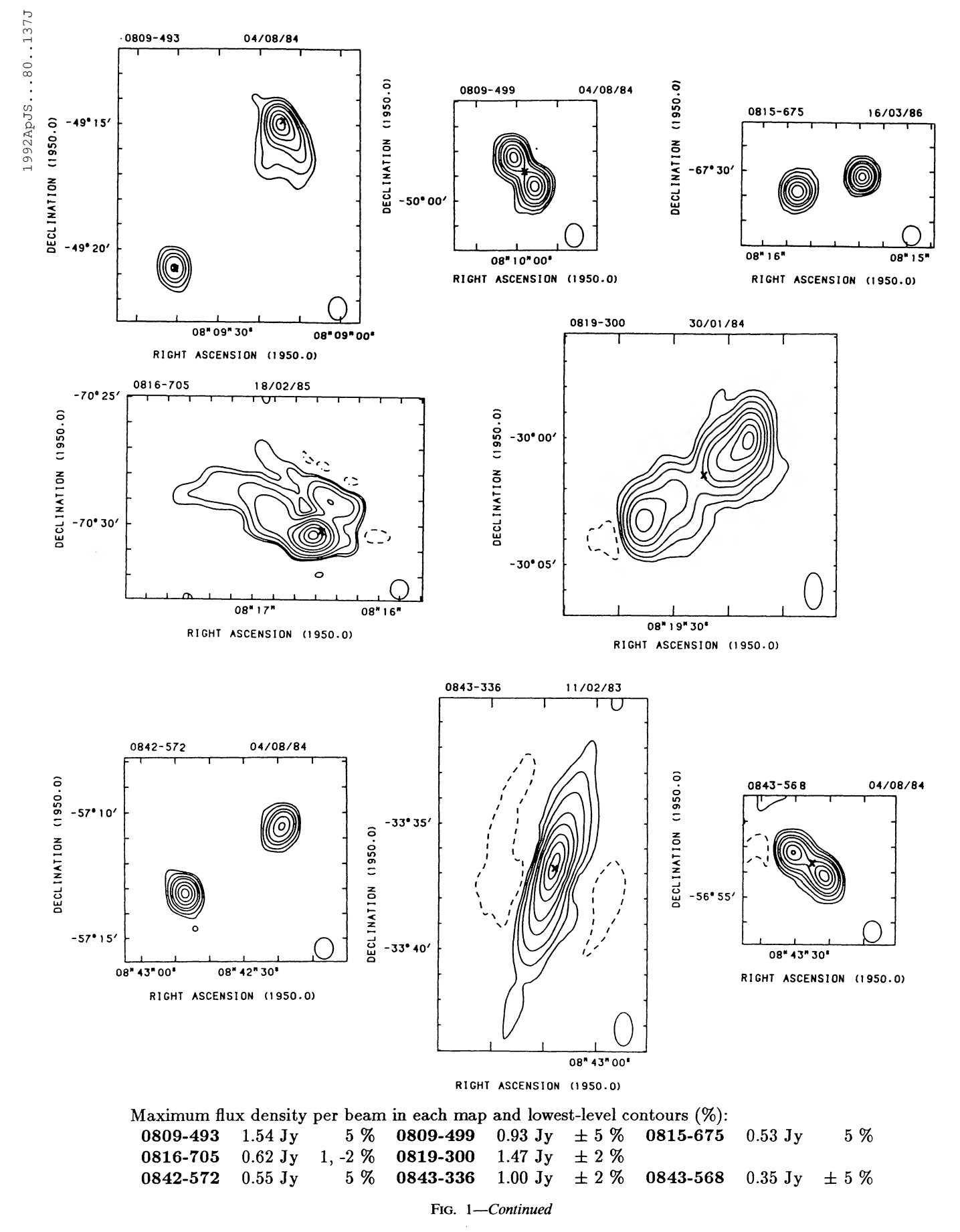
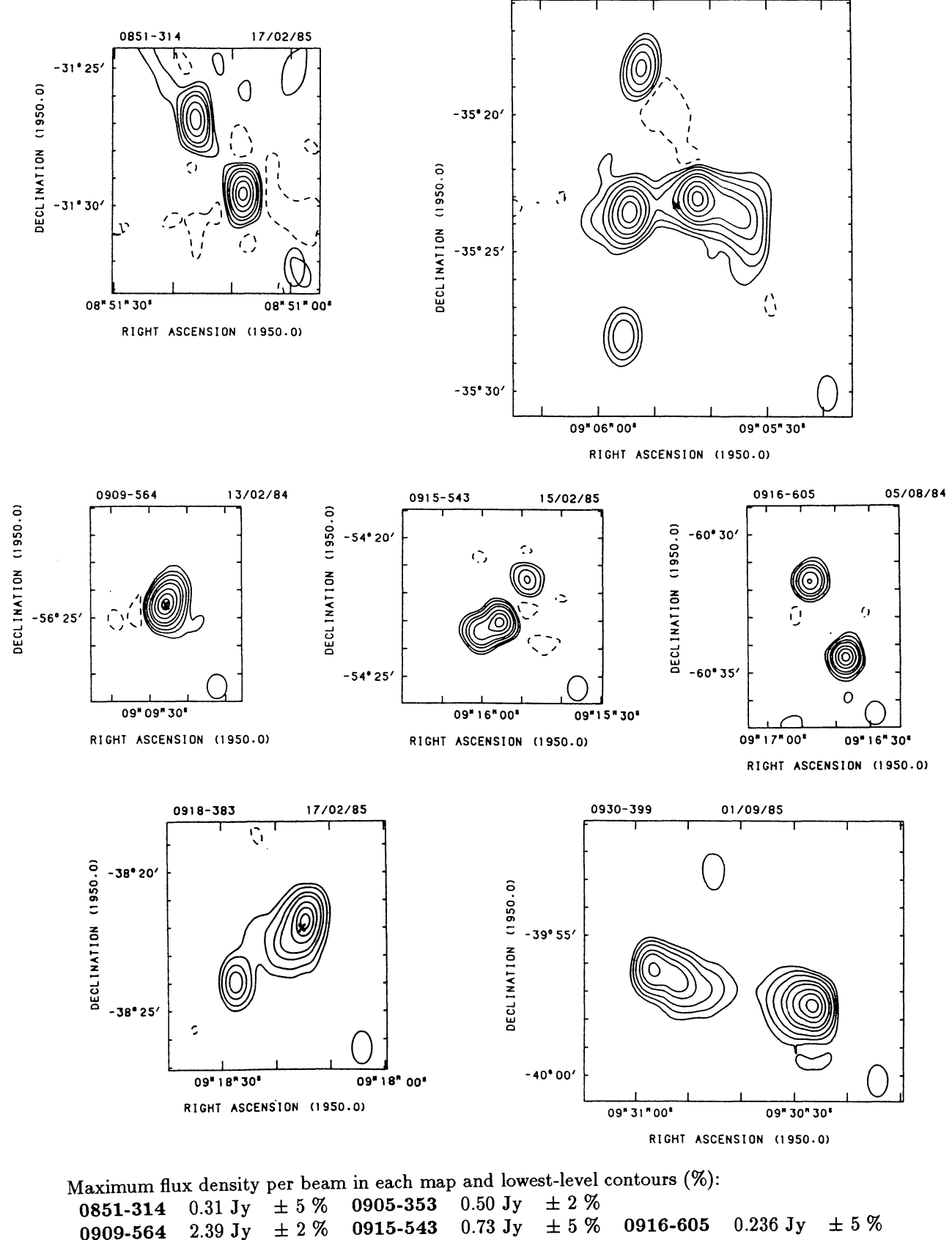


Fig. 1—Continued





157



07/07/85

0905-353

Fig. 1—Continued

0930-399

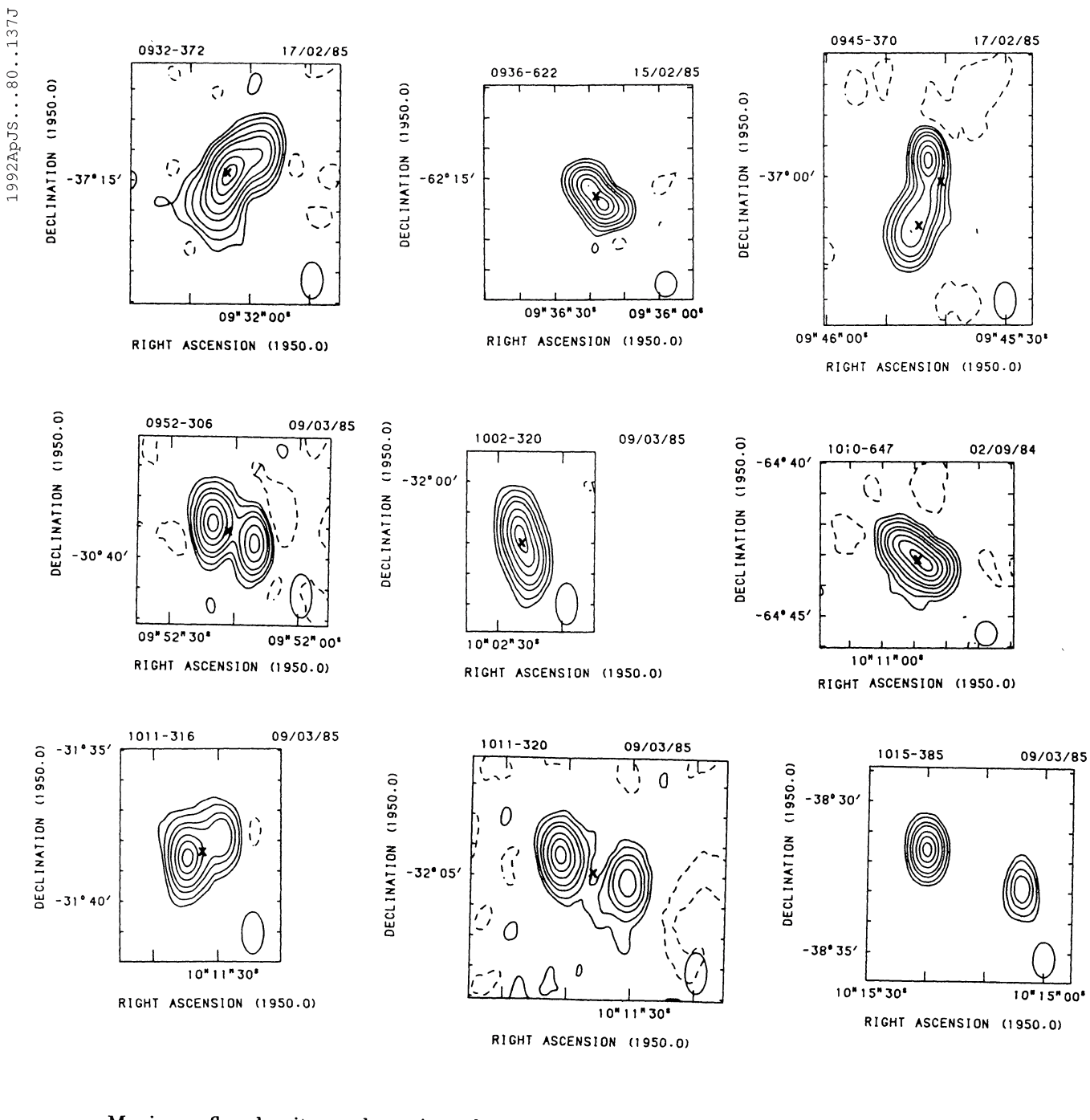
 \pm 5 %

0.48 Jy

0918-383

0.38 Jy

2 %



Maximum flux density per beam in each map and lowest-level contours (%): 0932-372 $0.54 \mathrm{~Jy}$ $\pm~2~\%$ 0936-622 $0.48 \,\mathrm{Jy}$ \pm 5 % 0945-370 0.32 Jy5, -2 % 0952 - 3060.44 Jy \pm 5 % 1002-320 0.74 Jy \pm 5 % 1010-647 1.77 Jy $\pm 2\%$ 1011-316 1.18 Jy \pm 5 % 1011-320 0.34 Jy±5% 0.61 Jy1015-385 5 %

FIG. 1—Continued

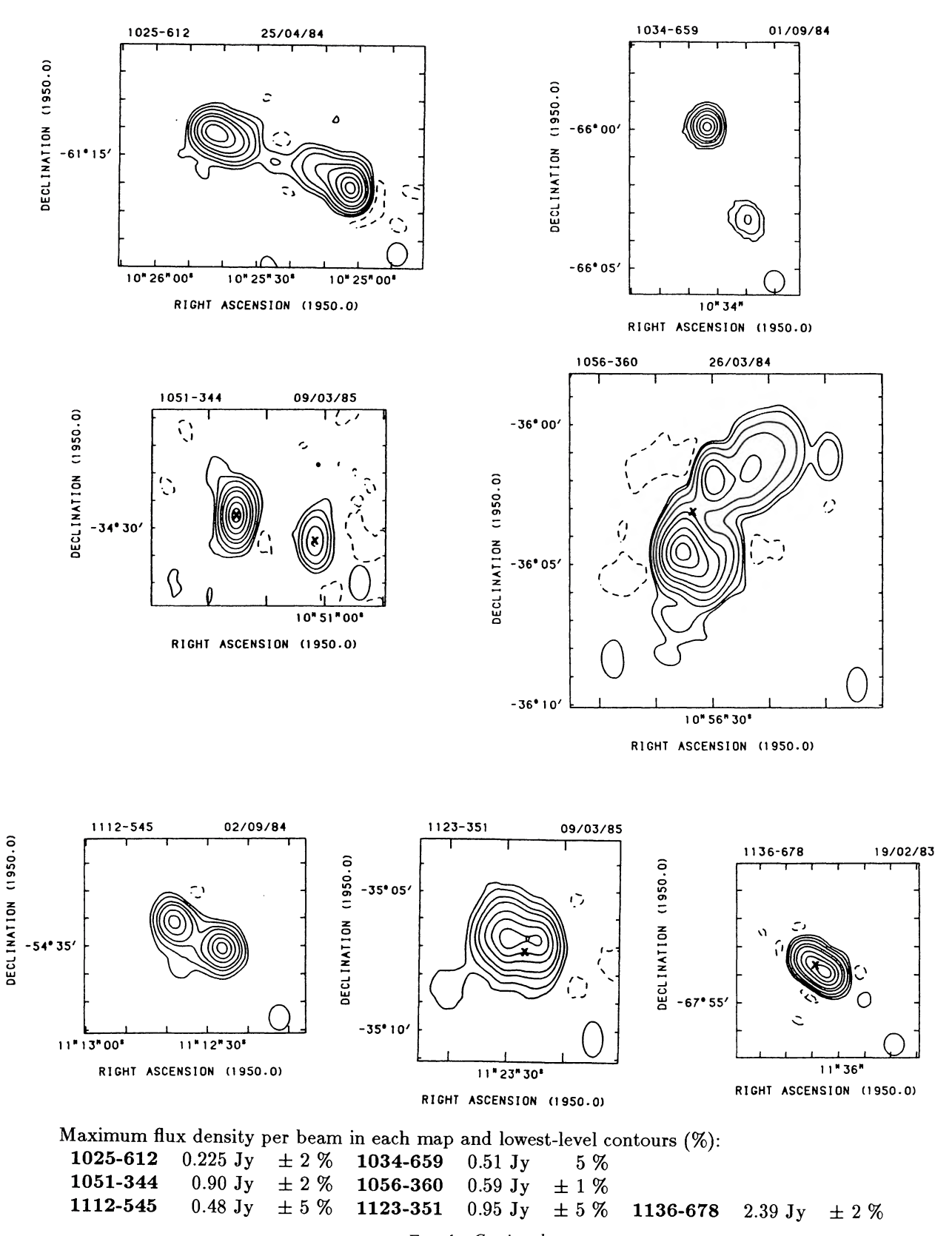
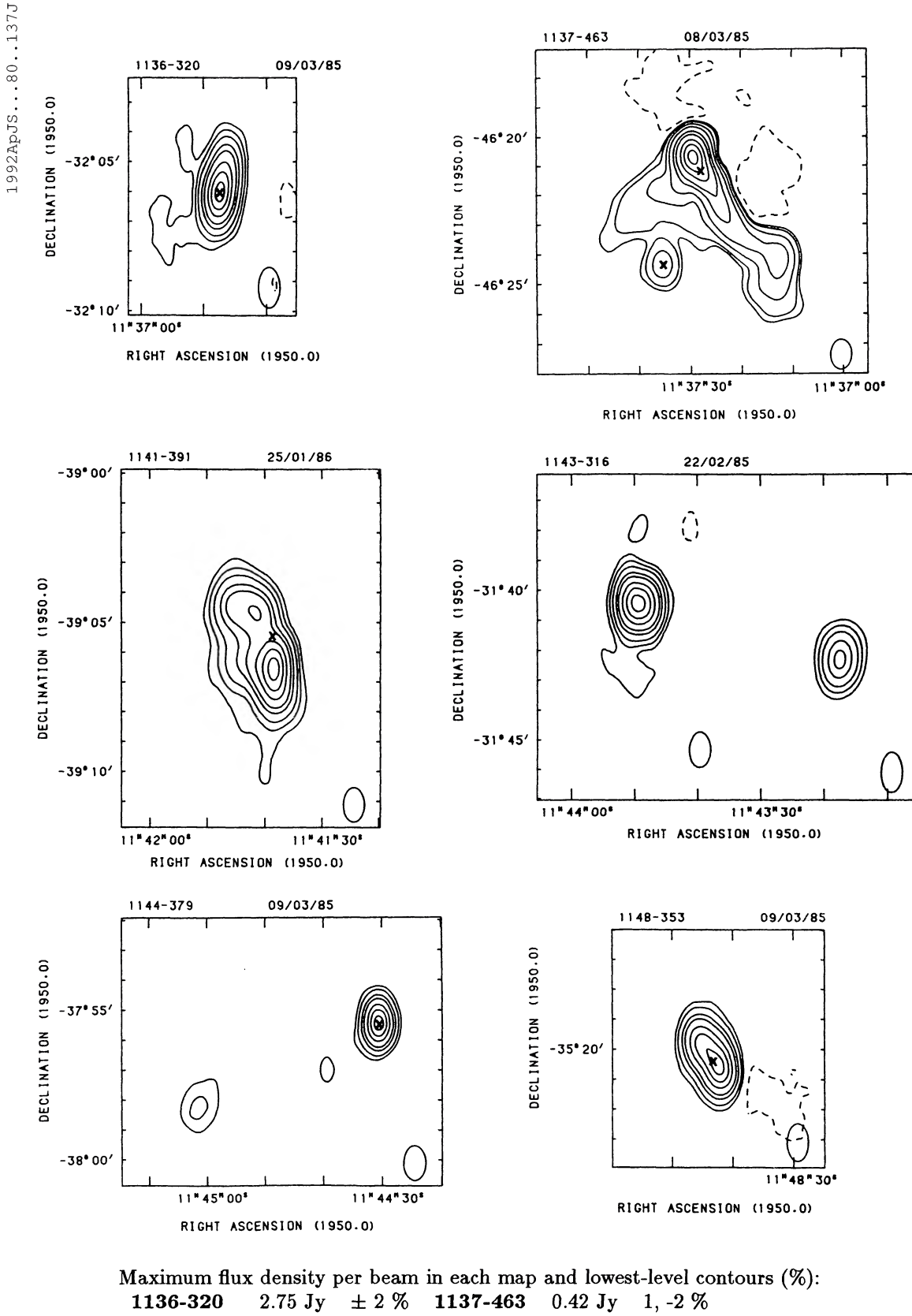


Fig. 1—Continued



1136-320 2.75 Jy $\pm 2\%$ 1137-463 0.42 Jy 1, -2 % 1141-391 0.170 Jy 2 % 1143-316 1.73 Jy $\pm 2\%$ 1144-379 1.69 Jy 5 % 1148-353 0.97 Jy $\pm 5\%$

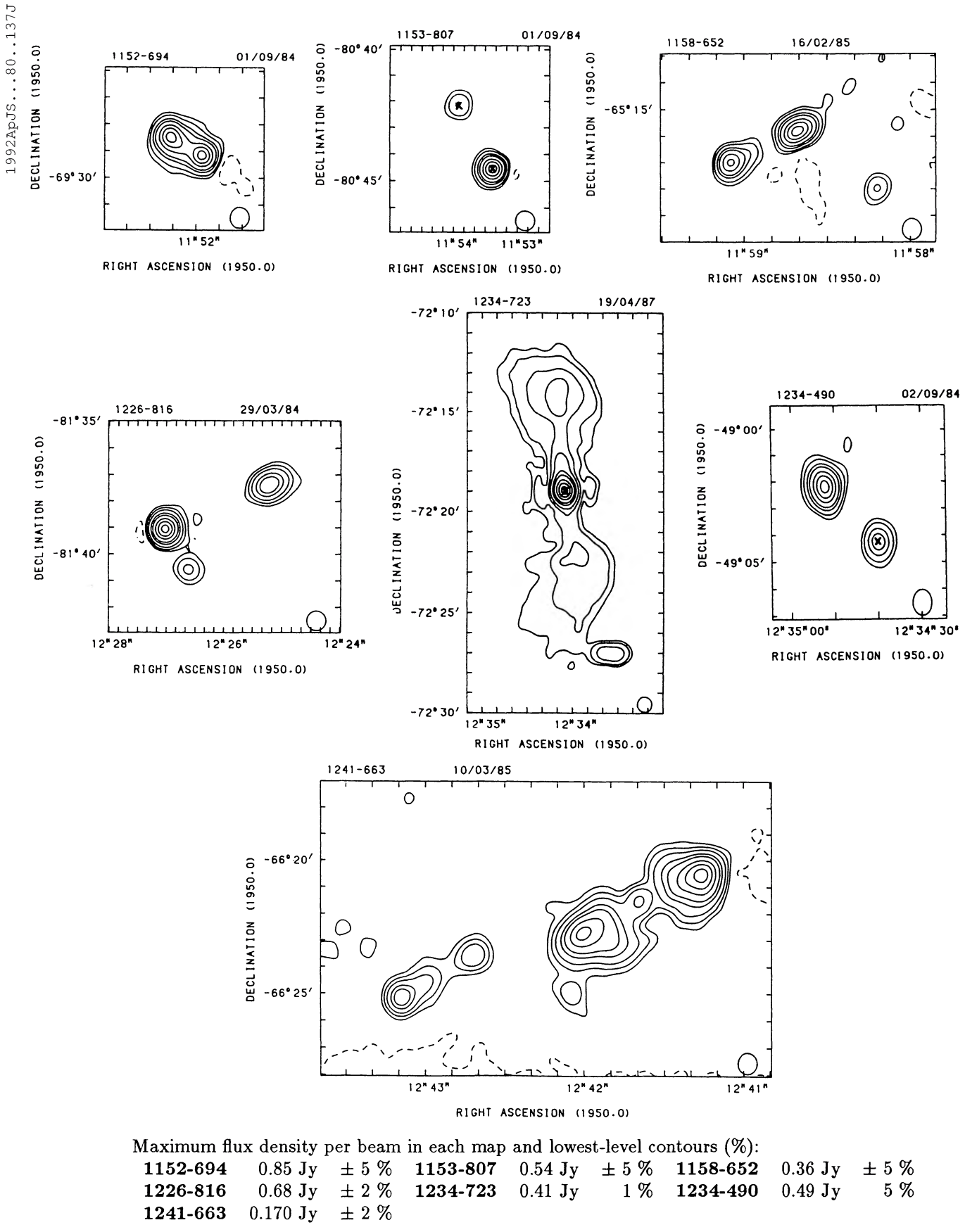
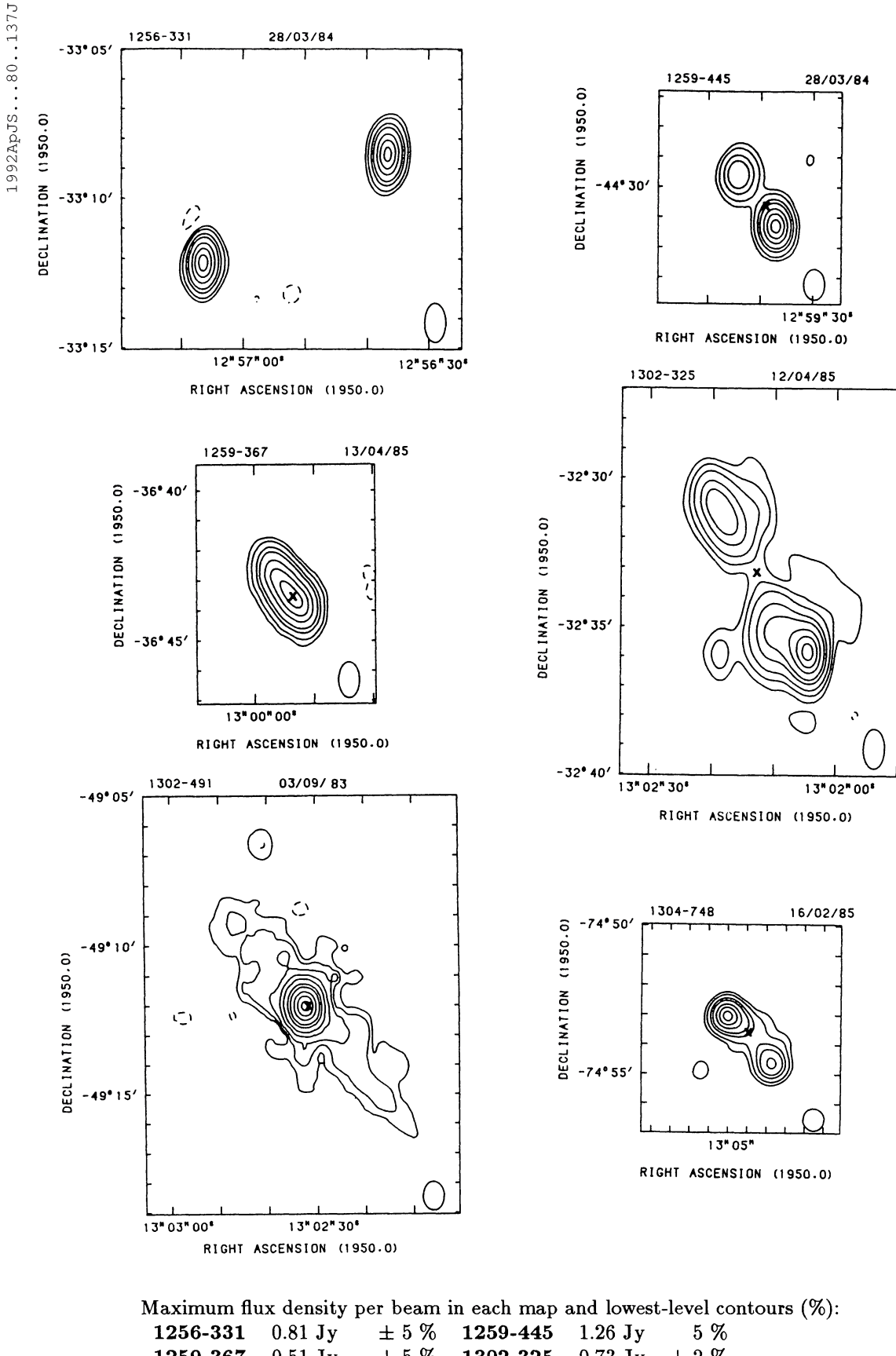
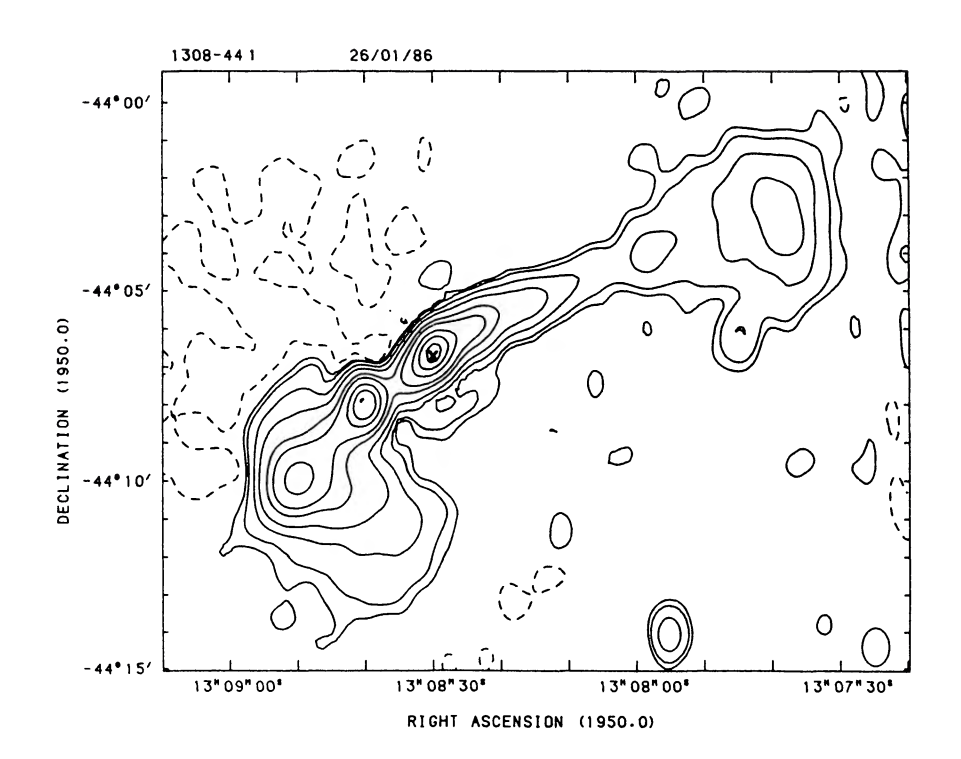
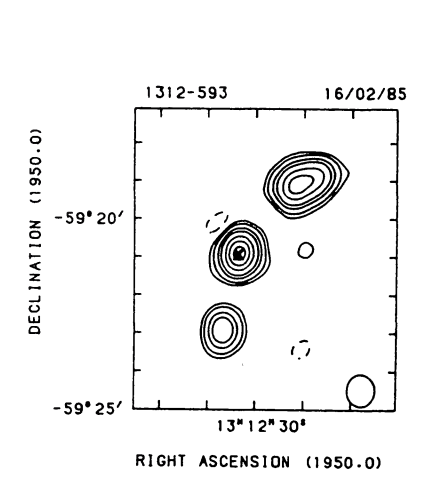


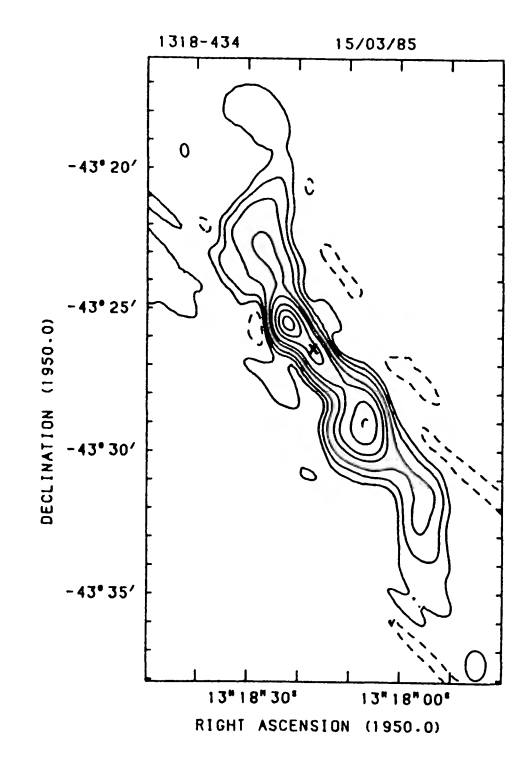
Fig. 1—Continued



1256-331	$0.81 \; \mathbf{Jy}$	\pm 5 %	1259-445	$1.26 \mathrm{Jy}$	5 %
1259-367	$0.51 \mathrm{~Jy}$	\pm 5 %	1302-325	$0.73 \mathrm{~Jy}$	$\pm~2~\%$
1302-491	5 3 Tv	$\pm 0.5\%$	1304-748	0.35 Ty	5 %

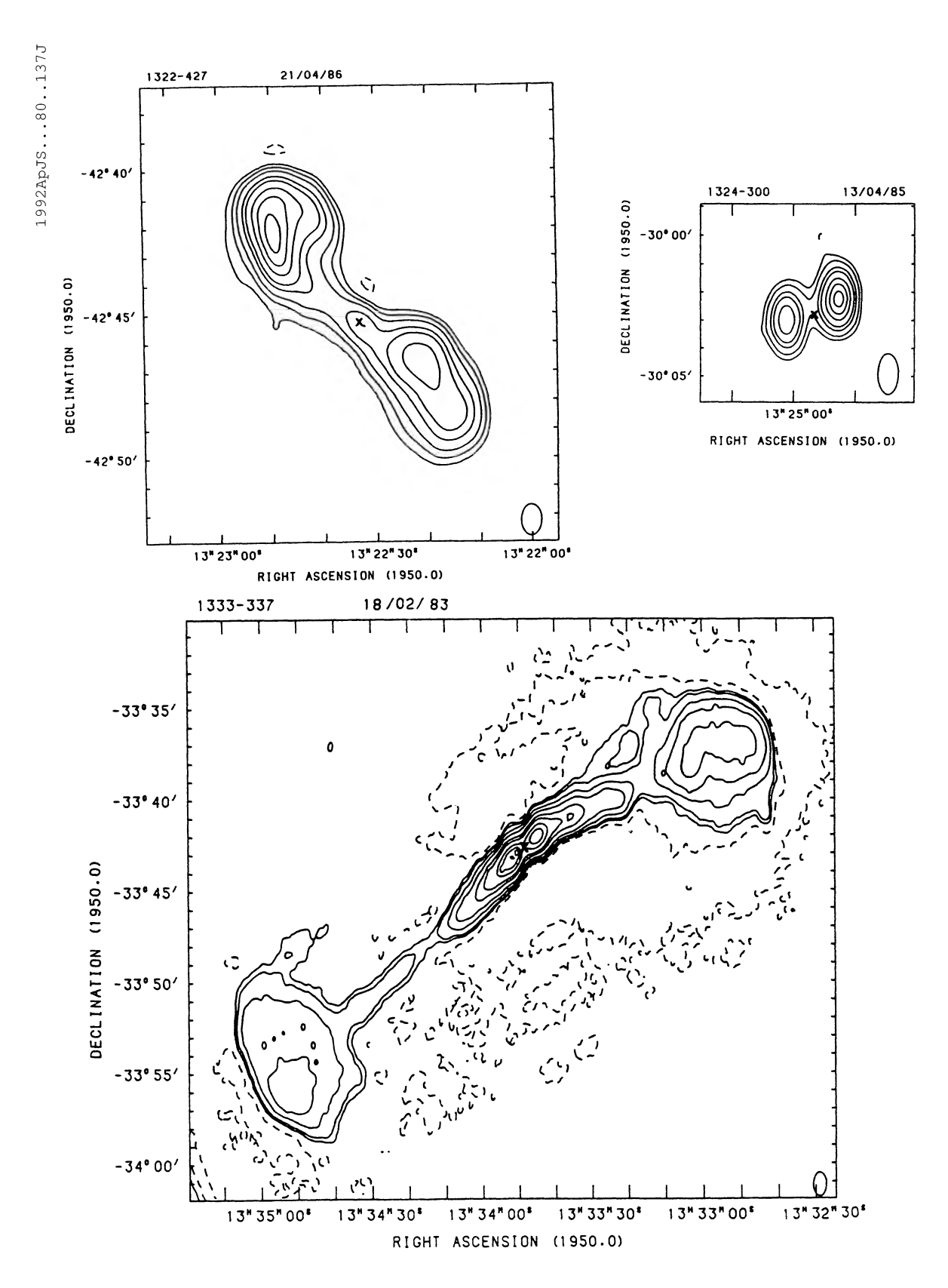






1308-441 0.223 Jy $\pm 1 \%$

1312-593 $0.45 \text{ Jy} \pm 5 \%$ 1318-434 $0.99 \text{ Jy} \pm 2 \%$



Maximum flux density per beam in each map and lowest-level contours (%): 1322-427 37 Jy \pm 2 % 1324-300 0.85 Jy 5 % 1333-337 1.11 Jy \pm 1 %

Fig. 1—Continued

Fig. 1—Continued

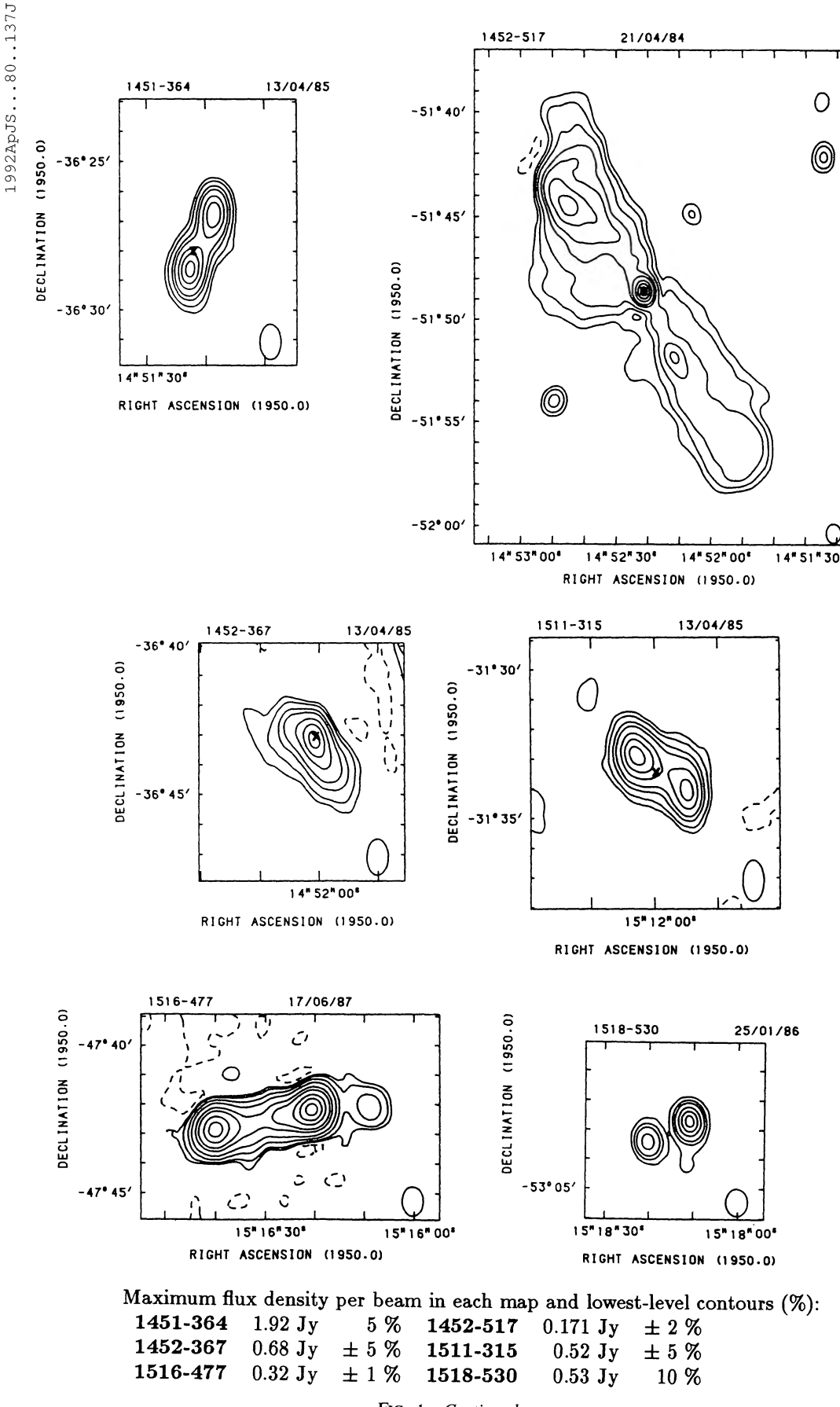
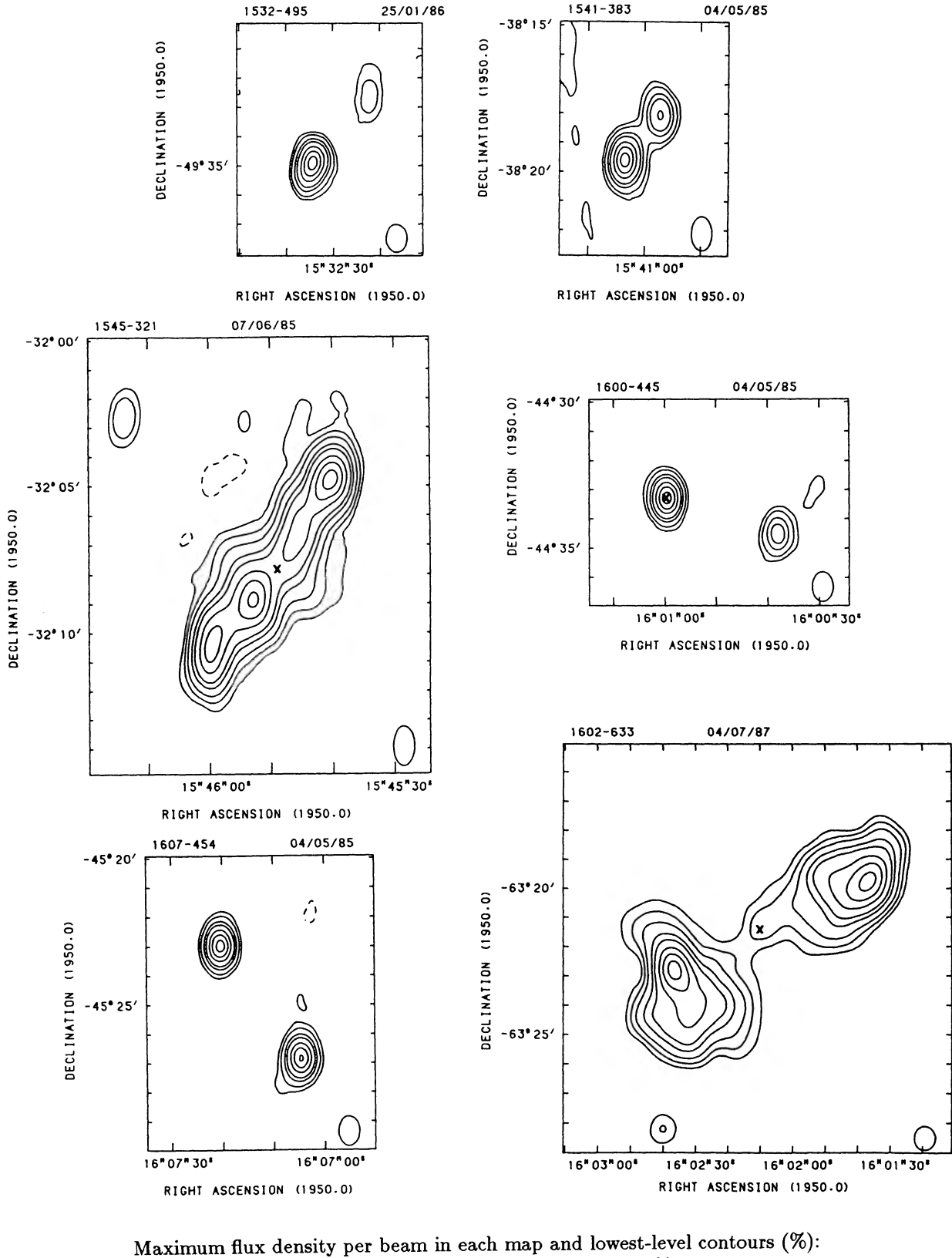


Fig. 1—Continued



0.55 Jy $0.43 \mathrm{Jy}$ $\pm~5~\%$ 1541-383 1532-495 ± 2 % 1600-445 1.14 Jy 5 % 0.32 Jy1545-321 0.74 Jy2 % $\pm 5\%$ 1602-633 $0.76 \mathrm{~Jy}$ 1607-454

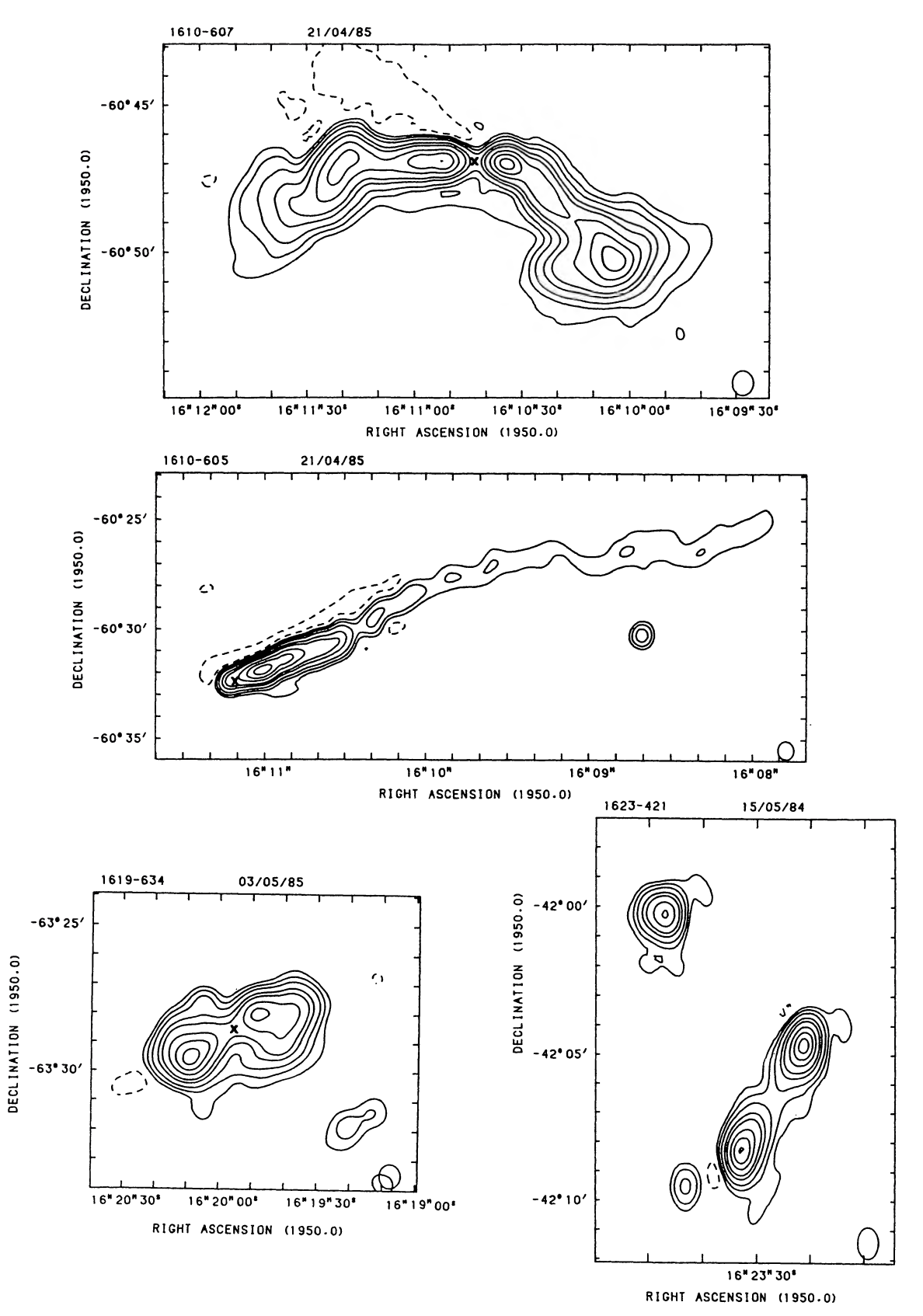
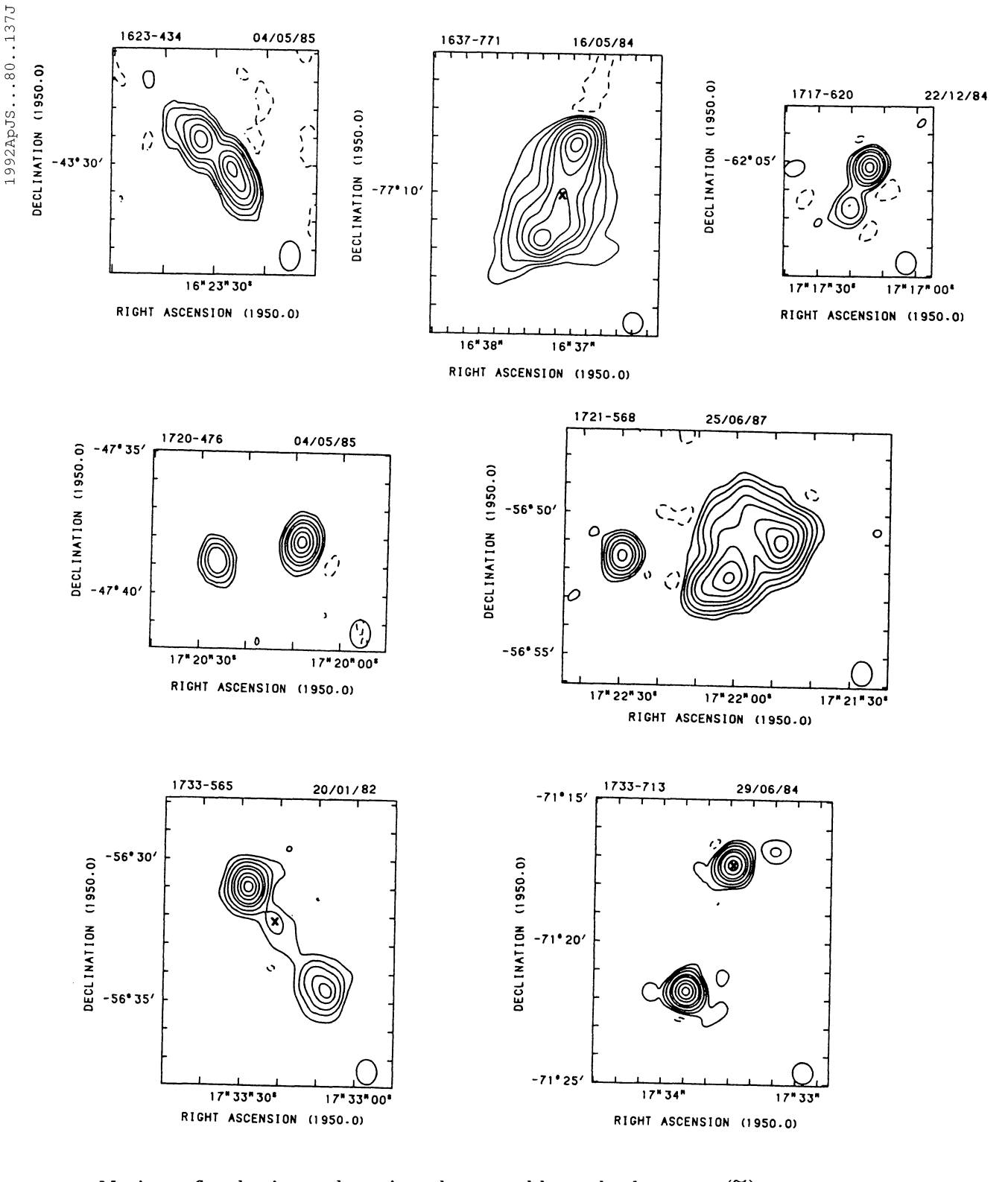


FIG. 1—Continued



 $\pm 2\%$ 1717-620 0.71 Jy $0.292 \text{ Jy} \pm 5 \%$ 1637-771 1623-434 1.12 Jy \pm 5 % 1720-476 0.34 Jy1721-568 0.107 Jy± 2 % 1733-565 5.8 Jy $\pm 2\%$ 1733-713 0.88 Jy $\pm 2\%$

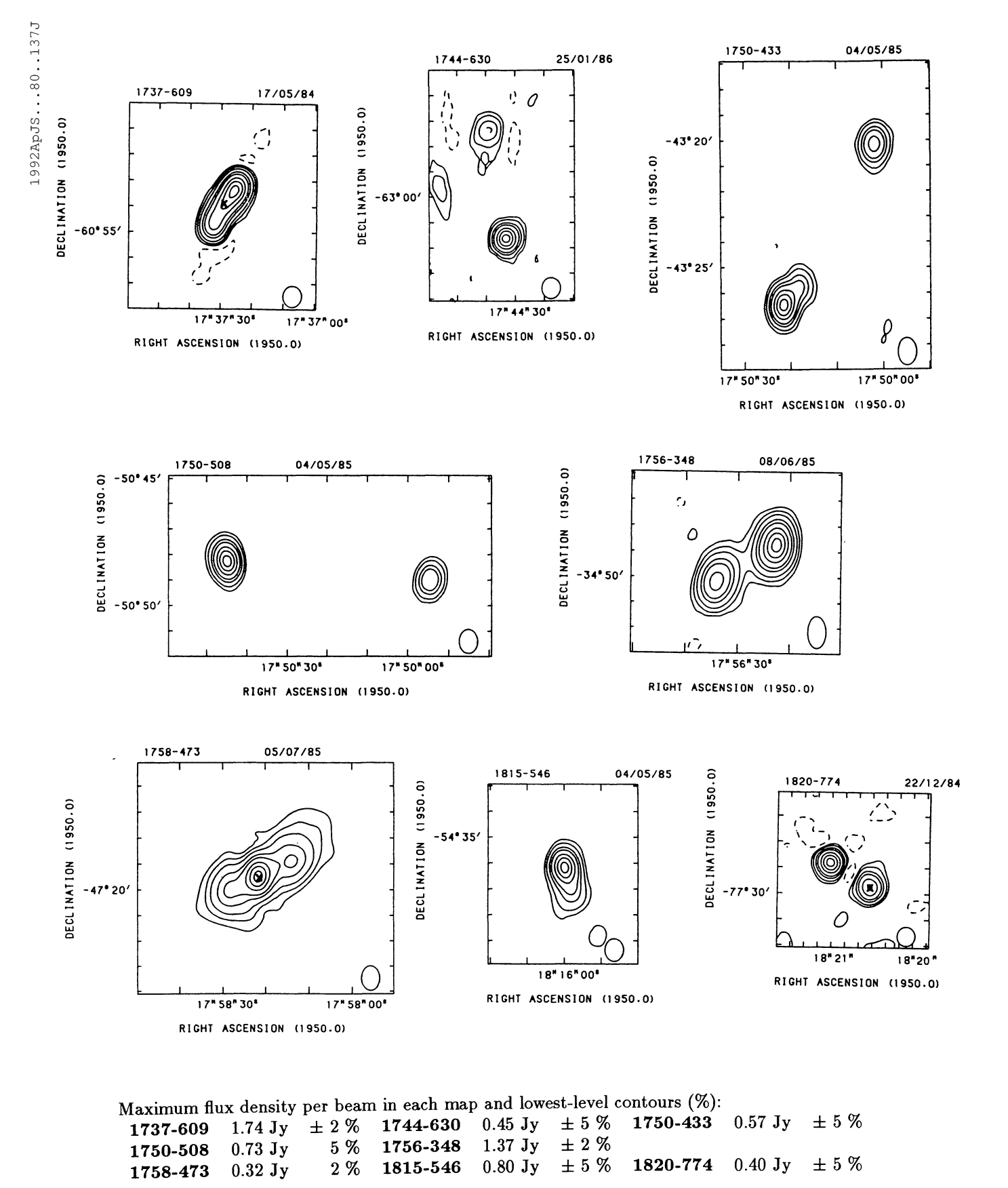
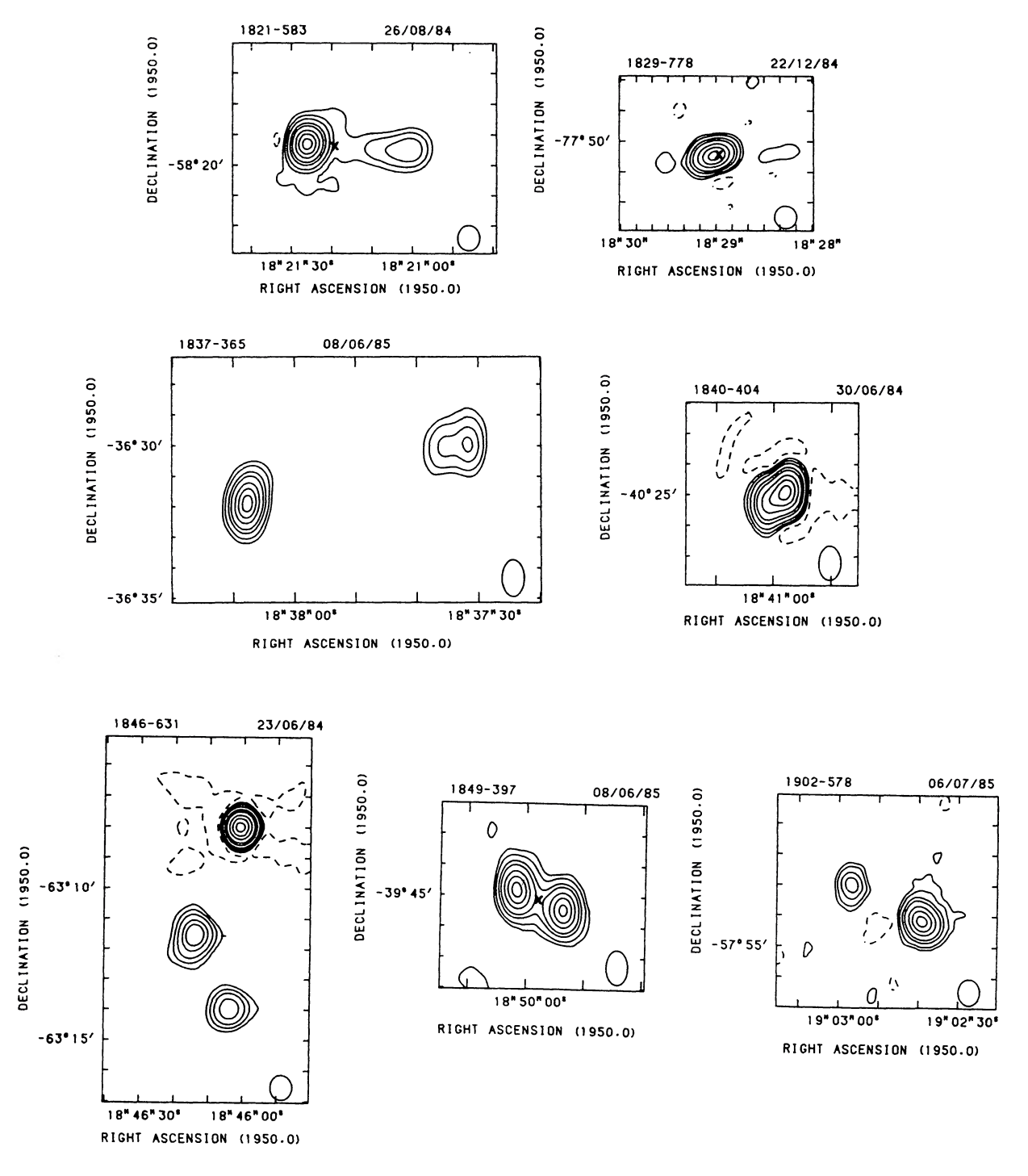
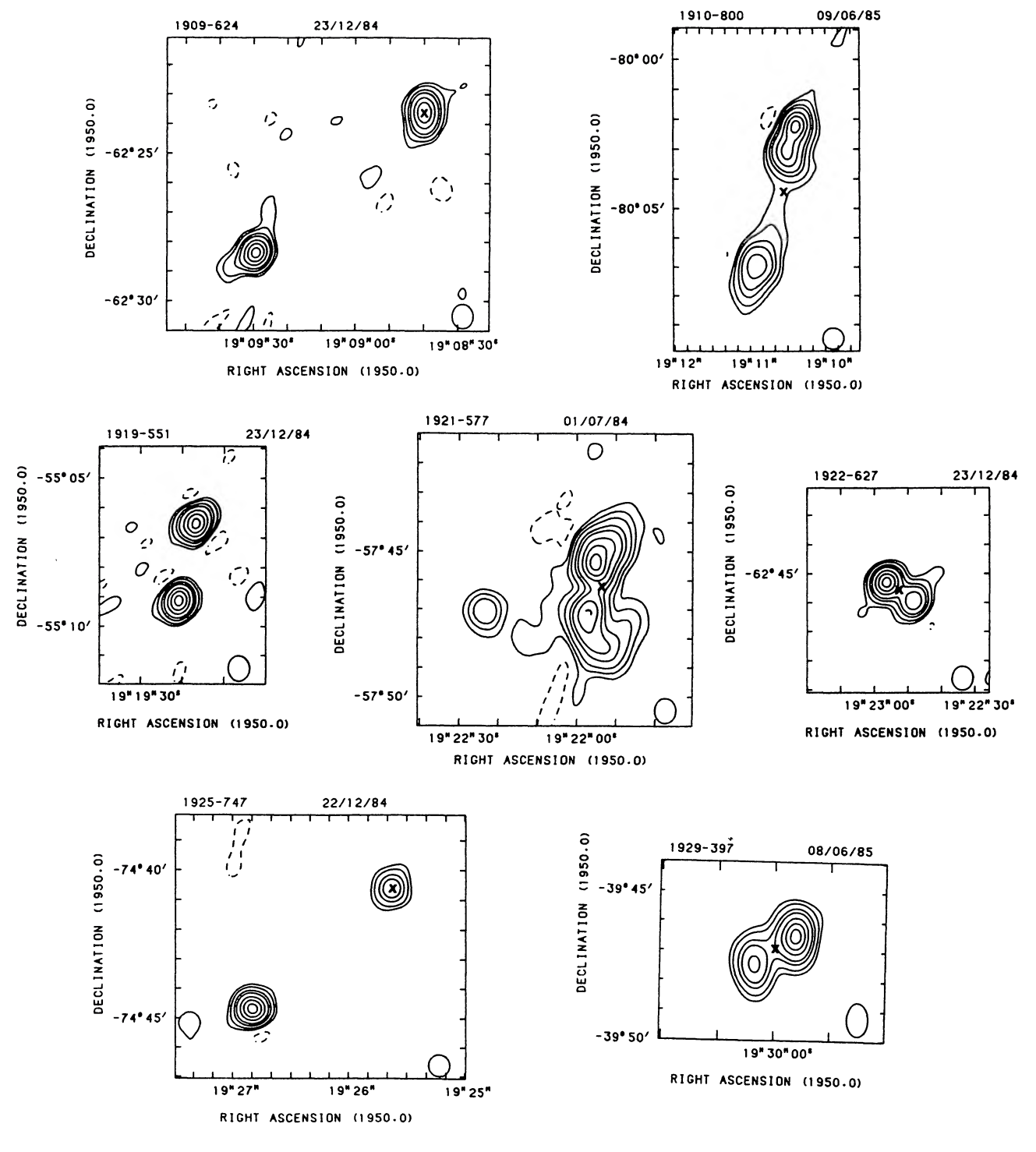


Fig. 1—Continued



 $1.52 \mathrm{~Jy}$ $\pm~2~\%$ 1821-583 1829-778 $0.52 \text{ Jy} \pm 5 \%$ 5 % 1837-365 0.92 Jy1840-404 2.52 Jy $\pm 2\%$ 1846-631 1.10 Jy $\pm 2\%$ 1849-397 0.36 Jy5 % 1902-578 $0.243 \text{ Jy} \pm 5 \%$

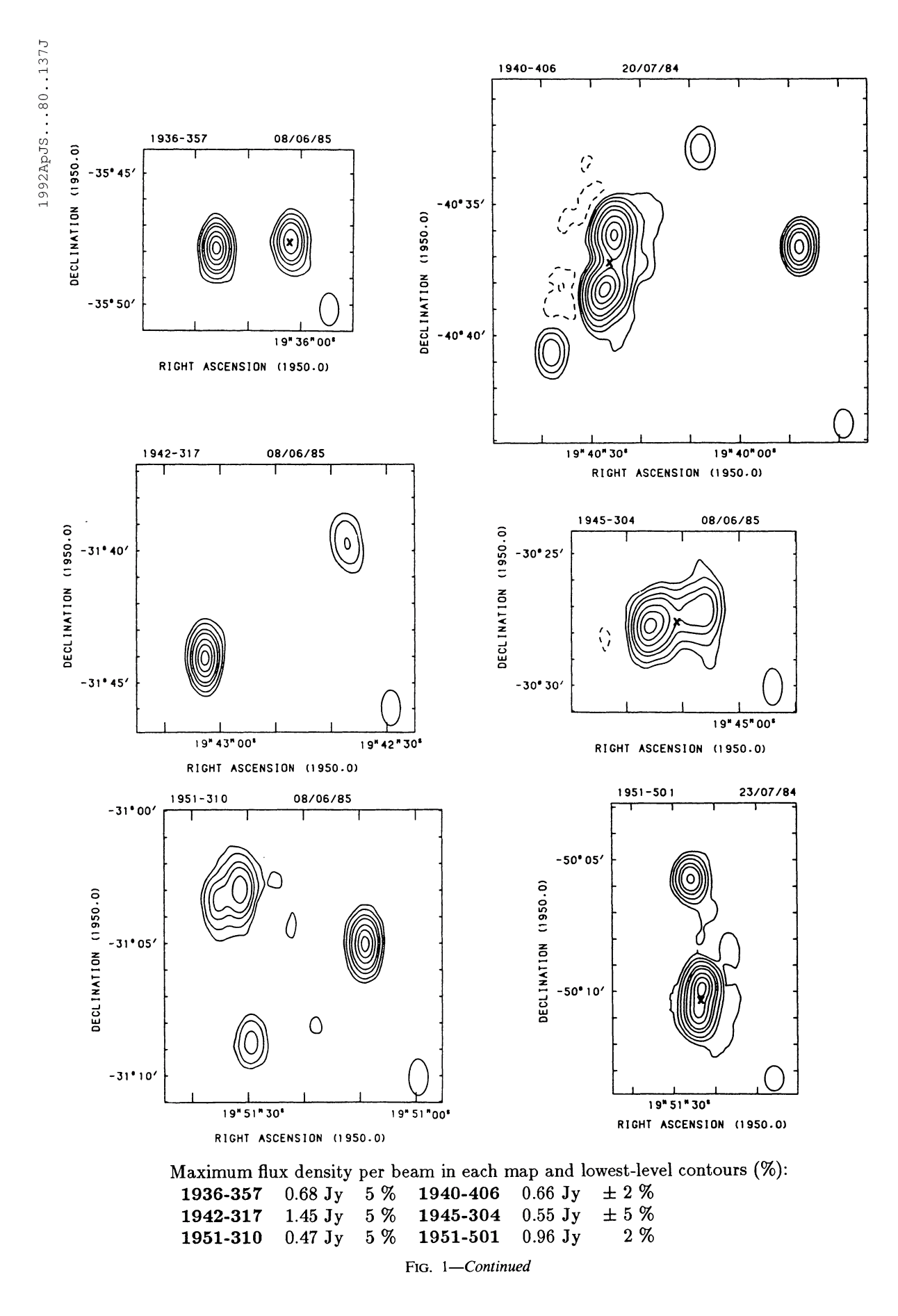
Fig. 1—Continued



Maximum flux density per beam in each map and lowest-level contours (%):

1909-624 0.38 Jy $\pm 5\%$ 1910-800 $0.33 \, \mathrm{Jy}$ $\pm~5~\%$ \pm 2 % \pm 5 % 1922-627 1.48 Jy $\pm 5 \%$ 1919-551 0.44 Jy1921-577 0.40 Jy1925-747 $0.67 \text{ Jy} \pm 5 \%$ 1929-397 2.13 Jy 5 %

Fig. 1—Continued



174

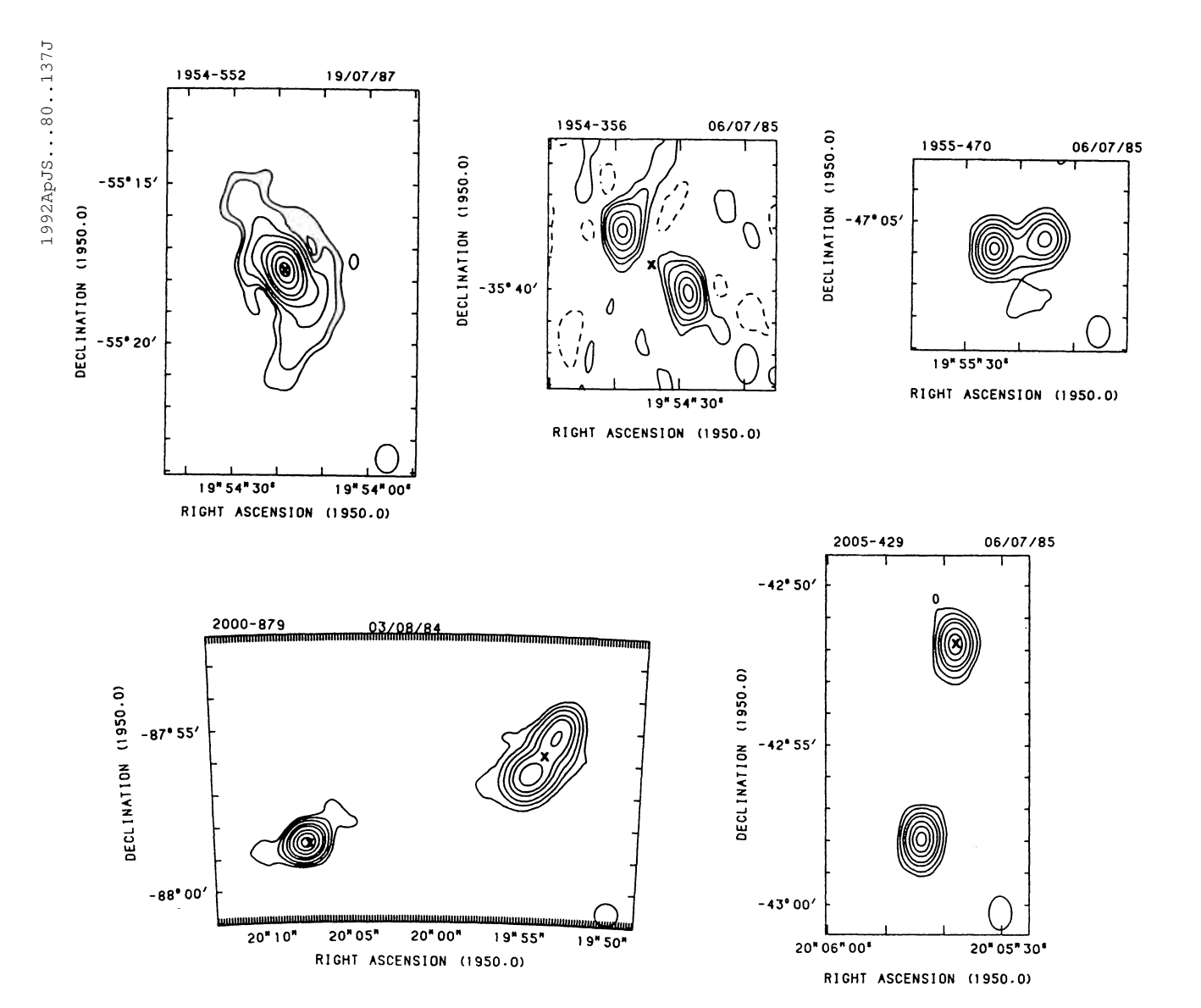
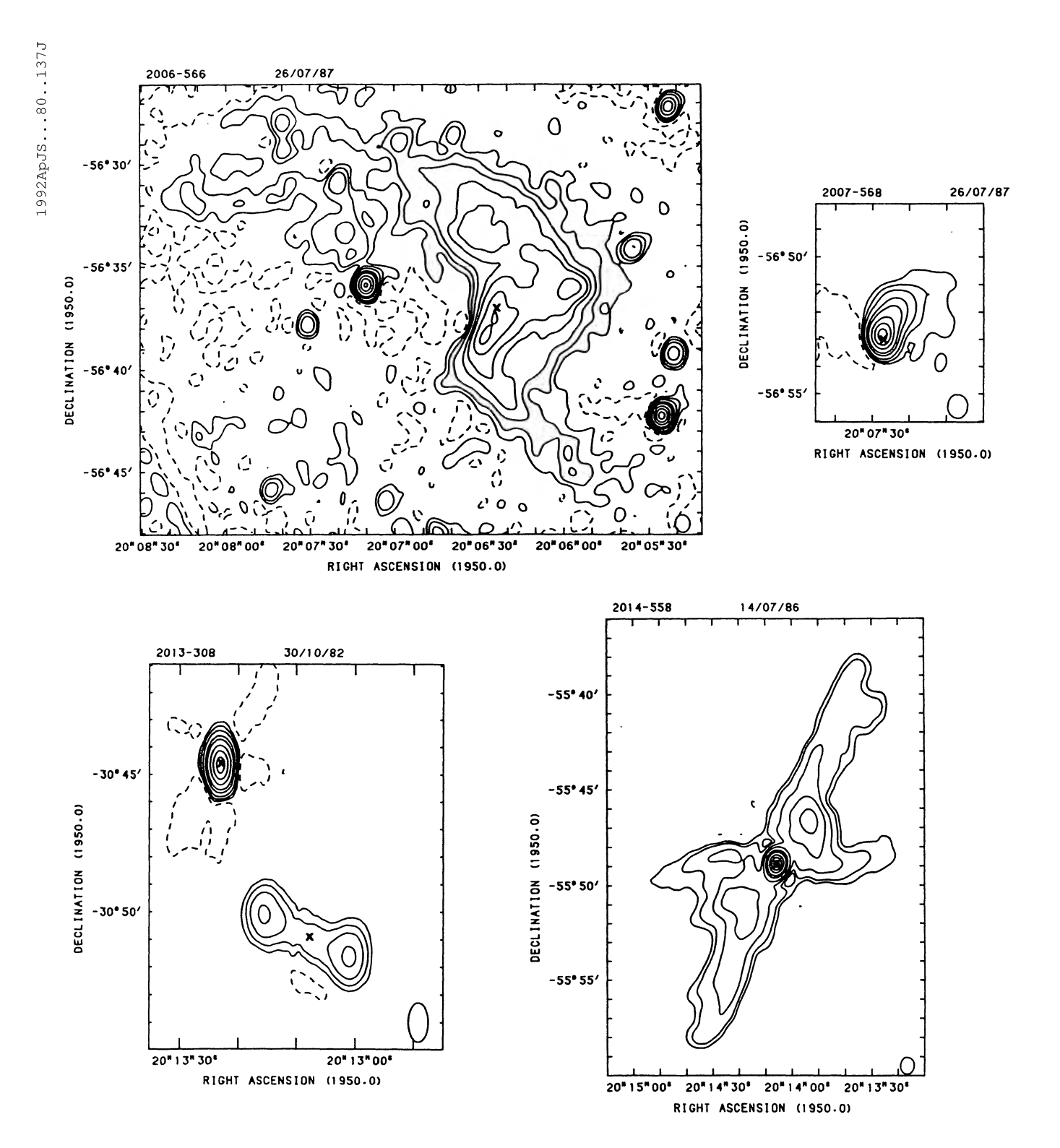
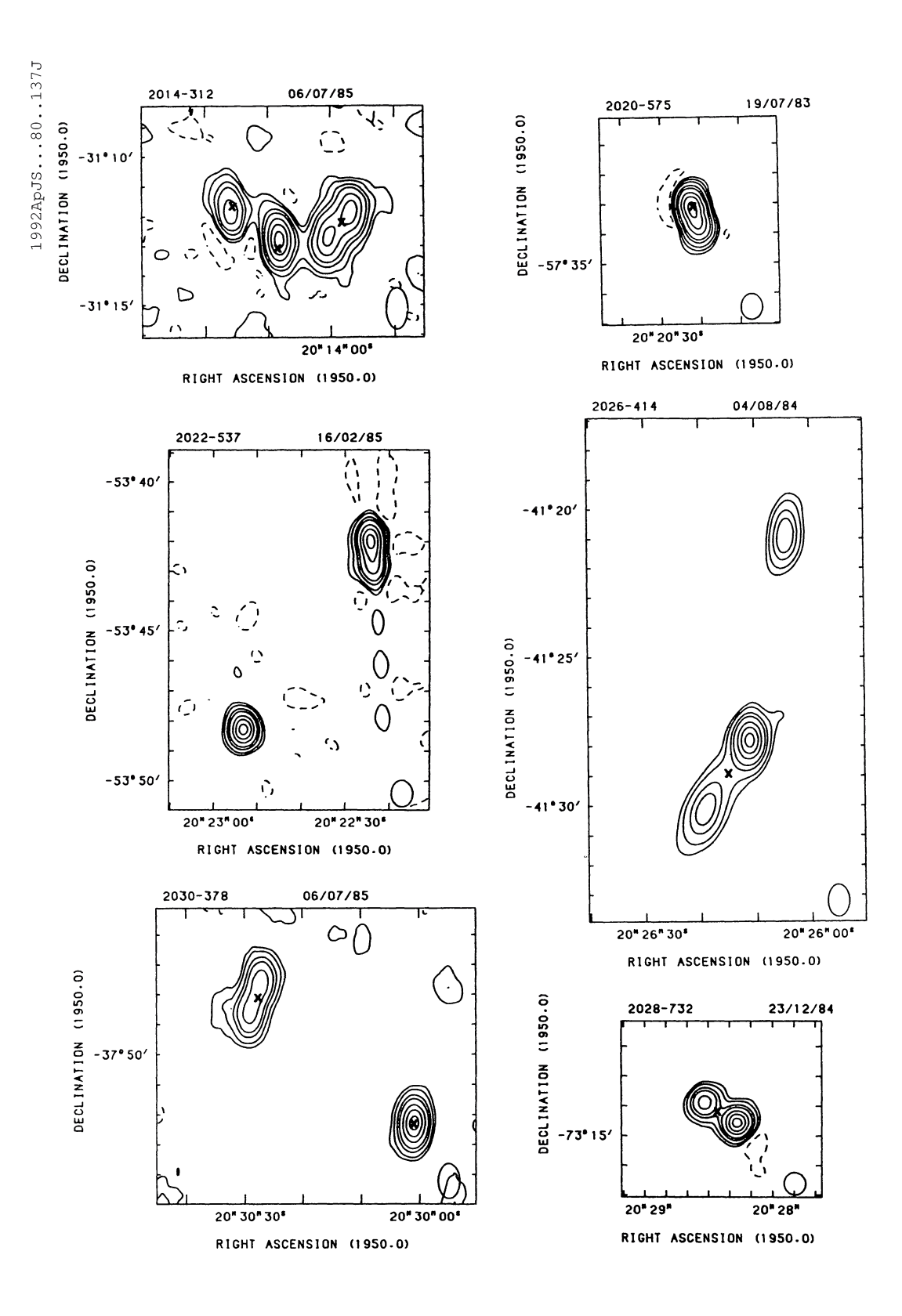


Fig. 1—Continued



Maximum flux density per beam in each map and lowest-level contours (%): 2006-566 0.076 Jy ± 2 % 2007-568 0.42 Jy ± 2 % 2013-308 1.25 Jy ± 2 % 2014-558 0.37 Jy ± 1 %

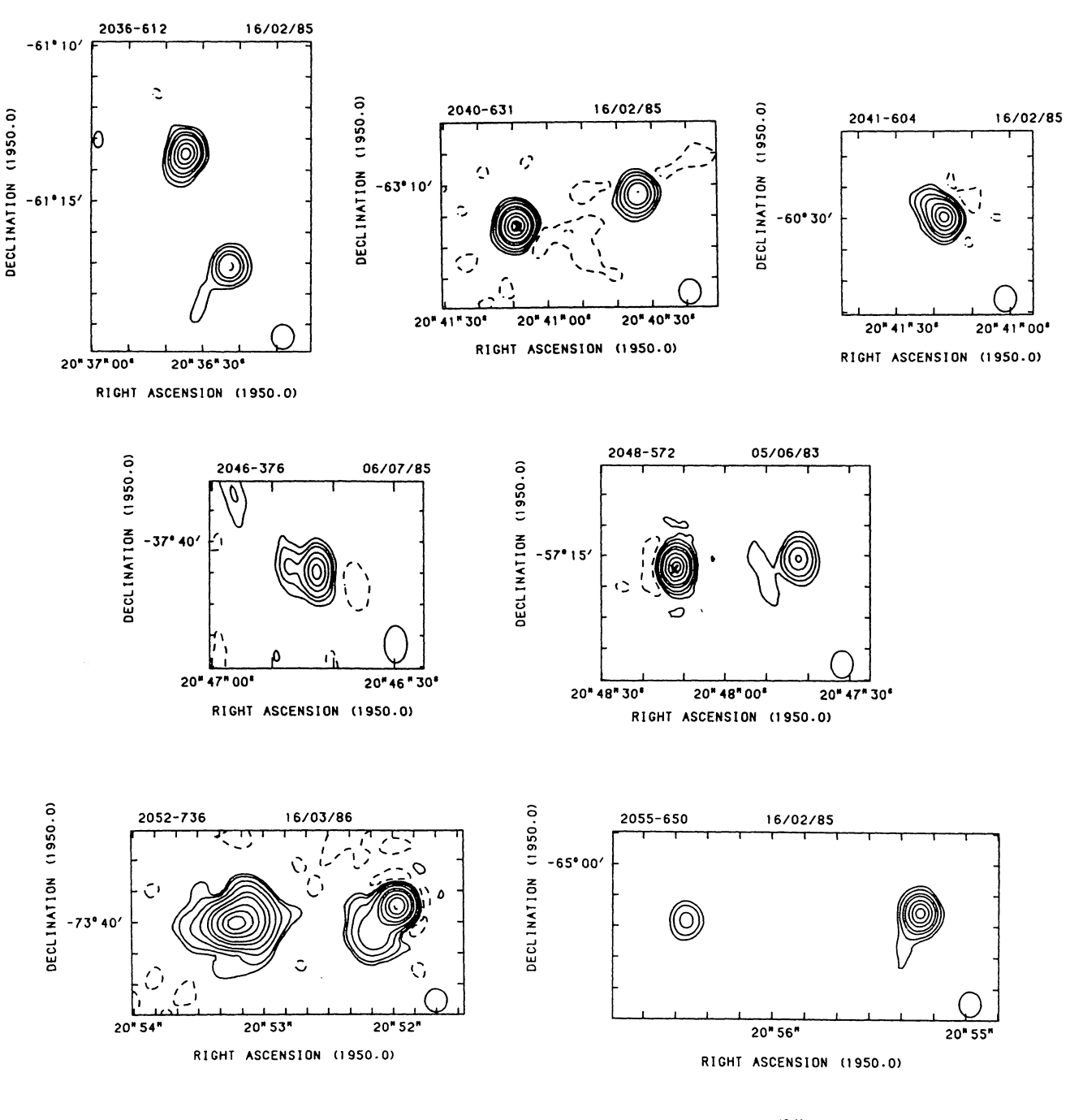
Fig. 1—Continued



Maximum flux density per beam in each map and lowest-level contours (%):

0.35 Jy \pm 5 % 2014-312 2020-575 3.1 Jy \pm 2 % \pm 5 % 0.73 Jy 5 % 2022-537 0.37 Jy2026-414 \pm 5 % 2030-378 0.32 Jy \pm 5 % 2028-732 1.15 Jy

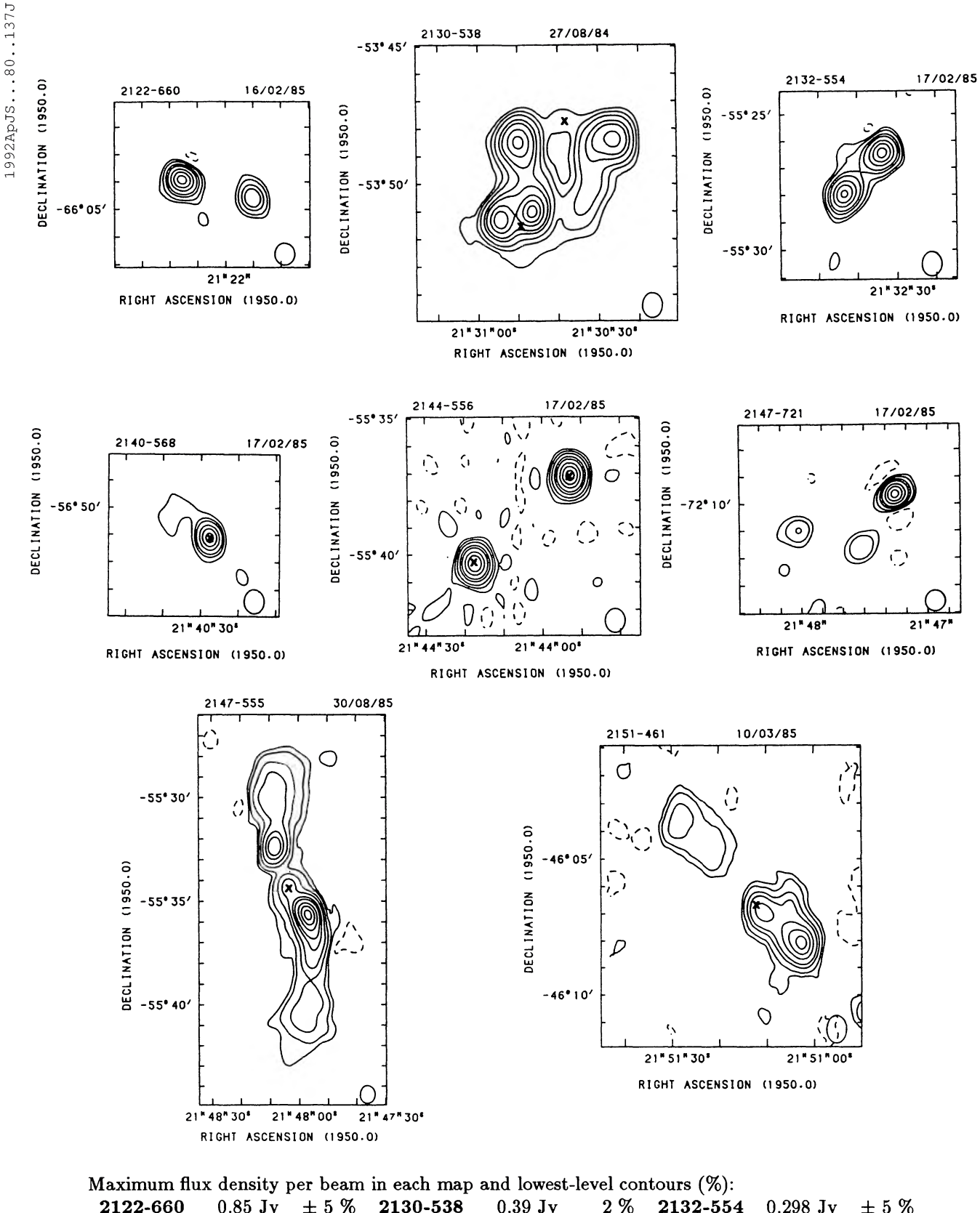
Fig. 1—Continued



1992ApJS...80..137J

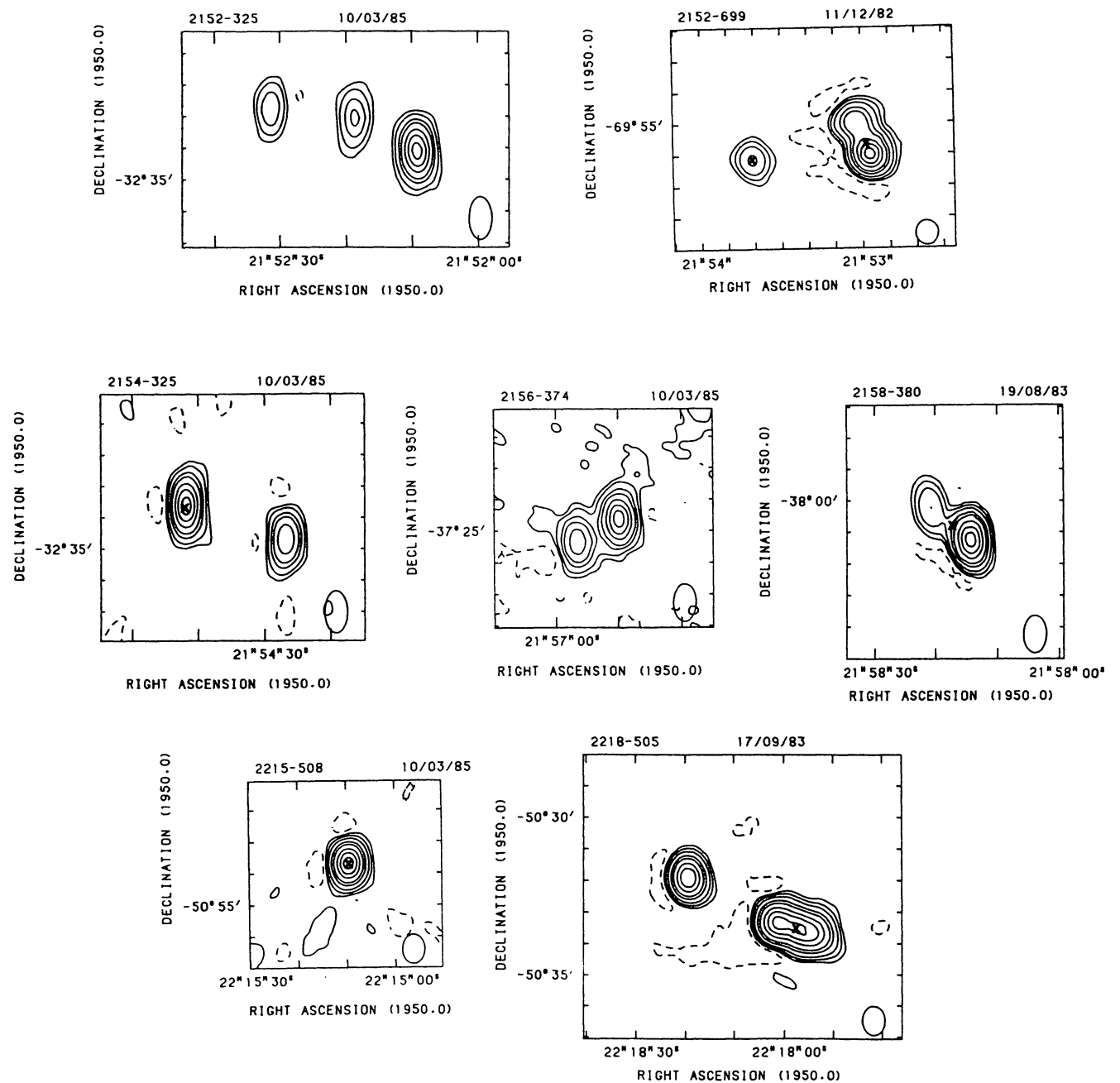
Maximum flux density per beam in each map and lowest-level contours (%): 3.8 Jy $\pm 5\%$ \pm 2 % 2041-604 2040-631 0.64 Jy0.41 Jy \pm 5 % 2036-612 \pm 2 % 2.26 Jy \pm 10 % 2048-572 2046-376 0.155 Jy5 % 2052-736 0.264 Jy± 1 % 2055-650 1.16 Jy

Fig. 1—Continued



2122-660 $0.85 \mathrm{~Jy}$ \pm 5 % 2130-538 0.39 Jy2 % 2132-554 \pm 5 % 0.298 Jy $0.63 \mathrm{~Jy}$ \pm 2 % 2140-568 0.160 Jy10 % 2144-556 2147-721 0.40 Jy $\pm 5\%$ 2147-555 0.58 Jy $\pm 1\%$ 2151-461 0.285 Jy \pm 5 %

Fig. 1—Continued



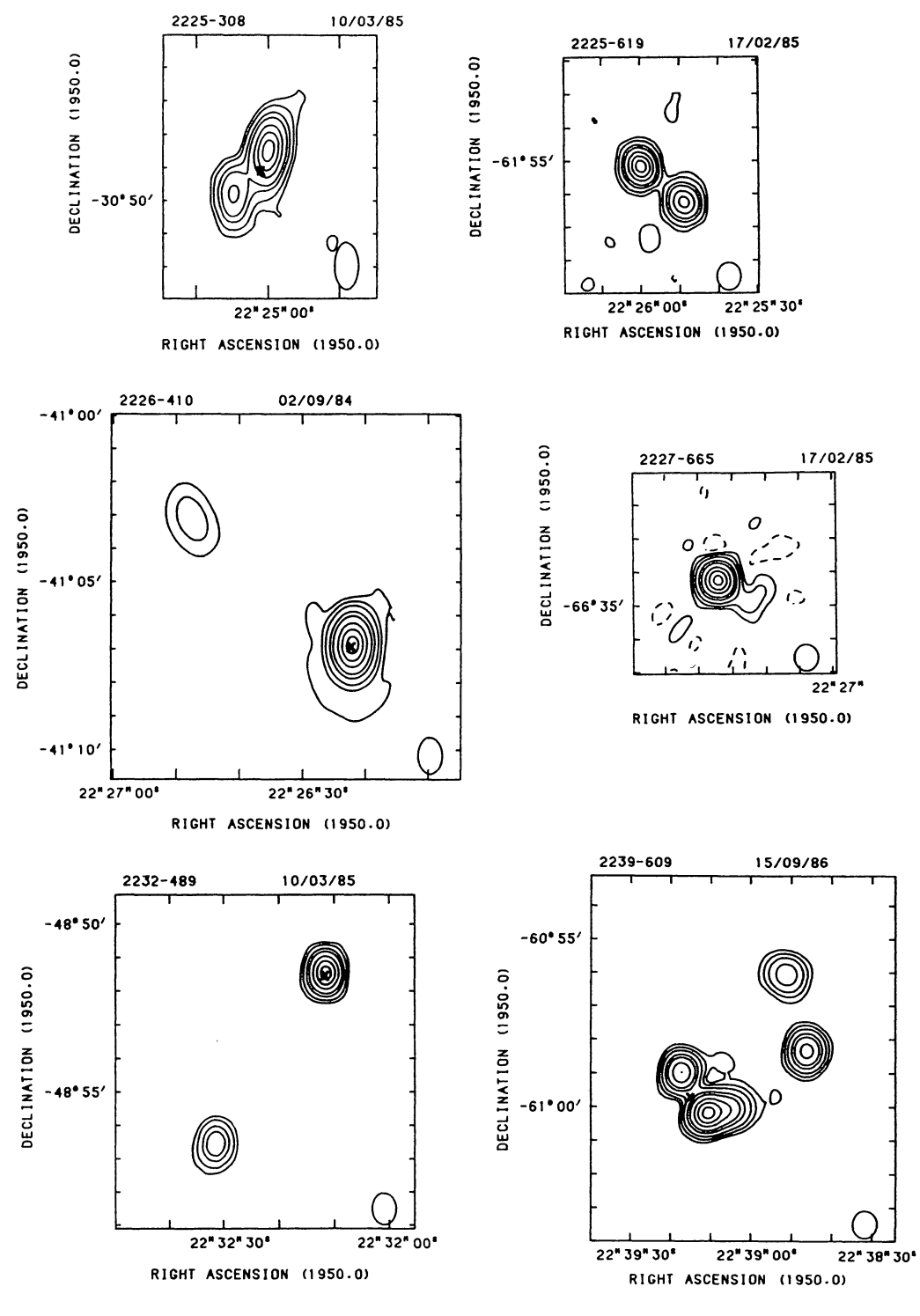
Maximum flux density per beam in each map and lowest-level contours (%):

2152-325 0.69 Jy $\pm 5\%$ **2152-699** 20.2 Jy $\pm 2\%$

2154-325 0.56 Jy $\pm 5 \%$ **2156-374** 0.54 Jy $\pm 5 \%$ **2158-380** 1.78 Jy $\pm 2 \%$

2215-508 1.48 Jy $\pm 2 \%$ **2218-505** 0.62 Jy $\pm 2 \%$

Fig. 1—Continued



Maximum flux density per beam in each map and lowest-level contours (%):

 $0.68 \mathrm{~Jy}$ 5 % 0.240 Jy $\pm 5\%$ 2225-308 2225-619 $\pm 2\%$ 2 % 1.15 Jy2226-410 $4.2 \mathrm{~Jy}$ 2227-665 2232-489 1.15 Jy 5 % 2239-609 0.58 Jy2 %

Fig. 1—Continued

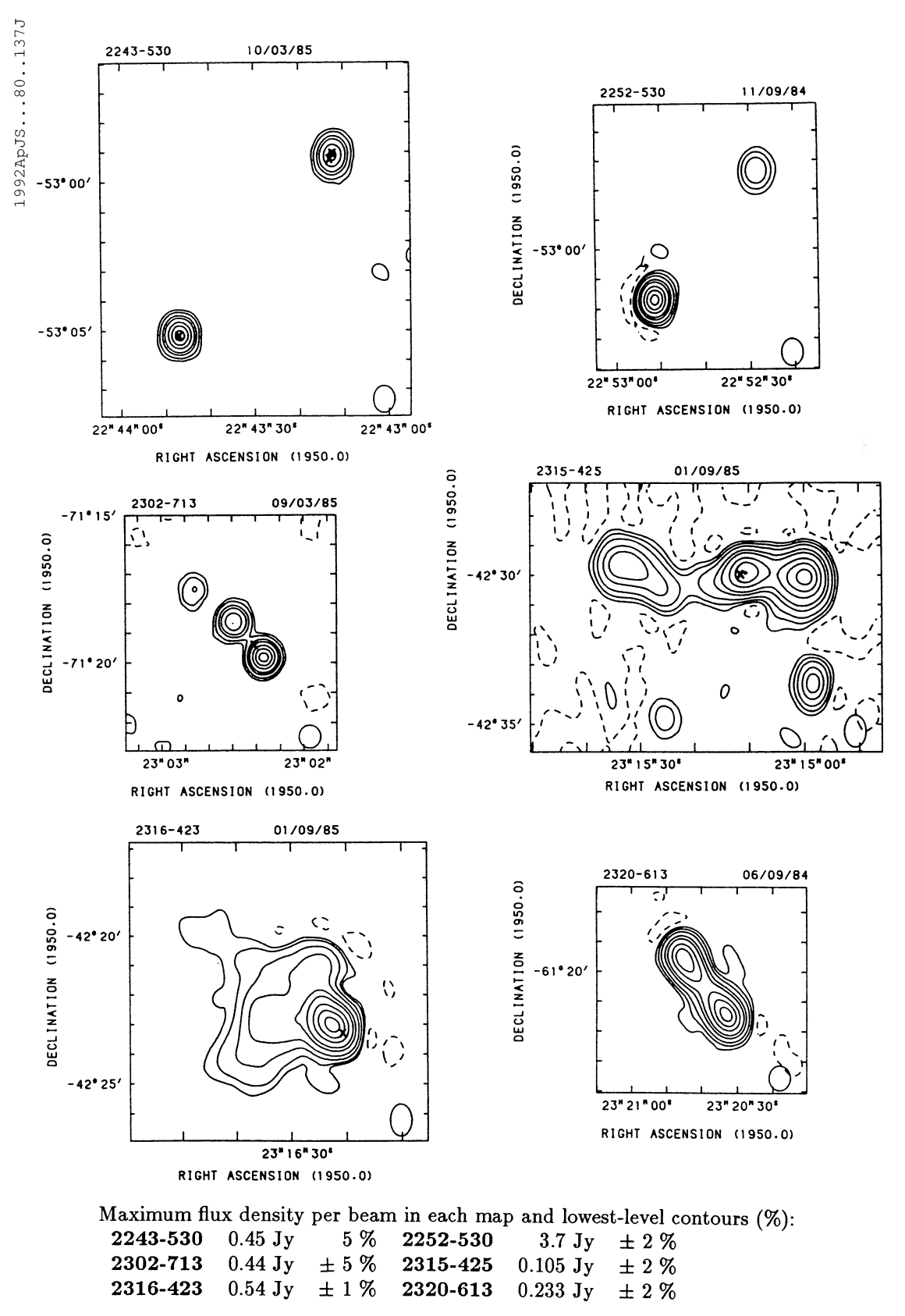


FIG. 1-Continued

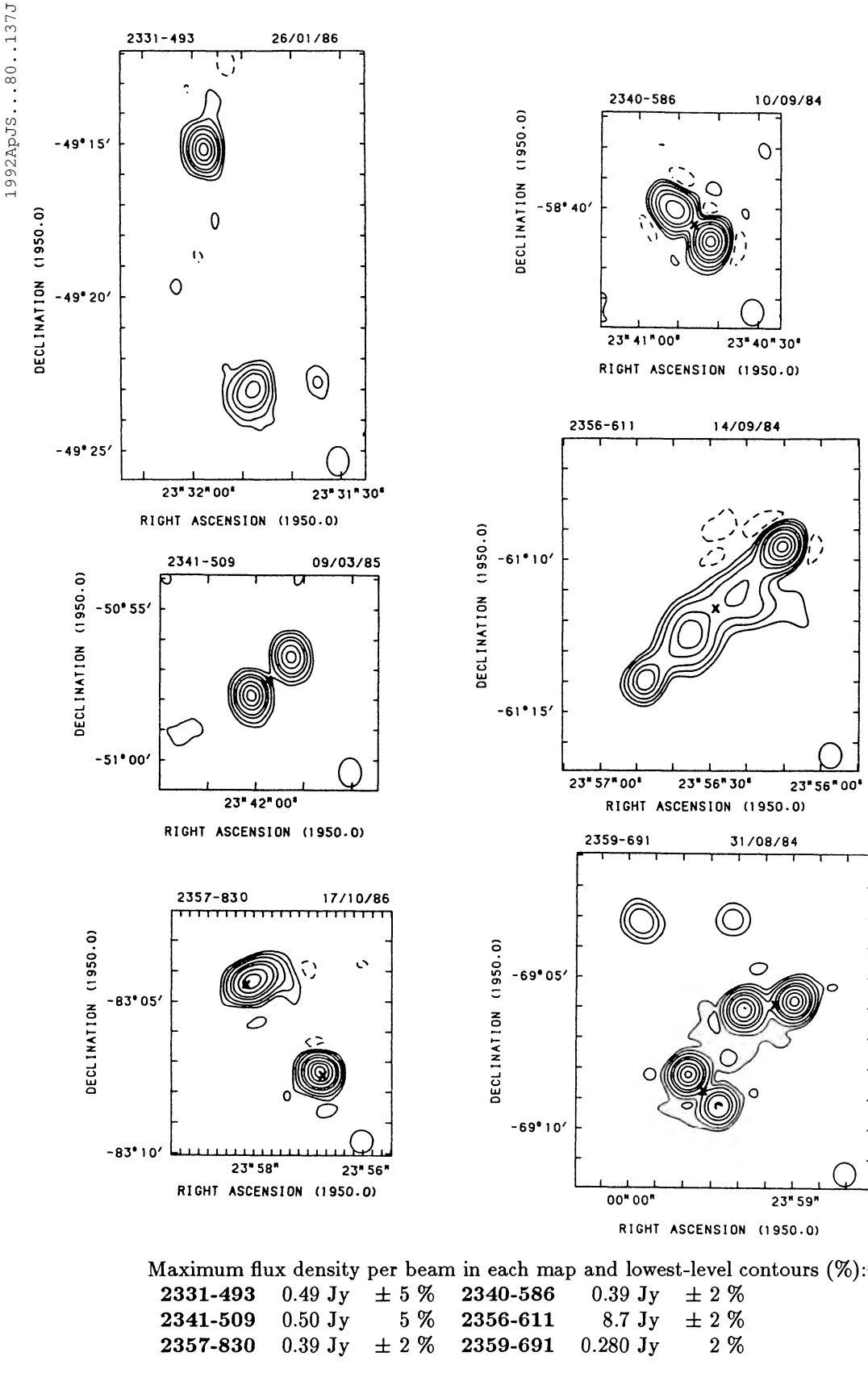


Fig. 1—Continued

184

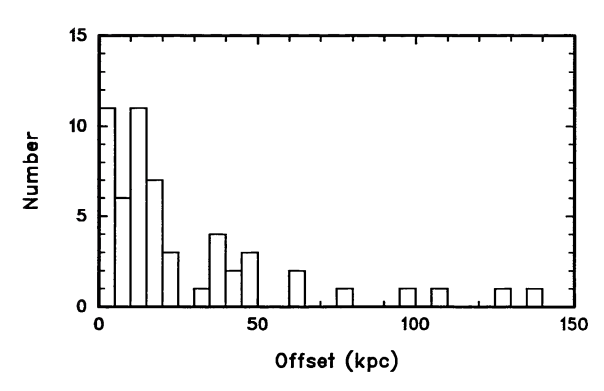


Fig. 2.—Distribution of offsets between the positions of the optical identification and the radio centroid for the sources which have measured redshifts. A Hubble constant $H_0 = 100 \text{ km s}^{-1} \text{ Mpc}^{-1}$ is used.

6. COMMENTS ON INDIVIDUAL SOURCES

We describe the radio structure of the 339 MRC sources in our southern sample, with notes listed according to source names in the 408 MHz catalog. Sources in the same field (with images in Fig. 1) are described together. Some MRC sources were found to be extended components of a larger source. Their MRC names are linked (with an asterisk *) in this section to show the single MOST source which is given the appropriate B1950 name in Table 1 based on the MOST centroid position. Similarly, adjacent sources flagged M in the MRC are linked (with a slash /) in these comments.

References are given to previously published images, or fits to structural models, but the reference list is not exhaustive for such extensively studied sources as Centaurus A and Fornax A.

The optical fields are also described, with any available optical identifications and redshifts. References are made to previous identifications, generally the first published with a finding chart, and to the source of the redshifts. Improved morphological data lead us to reject 25 earlier identifications suggested in the literature, as noted in the comments.

We make frequent reference to: the cluster catalog of Abell, Corwin, & Olowin (1989), hereafter ACO; Schilizzi & Mc-Adam (1975), hereafter SM; Slee, Siegman, & Mulhall (1982), hereafter SSM; Wall & Schilizzi (1979), hereafter WS.

0003-833—Double source with unresolved components. Galaxy 19.0 m at 00^h03^m55^s39 -83°22′50″.1, 13″ from the centroid along the major axis. There is a nearby galaxy 20.0 m at 00^h03^m56^s97 -83°22′57″.4.

0014-311/0015-311—Pair of unrelated sources, the south-west source slightly extended, the north-east a point source; Blank optical field for the two components.

0016-770/0017-769—Pair of unrelated point sources. Mapped by SM. Blank optical field for the two components. There is a possible object at the plate limit near 0016-770.

0020-747—Double source with extended components and a weak extension to the north-east. Galaxy 16.5 m at 00^h19^m55^s92 -74°44′52″4, 27″ from the centroid, see Savage et al. (1977). There is also a diffuse object 19.5 m at $00^{h}20^{m}02^{s}20 - 74^{\circ}44'36''.4, 4''$ from the centroid. The field is at the edge of the SMC and crowded with many faint objects.

0021-742—Pair of unrelated point sources. (The apparent

elongation of the south-east source is due to poor CLEANing.) Mapped by Clarke et al. (1976). Crowded field near the SMC hence no clear ID. There are many faint objects but no diffuse object brighter than 19.0 m.

0023-588/0024-589—Pair of unrelated sources (plus a third weaker source), the north-west source slightly extended, the south-east a point source. Blank optical field for the two components.

0028-505—Pair of unrelated point sources. Blank optical field for the two components and the centroid. The identification of Bolton & Savage (1977) with the 19.5 m galaxy at $00^{h}28^{m}15.16 - 50^{\circ}34'58.9$ is rejected.

0030-485—Double source with unresolved components. Stellar object 18.0 m at 00^h30^m53^s93 -48°35'47".6, 4" from the centroid. There is no other likely ID near the centroid or at the two components.

0032-738—Double source with extended components. Very crowded field at the edge of the SMC hence no clear ID.

0033-513/0034-513—Pair of unrelated point sources. Blank optical field for the two components. There is a galaxy 19.5 m at 00^h33^m51^s14-51°20′10″1, 20″ from the centroid, if the two are considered as a single source, but it is more likely that the radio sources are unrelated.

0043-424—Double source with extended components. Mapped by Slee (1977) and models fitted by Ekers (1969) and SSM. Galaxy 16.5 m at 00^h43^m55^s.76 -42°24′14″.3, 15″ from the centroid along the radio major axis, see Westerlund & Smith (1966) (z = 0.0528, Whiteoak 1972). There are two galaxies nearby, of 16.0 m at 00^h44^m02^s80 -42°24′53″.5 and 18.0 m at 00^h43^m48.44 –44°24′13″2, plus several fainter galaxies, in a cluster.

0046-585—Pair of unrelated point sources. Blank optical field for the two components and the centroid.

0058-507—Head-tail source with weaker structure (a second tail?) to the north. Galaxy 16.0 m at 00^h58^m33^s92 -50°48′17″8, 16″ from the radio peak consistent with the headtail morphology, see Savage, Bolton, & Wright (1977). In cluster A 2854 (ACO). There is another galaxy 16.0 m at 00^h58^m35^s19 -50°49′04″2.

0101-649—Triple source with extended lobes and a strong central component. Galaxy 19.5 m at 01 h01 m38 s33 -64°55′13″2, 4″ from the central peak of the radio triple. There is also a diffuse object 20.0 m nearby at 01^h01^m37.55 -64°55′11″5.

0103-453—Double source with extended components. Mapped by Slee (1977) and model fitted by SSM. Blank optical field for the centroid and the two components.

0107-371/0107-370—Pair of unrelated point sources. Blank optical field for the two components.

0108-348A/B—Pair of unrelated sources, the south-west source slightly extended, the north-east a point source. Blank optical field for the two components.

0110-692—Double source with unresolved components. Diffuse object 21.0 m at 01 h 10 m 00 s 38 - 69 o 15 5 4 ... 10 west of the centroid. There are two elongated galaxies nearby, 18.5 m at $01^{h}10^{m}02^{s}33 - 69^{\circ}15'07''.6$ and 19.0 m at $01^{h}10^{m}00^{s}96$ -69°16′11″.4. The faint object mentioned by Lasker & Smith (1974) is not visible on the SERC J image and as they suspected, should be rejected as a plate flaw.

0111-385—Double source with slightly extended compo-

 $\label{eq:table 2} TABLE~2$ Optical Identifications of the Radio Sources

									
MOST Source	RA (B1950) h m s	Dec (B1950)	Mag. bj	$_{ m z}^{ m redshift}$	MOST Source	RA (B1950) h m s	Dec (B1950)	Mag. bj	redshift z
0003-833 †	00 03 55.39	-83 22 50.1	19.0		0546-329	05 46 37.12	-32 59 31.1	13.0	0.037 †
0020-747	00 19 55.92	-74 44 52.4	16.5		0558-388 †	05 58 42.24	-38 53 56.9	15.5	0,00.
0030-485 †	00 30 53.93	-48 35 47.6	18.0 st		0608-658	06 08 50.35	-65 52 16.8	15.5	
				0.0500	•				
0043-424	00 43 55.76	-42 24 14.3	16.5	0.0528	0609-585 †	06 09 13.72	-58 30 28.2	17.5	
0058–507	00 58 33.92	-50 48 17.8	16.0		0610-316A	06 10 36.99	-31 38 07.4	18.5 Q	
0101-649 †	01 01 38.33	-64 55 13.2	19.5		0618-371	06 18 16.75	-37 10 18.5	14.5 db	0.0326
0110-692 †	01 10 00.38	-69 15 54.1	21.0			06 18 17.87	-37 10 18.7 J	14.0 00	0.0020
0114-476	01 14 14.84	-47 38 30.5	17.0	0.146	0620-526	06 20 36.77	-52 40 03.6	15.5	0.0511
0119-501 †	01 19 00.56	-50 07 49.6	20.5		0625-545	06 25 48.87	-54 30 39.8	16.0	0.052 †
0130-620 †	01 30 41.91	-62 02 06.5	20.0		0641-584	06 41 31.53	-58 27 03.0	17.5	,
0131-367	01 31 43.60	-36 44 56.6	13.5	0.0300	0649–557	06 49 23.72	-55 45 56.6	15.0	0.050 †
0150-480 †	01 50 39.29	-48 03 06.1	20.0		0651-603	06 51 15.50			0.000
0153-826	01 53 37.55	-82 40 01.2	21.0		0001 000		1	16.5 db	
0211-479	02 11 16.05	-47 58 13.7	19.5	0.2195	0700 505 1	06 51 16.09	-60 18 28.9	10.5	
0214-480	02 14 52.69	-48 03 01.0	15.5	0.0641	0703-595 †	07 03 08.73	-59 34 53.3	18.5	
0214 400	02 14 02.00	40 00 01.0	10.0	0.0041	0704–451	07 04 01.41	-45 08 31.5	18.0	
0218-452 †	02 18 05.90	-45 18 05.8	18.0		0707-359 †	07 07 26.61	-35 56 28.4	20.0	
0248-600A †	02 48 17.98	-60 01 18.5	21.0		0713-371A †	07 13 39.77	-37 10 43.0	20.0 st	
0248-600B †	02 48 37.47	-60 01 52.9	19.5 st		0715-362	07 15 20.82	-36 16 33.3	16.0	0.032 †
0250-682A †	02 50 30.76	-68 14 23.9	19.0 st		0718-340	07 18 56.22	-34 01 24.4	15.0	0.0297
0250–682B †	02 50 51.38	-68 15 21.3	19.5		0719–553	07 19 12.35	-55 19 38.0	19.5	0.216
0258-520 †	02 58 52.05	-52 02 38.3	15.0	0.060	0809-492 †	08 09 14.38	-49 14 55.5	16.5	
0305-417B †	03 05 38.77	-41 46 08.1	21.0		0809-493	08 09 41.20	-49 20 46.4	20.0 st	
0305-417A †	03 05 47.70	-41 47 02.5	19.5		0809-499 †	08 09 57.68	-49 58 50.3	20.5 st	
0305-418	03 05 54.45	-41 49 14.7	19.5		0816-704	08 16 26.30			0.000 1
0319-453 †	03 19 15.50	-45 25 54.6	15.0	0.063 †	0819-300	08 19 24.73	-70 30 17.0 -30 01 26.5	15.0 17.5	0.039 † 0.086
0320–373	03 20 47	-37 23 12	9.5	0.0061	0042 226	00 40 07 00	22 26 45 5	11.5	0.0072
0332-391	03 32 13.08	-39 10 36.0	15.5	0.063	0843-336	08 43 07.93	-33 36 45.5	11.5	0.0073
0336-356	03 36 34.37	-35 36 44.6	10.6	0.0049	0843-568 †	08 43 25.83	-56 53 39.2	16.5	0.062 †
0336–355	03 36 50.95	-35 32 35.9	18.0	0.0043	0905-353 †	09 05 45.85	-35 23 15.1	16.5	
0344–345	03 44 34.96	-34 32 00.8	15.5		0909-564 0918-383 †	09 09 25.68 09 18 14.81	-56 24 33.2 -38 22 04.6	19.5 st 19.5	
0057 071 1	00 57 50 50	27 00 10 2	10.5						
0357-371 †	03 57 56.58	-37 09 10.3	19.5		0932–372 †	09 32 03.24	-37 14 46.2	17.0	0.064 †
0408-479 †	04 08 44.66	-47 56 22.4	21.0		0936–622 †	09 36 18.10	-62 15 37.6	19.5	
0423-687 †	04 23 05.55	-68 44 43.1	16.0		0945-370 †	09 45 45.07	-37 01 29.2	16.5	0.041 †
0424-728 †	04 24 41.52	-72 52 48.2	19.0		0952-306	09 52 21.02	-30 39 07.9	19.5	
0427–539	04 27 58.57	-53 56 09.4	14.0 db	0.0392	1002–320	10 02 26.58	-32 02 07.1	18.0	
0429-616 †	04 29 35.21	-61 38 10.4	18.5	0.059	1010–647	10 10 49.98	-64 43 01.2	21.0	
0435-587A †	04 35 06.74	-58 44 06.8	20.0		1011-316 †	10 11 32.64	-31 38 27.6	21.0	
0450–387B †	04 50 08.70	-38 44 24.2	20.5		1011-320		-32 04 57.6	20.5	
0456–301 †	04 56 29.20	-30 11 37.1	17.0	0.062	1051-345	10 51 01.80	-34 30 34.1	20.0 st	
0456–470 †	04 56 36.55	-47 04 06.1	21.0		1051-344 †	10 51 15.24	-34 29 39.3	21.0 st	
0507-627 †	05 07 24.23	-62 46 13.8	20.0		1056-360	10 56 34.15	-36 03 17.2	17.0	0.070 †
0511-484A	05 11 27.21	-48 27 44.4	20.5	0.306	1123-351	11 23 26.40	-35 07 10.8	14.5	0.0329
0511-484B	05 11 44.00	-48 29 51.5	20.5		1136–678 †	11 36 07.94	-67 53 49.9	20.0	0.0028
0511-305	05 11 36.70	-30 32 14.7	16.0		1136-320 †	11 36 47.49			
0518-458	05 18 23.59	-45 49 42.5	16.5	0.0350	1130-320	11 37 27.45	-32 06 00.9 -46 21 12.6	21.5 16.0	0.068 †
	05 01 10 77				1137-464	11 37 35.24	-46 24 25.5	19.0 st	J.000
0521-478 †	05 21 13.77	-47 49 23.9	19.0						
0523-327	05 23 35.87	-32 44 49.9	16.0		1141-391	11 41 38.58	-39 05 36.3	16.0	0.056 †
	05 40 20.92	-61 44 01.6	16.0		1144-379	11 44 30.81	-37 55 31.5	19.0 BL	•
0540-617		CO FO 10 C	155		4440 000				
0540-628	05 40 29.82	-62 52 12.6	15.5		1148-353	11 48 43.06	-35 20 24.3	18.5	
	05 40 29.82 05 43 32.83	-62 52 12.6 -47 59 43.5	21.0		1148-353 1153-807A †	11 48 43.06 11 53 21.82	-35 20 24.3 -80 44 35.9	18.5 21.0	

TABLE 2—Continued

MOST Source	RA (B1950) h m s	Dec (B1950)	Mag. b _J	$egin{array}{c} \mathbf{redshift} \ \mathbf{z} \end{array}$	MOST Source	ŘA (B1950) h m s	Dec (B1950)	Mag.	redshift z
1234-723	12 34 05.52	-72 19 00.1	15.5	0.0234	1954-552	19 54 18.86	-55 17 41.9	15.0	0.0600
1234-490B †	12 34 39.71	-49 04 17.0	20.0		1954-356 †	19 54 34.24	-35 39 11.1	20.0	
1259-445 †	12 59 38.38	-44 30 33.5	21.5		2005-428	20 05 38.23	-42 51 53.5	21.0 st	
1259-367	12 59 53.87	-36 43 30.2	20.0		2006-565	20 06 22.18	-56 36 49.7	17.5	0.0576
1302-325 †	13 02 12.95		} 18.0 db		2007-568	20 07 27.48	-56 53 04.4	17.0	0.053
1992 929	13 02 13.07	-32 33 13.4	18.0 ac	•					
		02 00 1011			2007-879 †	20 07 24.2	-87 58 29.4	21.0	
1302-492	13 02 31	-49 12 12	9.3	0.0018	2013-308	20 13 07.67	-30 50 46.2	16.5	
1304–748 †	13 04 48.45	-74 53 36.1	20.5	0.0010	2013-307	20 13 23.16	-30 44 34.5	19.5 st	
1308-441	13 08 30.44	-44 06 45.1	14.5	0.051 †	2013-312 †	20 13 58.86	-31 12 17.9	21.0	
1312-593B †	13 12 33.49	-59 20 55.1	21.5	0.001	2014-312	20 14 09.20	-31 13 10.5	21.0	
1318–434	13 18 17.36	-43 26 34.0	12.0	0.011	2014-311	20 14 16.10	-31 11 38.3	20.5	
	20 20 21.100	10 20 0 110	12.0	0.011			01 11 00.0	2010	
1322-427	13 22 33	-42 45 24	7.7	0.0018	2014-558	20 14 06.21	-55 48 51.6	16.5	0.0608
1324-300	13 24 56.67	-30 02 45.1	18.0	0.0010	2020-575 †	20 20 21.60	-57 33 26.9	18.5	0.352
1333-337	13 33 47.52	-33 42 42.4	11.0	0.0124	2026-414	20 26 15.06	-41 28 51.6	21.5	
1343-377 †	13 43 27.24	-37 43 16.6	15.0	0.037	2028-732	20 28 24.95	-73 14 13.2	18.0 Q	0.455
1355-416	13 55 57.30	-41 38 19.5	15.0 Q		2030-378A †	20 30 01.13	-37 52 26.2	21.5 st	
					2030-378B †	20 30 27.65	-37 48 05.2	21.0	
1413-364	14 13 31.83	-36 27 01.5	17.5		•				
1416-517 †	14 16 29.69	-51 44 46.3	21.5 st		2041-631 †	20 41 09.29	-63 11 21.9	21.0	
1421-382	14 21 11.90	-38 13 13.4	17.0 Q	0.41	2048-572	20 48 12.78	-57 15 31.8	12.0	0.0113
1425-479 †	14 25 38.68	-475845.2	17.5		2130-538	21 30 38.32	-53 47 40.5	15.5	0.0781
1437–368 †	14 37 27.32	-36 52 40.5	20.0			21 30 49.18	-53 51 33.6	15.5	0.0763
•					2140-568 †	21 40 27.79	-56 51 06.9	16.0	
1451–364 †	14 51 21.96	-36 28 09.1	20.0		•				
1452-367 †	14 52 01.44	-36 42 59.7	16.5		2143-556 †	21 43 53.10	-55 37 04.1	19.5 st	
1452-517	14 52 21.49	-51 48 39.7	16.5	0.016 †	2144-556	21 44 17.63	-55 40 19.4	19.5 st	
1511-315	15 11 59.96	-31 33 27.0	21.0		2148-555	21 48 03.98	-55 34 18.2	14.5	0.035
1545-321 †	15 45 49.00	-32 07 48.0	17.5		2151-461 †	21 51 12.80	-46 06 43.0	17.5	
					2152-699	21 52 58.50	-69 55 41.2	14.0	0.0266
1600-445A †	16 00 59.65	-44 33 20.1	20.5		2153-699 †	21 53 40.86	-69 56 11.4	20.0	
1602–633	16 02 09.99	-63 21 21.9	17.5	0.0591	•				
1610–605	16 11 13.07	-60 32 26.0	14.5	0.0162	2154-325B	21 54 42.08	-32 33 43.6	17.0 st	
1610-608	16 10 43.12	-60 46 54.3	13.5	0.0167	2158-380	21 58 17.19	-38 00 52.8	14.5	0.0333
1619-634 †	16 19 56.06	-63 28 35.7	17.5		2215-508 †	22 15 09.65	-50 53 43.9	18.5 st	
					2217-505 †	22 17 57.87	-50 33 32.3	20.5	
1637–771	16 37 05.24	-77 10 08.1	16.0	0.0438	2225-308	22 25 01.08	-30 49 03.1	16.5	
1733-565	17 33 21.48	-56 32 16.6	18.0	0.0985					
1733-712 †	17 33 28.57	-71 17 13.7	20.5		2226-411	22 26 22.12	-41 06 55.1	20.0 st	
1737–608 †	17 37 28.82	-60 53 51.4	20.0		2232-488	22 32 11.40	-48 51 31.2	17.0 st	
1758–473 †	17 58 21.51	-47 19 30.7	18.5 st	į	2239-609 †	22 39 15.93	-60 59 44.5	20.5	
					2243-529 †	22 43 12.76	-52 59 03.4	17.0 db	
1820-774 †	18 20 31.58	-77 29 44.4	20.0			22 43 13.16	-52 59 17.0	17.0	
1821–583 †	18 21 19.63	-58 19 19.3	20.0		2243-530 †	22 43 47.00	-53 05 11.9	21.5	
1829-778 †	18 28 59.04	-77 50 24.5	20.5						
1849–397 †	18 49 57.92	-39 45 10.2	19.5		2302-713	23 02 20.28	-71 19 23.0	17.0 Q	0.384
1908–623 †	19 08 40.03	-62 23 36.5	20.0		2315-425 †	23 15 11.11	-42 29 57.3	15.0	
					2316-423	23 16 20.94	-42 23 14.1	14.5	
910-800 †	19 10 40.03	-80 04 28.6	21.0	İ	2340-586	23 40 46.39	-58 40 31.7	18.5	
1921-577	19 21 53.30	-57 46 16.1	16.5		2341-509 †	23 41 57.71	-50 57 17.0	21.0 st	
922-627 †	19 22 53.55	-62 45 37.1	17.5 st						
1925-746 †	19 25 38.03	-74 40 38.5	21.0		2356-611	23 56 29.44	-61 11 41.8	17.0	0.0964
1929–397	19 30 00.06	-39 46 52.1	15.5		2356-831 †	23 56 41.63	-83 07 34.6	16.0	
					2357-830 †	23 58 07.73	-83 04 36.3	16.0	
1936-357B †	19 36 01.93	-35 47 42.9	17.0		2359-690 †	23 59 07.12	-69 05 54.4	19.0 st	
1940-406 †	19 40 26.30	-40 37 24.4	20.0		2359-691	23 59 33.31	-69 08 44.4	17.0 st	
1945–304 †	19 45 12.07	-30 27 37.1	21.5		•				
1951–501	19 51 23.61	-50 10 21.7	20.0						
1953-879 †	19 53 41.8	-87 55 52.3	21.5						

Notes.—Columns give: radio source name; flags; optical position; optical magnitude; redshift. Key: st—stellar image, probably a QSO. Q—confirmed QSO; BL—confirmed BL Lac object; db—double galaxy. New identifications (from the SERC IIIaJ survey) and redshifts from this study are flagged †.

nents. Blank optical field for the centroid and the two components.

0113-808—Pair of unrelated point sources. Blank optical field for the two components.

0113-475*0114-476—Giant complex source; an edge-brightened double with broad outer lobes and two inner lobes (but no MOST core component). Model fitted by Ekers (1969). Mapped by SM and Danziger & Goss (1983). Galaxy 17.0 m at $01^h14^m14^s84-47^o38'30''.5$, midway between the two inner lobes of the radio structure, see Westerlund & Smith (1966) (z=0.146, Danziger, Goss, & Frater 1978).

0118-501B/A—Pair of unrelated sources, the north a point source, the south source a double with unresolved components. Diffuse object 20.5 m at 00^h19^m00.56 -50°07′49″.6, 4″ from the north source. Blank optical field for the south source.

0130-620—Double source with extended components. Galaxy 20.0 m at 01 h30 m41 s91 -62 02 06 5, 4" from the centroid, plus nearby galaxy 20.0 m at 01 h30 m41 s49 -62 01 52 6, 10" from the centroid. The first galaxy is taken as the ID, but the second is the ID of Bolton & Savage (1977) which is rejected.

0131-367B*A—Complex source; an edge-brightened double, with no MOST core component. Models fitted by Ekers (1969) and SSM. Mapped by SM, Slee (1977), Ekers et al. (1978) and Ekers et al. (1989). The last shows a core component in the VLA image. Dust-lane galaxy NGC 612, 13.5 m at $01^h31^m43.60^-36^\circ44.56.6$, 32" from the centroid with z=0.0300 (Westerlund & Smith 1966). See Ekers et al. (1978) for a detailed discussion of the galaxy.

0150–480—Double source with extended components. Galaxy 20.0 m at 01^h50^m39^s29 –48°03'06".1, 13" north of the centroid.

0153-826—Double source with extended components. Diffuse object 21.0 m at 01^h53^m37^s.55 -82°40′01″.2, 9″ from the centroid. There are two other diffuse objects, 21.0 m, nearby at 01^h53^m36^s.55 -82°39′55″.5 and 01^h53^m34^s.08 -82°39′53″.9, indicating a faint cluster.

0156-483/0156-482—Pair of unrelated point sources. Blank optical field for the two components and the centroid. The galaxy suggested by Bolton & Savage (1977) is rejected.

0208-418—Pair of unrelated sources, the west source slightly extended, the east a point source. Blank optical field for the two components and the centroid.

0210-432—Pair of unrelated sources, the west source slightly extended, the east a point source. Blank optical field for the two components and the centroid.

0211-479*0211-480—Giant, edge-brightened double source with extended lobes but no MOST core or bridge emission. Mapped by SM and Danziger et al. (1978). White, Mc-Adam, & Jones (1984) published MOST and FST images of this source and nearby sources 0214-480 and 0214-483 which have similar position angles. The redshifts indicate that they are unlikely to be related and so the alignment is coincidental (White et al. 1988). Galaxy 17.5 m at $02^h11^m16.05-47^\circ58'13.7$ 7 plus several fainter galaxies within a cluster, see Tritton & Schilizzi (1973) (z = 0.2195, White et al. 1988, who give $b_J = 17.8$).

0213-406—Strong point source plus nearby double source with edge-brightened lobes. Although the strong source is nearly aligned on the axis of the double, they are considered unrelated. Blank optical field for the two sources. There is a

18.0 m galaxy nearby at $02^h13^m35^s73 -40^\circ40'58''.1$ but this is unlikely to be the ID.

0214–480—Complex source, an edge-darkened double with strong inner lobes but no MOST core component. The outer structure is bent into a "Z"-shape. Model fitted by Ekers (1969). Mapped by SM, Christiansen et al. (1977), and White et al. (1984). Galaxy 15.5 m at $02^h14^m52^s69 - 48^\circ03'01''0$, 11" from the centroid and between the two inner lobes of the radio structure, see Tritton & Schilizzi (1973) (z = 0.0641, White et al. 1988). In cluster AS 239 (ACO).

0218–452—Triple source with extended components. The morphology is unusual for a triple in that one outer component is much stronger than the other two components, suggesting a head-tail source. Galaxy 18.0 m at 02 h 18 m 05 s 90 – 45° 18′ 05″, 12″ from the central peak of the triple radio structure, along the radio axis. The triple is asymmetric in flux, so this galaxy is 72″ from the centroid.

0230-666—Pair of unrelated point sources. Blank optical field for the two components.

0231-383—Pair of unrelated point sources. Blank optical field for the two components.

0248-600—Pair of unrelated point sources. Diffuse object 21.0 m at $02^{h}48^{m}17^{s}98-60^{\circ}01'18''.5$, 5" from the west source and a stellar object 19.5 m at $02^{h}48^{m}37^{s}.47-60^{\circ}01'52''.9$, 3" from the east source.

0250–682—Pair of unrelated sources, the west a point source, the east source extended, possibly with a head-tail morphology. Mapped by Clarke et al. (1976). Stellar object 19.0 m at 02^h50^m30^s.76 –68°14′23″9, 2″ from the west source and galaxy 19.5 m at 02^h50^m51^s.38 –68°15′21″3, 5″ from the centroid of the east source.

0251-677—Double source with unresolved components. Blank optical field for the centroid.

0254–484—Single point source. This source should not have been flagged as extended in the MRC. Blank optical field. 0258–520—Double source with extended components. Gal-

axy 15.0 m at $02^h58^m52^s05 - 52^\circ02'38''3$, 19" from the centroid. In cluster A 3078 with cluster redshift z = 0.060 (ACO).

0305-417—Triple group with the two outer sources slightly extended. The structure is not like a typical triple (two lobes plus a core) and is probably three unrelated sources or a cluster. Diffuse object 21.0 m at 03h05m38s77 -41°46′08″1, 6″ from the west component, galaxy 19.5 m at 03h05m47s70 -41°47′02″5, 5″ from the central component, and galaxy 19.5 m at 03h05m54s45 -41°49′14″7, 4″ from the east component.

0319-453*0317-456—Giant complex source, considered an edge-brightened, asymmetrical double with the nearby unflagged MRC source 0317-456 as one lobe. One of the largest sources in the sample. The weak ridge continues for about half the distance between the two sources. There are hotspots near the end of the extended lobes and steps on the ridge line but no clear core component in the MOST image. See Jones (1989). Mapped by Slee (1977) and model fitted by SSM. Dust-lane galaxy, 15.0 m at $03^{\text{h}}19^{\text{m}}15^{\text{s}}50$ – $45^{\circ}25'54''.6$, listed in Arp & Madore (1987) as AM 0319-452 lies between the centroid and the midpoint of the lobes along the axis. A recent AT image shows a weak core component at this position (L. Saripalli 1991, private communication; z = 0.063, Jones 1989). There is a galaxy 16.5 m, probably an edge-on spiral, at $03^{\text{h}}18^{\text{m}}44^{\text{s}}.07$ – $45^{\circ}31'15''.5$, 2'' from another faint peak on the

axis of the radio source but this galaxy is not the ID of the large double. The ID proposed by Tritton & Whitworth (1973) for the north-east lobe, 0319-453, is rejected.

0320-373—Fornax A, a complex source with a compact core component and very large diffuse lobes showing much structure. It is an edge-brightened double although not a powerful radio source. The MOST image has a negative "bowl" due to the lack of short-spacing data and has not been CLEANed. Fornax A has been extensively studied so only a few references are given here. Mapped by Cameron (1971), Gardner & Whiteoak (1971), and Ekers et al. (1983). SO Galaxy, 9.5 m, NGC 1316 at $03^{\rm h}20^{\rm m}47^{\rm s}-37^{\circ}23'12''$ (Lauberts 1982) coincident with the central peak of the radio source (z=0.0061, Palumbo et al. 1983). This is a well-known ID, one of the earliest extragalactic radio sources identified (Mills 1954).

0332-391A*B—Complex structure with two edge-dark-ened lobes, bent into a wide-angle-tail. Model fitted by Ekers (1969) but with a poor fit as a core-halo structure. Mapped by SM, WS and Ekers et al. (1989). The last shows a core component in the VLA image. Galaxy 15.5 m at $03^h32^m13^s08-39^\circ10'36''0$, see Bolton, Clarke, & Ekers (1965), 57'' from the centroid but between the two peaks of the bent radio structure (z = 0.063, Smith 1983). In cluster A 3135 (ACO). There is another galaxy 15.5 m nearby, towards the north at $03^h32^m16^s48-39^\circ09'32''.6$, only 30'' from the centroid but outside the radio structure, plus several more galaxies in the cluster

0336-356/0336-355—Pair of unrelated sources, the south-west source a triple with extended components and the north-east source a strong double with unresolved components. Models fitted by Ekers (1969) and SSM. Mapped by SM, Slee (1977), and Ekers et al. (1989). Galaxy 10.6 m, NGC 1399, at $03^{h}36^{m}34^{s}37$ $-35^{\circ}36'44''.6$, 18'' from the centroid of the south-west source, see Mills et al. (1960) (z = 0.0049, Palumbo et al. 1983). In cluster AS 373 (ACO). Galaxy 18.0 m at $03^{h}36^{m}50^{s}95$ $-35^{\circ}32'35''.9$, 13'' from the centroid of the north-east source, see Schilizzi & McAdam (1970). There is a faint cluster near the north-east source with a 20.5 m object at $03^{h}36^{m}51^{s}16$ $-35^{\circ}32'18''.4$.

0344-345—Complex source with at least three extended components and diffuse bridge emission. The nearby point source 0345-345 is close to the axis but probably unrelated. Models fitted by Ekers (1969) and SSM. Mapped by SM, Slee (1977), WS, and Ekers et al. (1989). The last shows a core component in the VLA image. Galaxy 15.5 m at 03 h44 m34 s96 -34°32′00″8, 9″ from the centroid, see Bolton et al. (1965). There are several more galaxies in a cluster, some within the bounds of the radio structure, notably a face-on spiral 15.0 m at 03 h44 m45 s02 -34°32′00″7, an elliptical galaxy 16.0 m at 03 h44 m39 s74 -34°32′15″5, a galaxy 16.0 m at 03 h44 m33 s56 -34°33′35″6 and a galaxy 17.5 m at 03 h44 m24 s32 -34°31′18″0. These may be associated with the diffuse radio structure.

0357-506—Double source with slightly-extended components. Blank optical field. There is a galaxy 19.0 m at 03^h57^m45.32 -50°40′51″.3 but this is well off the radio axis. This is probably the object suggested by Wall & Cannon (1973) but rejected by Bolton & Savage (1977).

0357-371—Single extended peak. Galaxy 19.5 m at $03^h57^m56^s58-37^\circ09'10''.3$, 18" from the centroid. There is a faint cluster with a galaxy 20.0 m to the north of the first at $03^h57^m56^s.72-37^\circ08'52''.7$, 3" from the centroid, but the first

galaxy is taken as the ID. This second galaxy was the ID of Wall & Cannon (1973) (who stated that it was the brighter of the two) and is rejected.

0408-479—Single peak; extended EW. Diffuse object 21.0 m at $04^h08^m44^s66-47^\circ56'22''.4$, less than 1" from the centroid, within a faint cluster.

0412-441—Pair of unrelated point sources. Blank optical field for the two components.

0423-687—Double source with extended components. Galaxy 16.0 m at 04^h23^m05^s55 -68°44′43″1, 14″ from the centroid. In cluster AS 450 (ACO).

0424-728—Complex source, an edge-brightened double (the north hotspot prominent) with a bent ridge-line and a weak core component. Mapped by Clarke et al. (1976). The slightly extended source to the east is unrelated. Galaxy 19.0 m at 04^h24^m41^s.52 -72°52′48″.2, 6″ from the centroid.

0427–539B*A—Complex source; appears to be a head-tail source with a strong double peak at the head, a bent tail and a weak extension to the north-east. Model fitted by Ekers (1969). Mapped by SM, Christiansen et al. (1977) and WS. Recent MOST and FST images (McAdam, White, & Bunton 1988) suggest that the morphology is a wide-angle-tail in projection. db galaxy 14.0 m, IC 2082, at $04^h27^m58^s57-53^\circ56'09''.4$, 76" from the radio centroid, but the fainter nucleus is close to the radio peak, consistent with the head-tail morphology, see Westerlund & Smith (1966) (z = 0.0392, Burbidge & Burbidge 1972). In cluster AS 463 (ACO). There is a 17.0 m galaxy in the cluster, at $04^h27^m30^s88-53^\circ57'01''.0$, near where the radio tail bends sharply, which may be associated with this bending.

0429–616—Complex source, a double with extended lobes and bent morphology with an extension to the north-west. Mapped by Clarke et al. (1976). There are several weak sources to the north-east (e.g., the head-tail source in the corner of the MOST image). Galaxy 18.5 m at $04^h29^m35^s21$ –61°38′10″4, 62″ north of the centroid but consistent with the bending of the structure towards the north-west. In cluster A 3266 with z = 0.059 (ACO). There is a brighter galaxy nearby, 16.5 m at $04^h29^m42^s52$ –61°38′24″9, 65″ north-east of the centroid and offset from the radio ridge line. A higher resolution FST image confirms that the radio structure is more consistent with the fainter galaxy as the ID.

0435–587A/B—Pair of unrelated point sources. Blank optical field for the east source and galaxy 20.0 m at 04^h35^m06^s74 –58°44′06″8, 2″ from the west source.

0437-662—Pair of unrelated point sources. Blank optical field for the two components.

0450-387B/A—Pair of unrelated sources, the west source a double with slightly extended components and the east source slightly extended. Diffuse object 20.5 m at 04h50m08s70-38°44′24″2, 10″ from the centroid of the west source and blank optical field for the east source.

0456–301—Extended diffuse source with no small-scale structure in the MOST image. Models fitted by SSM and Ekers (1969) and mapped by Slee (1977). Galaxy 17.0 m in cluster A 3297 (ACO) has distorted wispy structure, at $04^h56^m29^s20-30^\circ11'37''1,21''$ from the centroid. VLA data suggest that this galaxy may be the ID at the center of wide-angle-tail radio structure; z=0.062 (A. Unewisse 1991, private communication). There is also a galaxy 16.5 m at $04^h56^m32^s59-30^\circ11'48''9,25''$ from the centroid. The diffuse structure seen

in the MOST image may be associated with the whole cluster as a halo.

0456-470—Double source with extended components. Diffuse object 21.0 m at 04^h56^m36.55-47°04′06″1, 20″ from the centroid, along the radio axis. There is a galaxy 16.5 m nearby at 04^h56^m42.44 -47°05′29″6, but this is 30″ south of the south-east peak of the double.

0507-627—Double source with unresolved components. Galaxy 20.0 m at 05\(^h07\)^m24\(^s23\) -62\(^o46'13''.8\), 8" from the centroid

0511–484—Three separate unrelated sources: a weak point source, a double source with extended components and a slightly extended source. Mapped by SM, WS, and Robertson & Smith (1981). Galaxy 20.5 m at $05^h11^m27^s21-48^\circ27'44''.4$, 35" from the centroid of the double, but along the axis and near the midpoint of the lobes. This ID is from Robertson & Smith (1981) who claim that it has peculiar morphology and give z=0.306. There are two galaxies toward the north-east 20.5 m at $05^h11^m32^s32-48^\circ27'26''2$, 20" from the centroid and 21.0 m at $05^h11^m30^s75-48^\circ27'22''.0$, 10" from the centroid. The nearby radio source to the south-east is identified with a galaxy 20.5 m at $05^h11^m44^s00-48^\circ29'51''.5$ and the source to the west has a blank optical field, see Robertson & Smith (1981).

0511-305—Complex source, an edge-brightened double with rotation-symmetry bending in the inner lobes. Models fitted by Ekers (1969) and SSM. Mapped by Wall & Cole (1973), SM, Slee (1977), Swarup (1984), and Ekers et al. (1989). (Note that the Culgoora-3 data refer to the south lobe only.) The structure changes with frequency indicating spectral index differences over the source. Galaxy 16.0 m at 05^h11^m36^s70 -30°32′14″.7, 33″ from the centroid along the radio axis, see Bolton et al. (1965). There is a long wisp from this galaxy to the west on the SERC J image. There are several nearby galaxies including one 18.0 m at 05^h11^m41^s70 -30°31′18″.9 near the midpoint of the two lobes.

0518–458—Complex source, Pictor A, an edge-brightened double (the west hotspot prominent) with a core component. Models fitted by Ekers (1969) and SSM. Mapped by Gardner & Whiteoak (1971), SM, Schwartz, Whiteoak, & Cole (1974), Slee (1977), and Christiansen et al. (1977). Galaxy 16.5 m at $05^{h}18^{m}23^{s}.59$ – $45^{o}49'42''.5$, 40'' from the centroid and 15'' west from the central peak. This is the same as the faint 19 m ID of Bolton et al. (1964) but our brighter magnitude is supported by V = 15.77 of Westerlund & Wall (1969) (z = 0.0350, Schmidt 1965).

0521-478—Double source with extended components; considered as one source although there is no bridge emission in the MOST image. Galaxy 19.0 m at 05^h21^m13^s77-47°49′23″9, 16″ from the centroid, along the major axis.

0523-327—Complex source, an edge-darkened double with reflection-symmetry bending of the outer lobes. Model fitted by SSM. Mapped by Slee (1977) and Ekers et al. (1989). Galaxy 16.0 m at 05^h23^m35^s87-32°44′49″9, 19″ from the centroid, see Bolton et al. (1965). In cluster AS 527 (ACO).

0534-613—Pair of unrelated point sources. Blank optical field for the two components. Some faint objects but no obvious ID near the centroid.

0540-617—Double source with extended components. Galaxy 16.0 m at 05^h40^m20^s92 -61°44′01″6, 8″ from the centroid, see Bolton & Savage (1977). In cluster A 3362 (ACO).

0540-628—Double source with extended components. Galaxy 15.5 m at 05^h40^m29^s82 -62°52′12″.6, 17″ from the centroid along the major axis, see Bolton & Savage (1977).

0543-479—Pair of unrelated sources, the south-west a point source, the north-east source slightly extended. Diffuse object 21.0 m at 05^h43^m32.83 -47°59′43″5, 2″ from the south-west source and blank optical field for the north-east source. There is a faint cluster near the north-east source.

0546-330*0546-329—Complex source, with extended lobes which trail off towards the east, a strong, narrow bridge and core emission. It is an edge-brightened double although not a powerful radio source. Mapped by Ekers et al. (1989), including high-resolution VLA observations of the core component. Galaxy 13.0 m at $05^h46^m37^s12-32^\circ59'31''1,30''$ from the centroid but at the radio core, see Shimmins & Bolton (1974) (z=0.037, this paper). There is a 15.5 m galaxy nearby at $05^h46^m44^s84-33^\circ00'58''.0$.

0558–388/0559–389—Pair of unrelated sources: the north-west source is a double with extended components, the south-east is a point source. Galaxy 15.5 m at 05^h58^m42^s24 –38°53′56″9, 26″ from the centroid of the north-west source and near the peak. In cluster AS 559 (ACO). Blank optical field for the south-east source.

0608-658—Double source with extended lobes, unusual in that the major axis of extension is perpendicular to the lobe separation, with an additional peak at the south end of the source. Galaxy 15.5 m at 06 h08 h50 h35 -65 h52 h6.8, 88" from the centroid at the southern peak of the radio structure, indicating a highly bent radio structure. Stellar object at 06 h08 h47 h85 -65 h0.35 h6. 20" from the centroid and between the two radio peaks, confirmed as a star by AAT spectroscopy.

0609-585—Pair of components: 0.54 Jy at 06^h09^m06^s8 -58°30′55″ and 0.135 Jy at 06^h09^m24^s9 -58°29′22″; both extended and considered to be lobes of one source. Galaxy 17.5 m at 06^h09^m13^s72 -58°30′28″.2, 27″ from the centroid of the double, along the radio axis. There is another galaxy nearby at 06^h09^m15^s73 -58°31′11″.3 with a core 18.0 m and a faint halo.

0610-316—Pair of sources, probably unrelated. The weak west source is extended with major axis toward the strong east point source. It is possible that this is a core-jet structure. Stellar object 18.5 m at 06^h10^m36^s99 -31°38′07″.4, 5″ west of the strong compact peak. This object was suggested by Peterson, Bolton, & Shimmins (1973) as a QSO with weak UV excess. Blank optical field for the weaker extended source to the west.

0611-557—Pair of unrelated sources, the north a point source, the south source extended. Blank optical field for the two components.

0616–487—Pair of unrelated sources, both extended, with a head-tail structure for the north-east source. Blank optical field for both sources. There is a galaxy 15.5 m at 06^h16^m55^s17–48°43′41″.5 between the sources, near the edge of the north-east source. This galaxy is the ID suggested by Bajaja (1970), but the radio morphology does not appear to support this ID.

0618-371—Double source with extended components. Models fitted by Ekers (1969) and SSM. Mapped by Schwartz et al. (1974), Slee (1977), and Ekers et al. (1989). db galaxy 14.5 m with the two cores at $06^{h}18^{m}16^{s}75 - 37^{\circ}10'18''.5$ and $06^{h}18^{m}17^{s}87 - 37^{\circ}10'18''.7$, around 6" from the centroid, see Bolton et al. (1965) (z = 0.0326, Burbidge & Burbidge 1972).

0620-526—Complex source with a strong core and bent edge-darkened lobes. Galaxy 15.5 m at 06^h20^m36^s77

 $-52^{\circ}40'03''.6$, 62" from the centroid but 7" from the radio peak, consistent with the head-double-tail morphology, see Tritton (1972) who gives z = 0.0511. (The image on the SERC J survey is obscured by a bright star so the ESO R survey was used and the b_J -magnitude is uncertain.)

 $06\overline{25}-54\overline{5}$ —Complex source, a double with edge-darkened lobes. The north lobe is bent sharply to the west. Galaxy 16.0 m at $06^{h}25^{m}48.87 -54^{\circ}30'39''.8$, 20" from the centroid and between the two inner peaks of the radio structure, see Savage (1976) (z = 0.052, this paper). In cluster A 3395 (ACO).

0629-729—Pair of unrelated sources, the west a point source, the weak east source slightly extended. Blank optical field for the two components.

0641-584—Double source with extended components. Galaxy 17.5 m at 06^h41 ^m31 *53 -58°27′03″0, 2″ from the centroid, see Savage et al. (1976).

0645-729—Double source with extended components. Blank optical field for the centroid.

0649-557—Double source with extended components. Galaxy 15.0 m at $06^{h}09^{m}23^{s}.72-55^{o}45'56''.6$, 5" from the centroid, in a cluster, see Savage et al. (1976) (z = 0.050, this paper).

0651-603—Single extended source with a weak extension to the north-west. db galaxy 16.5 m with the two cores at 06^h51^m15^s50 -60°18′33″.7 and 06^h51^m16^s09 -60°18′28″.9, around 11″ from the centroid, see Savage et al. (1976).

0655-486—Double source with unresolved components. The weak extension to the west is not reliable. Blank optical field for the centroid and the two components. There is a bright star nearby which obscures the position of the south-east radio peak with a diffraction spike but does not significantly obscure the centroid position.

0703-595—Double source with extended components and with the south component bent. Galaxy 18.5 m at $07^h03^m08.73-59^\circ34'53''3,21''$ from the centroid and near the midpoint of the lobes. There is a nearby galaxy 19.5 m at $07^h03^m07.59-59^\circ34'33''2,6''$ from the centroid.

0703-451—Double source with extended components and a weaker point source to the west (considered unrelated although nearby, and on the axis of the double). Mapped by SM. Galaxy 18.0 m at $07^{h}04^{m}01^{s}41-45^{\circ}08'31''.5$, 12" from the centroid, see Lü (1970a).

0707–359B*A—Complex source, an edge-brightened double, with two compact outer components, the south-east one stronger. Two weaker inner components extend away from the axis joining the outer components and give a slight twist to the structure. Mapped by SM and WS. Galaxy 20.0 m at 07h07m26f61-35°56′28″4, near the center of the extended inner double of the radio structure and the point of symmetry. This is far from the overall centroid, however, since the two outer components are asymmetric in flux. The 18.5 m object at 07h07m35f12-35°57′32″5, suggested by Schilizzi (1975), is 17″ from the centroid, but is stellar on the SERC J survey and hence less likely to be the correct ID. The 18.0 m object proposed by Lü (1970a) at 07h07m37f33-35°56′38″5 is also stellar and well away from the radio structure and so is rejected.

0713-371—Pair of unrelated point sources. Stellar object 20.0 m at 07^h13^m39^s.77 -37°10′43″.0, 3″ from the south-west source. There is also a 21.5 m object nearby at 07^h13^m39^s.25 -37°10′44″.4, 4″ from this source. Blank optical field for the north-east source.

0715-362—Complex source, an edge-darkened double

with a bent ridge-line. Models fitted by Ekers (1969) and SSM. Mapped by SM and Slee (1977). Galaxy 16.0 m at $07^{h}15^{m}20^{s}82 - 36^{\circ}16'33''3$, 34" from the centroid and between the two inner peaks, see Bolton et al. (1965) (z = 0.032, this paper).

0718-340—Double source with unresolved components. Model fitted by Ekers (1969). Mapped by Ekers et al. (1989) with the VLA image showing a core component. Galaxy 15.0 m at $07^h18^m56^s22-34^\circ01'24''.4$, 3" from the centroid, see Bolton et al. (1965) (z = 0.0297, Burbidge & Burbidge 1972).

0719-553—Single extended peak. Galaxy 19.5 m at $07^{h}19^{m}12^{s}35-55^{\circ}19'38''.0$, 3" from the centroid, in a faint cluster, see Hunstead et al. (1971) (z=0.216, Spinrad, Kron, & Hunstead 1979).

0724-375/0724-374—Pair of unrelated point sources. Blank optical field for the two components. For both components diffraction spikes from nearby bright stars may obscure faint objects.

0747-673—Pair of unrelated point sources. Blank optical field for the two components.

0807-389—Double source with extended components. Mapped by Slee (1977) and model fitted by SSM. Blank optical field at the centroid.

0809–492/0809–493—Pair of unrelated sources, the north-west source extended, possibly as a head-tail, the east a point source. Galaxy 16.5 m at 08^h09^m14^s38 –49°14′55″5, 8″ from the peak of the north-west source and consistent with the head-tail morphology. Stellar object 20.0 m at 08^h09^m41^s20 –49°20′46″4, 5″ from the south-east source. There is another object at 08^h09^m40^s64 –49°20′43″4, 2″ from the south-east source at the plate limit.

0809–499—Double source with slightly-extended components. Diffuse object 20.5 m at 08^h09^m57^s68 –49°58′50″3, 5″ from the centroid.

0815-675—Pair of unrelated point sources. Blank optical field for the two components.

0816-705—Complex source with a strong core and two edge-darkened lobes which are sharply bent. Galaxy 15.0 m, the brightest in a cluster, at $08^h16^m26^s30$ $-70^\circ30'17''.0$, 57'' from the centroid but near the radio peak, consistent with the head-tail morphology, see Savage et al. (1976) (z = 0.039, this paper). The two next brightest galaxies in the cluster, both 15.5 m, are at $08^h16^m15^s.31$ $-70^\circ30'23''.6$ and $08^h16^m59^s.47$ $-70^\circ28'48''.5$. It is possible that interaction with these affects the radio structure.

0819-300.4*B—Complex source, an edge-brightened double. Models fitted by Ekers (1969) and SSM. Mapped by Wall & Cole (1973), SM, and Slee (1977). Galaxy 17.5 m at $08^h19^m24^s.73 -30^\circ01'26''.5$, 12" from the centroid, see Bolton & Ekers (1966) (z = 0.086, Danziger & Goss 1983).

0842-571/0842-572—Pair of unrelated sources, the north-west source slightly extended, the south-east a point source. Blank optical field for the two components.

0843-336—Single elongated peak (with no small-scale structure in the MOST image). Model fitted by Ekers (1969). Mapped by Schwartz et al. (1974) and Danziger & Goss (1983). The latter find a compact nucleus from a high-resolution VLA image. Galaxy 11.5 m, NGC 2663, at $08^h43^m07^s93-33^\circ36'45''.5$, center 6" from the centroid, see Lü (1970a) (z=0.0073, Burbidge & Burbidge 1972).

0843-568—Double source with extended components. Gal-

axy 16.5 m at $08^{h}43^{m}25^{s}83 - 56^{\circ}53'39''.2$, 4" from the centroid (z = 0.062, this paper).

0851-314—Pair of unrelated point sources. Blank optical field for the two components.

0905–353—Complex source, asymmetric double structure with the west lobe edge-darkened and bent towards the south. There are two sources nearby, to the north and south of the east lobe, almost collinear, but it is considered that these sources are unrelated and that the alignment is coincidental. Galaxy 16.5 m at 09 h05 m45 s85 -35 23 15 1, 21 from the centroid, confused with a star to the south. There is a galaxy 18.0 m at 09 h05 m36 s02 -35 23 58 y9, which may be associated with the bend in the radio structure if it is in the same cluster.

0909-564—Single extended peak. Crowded field, $b=-5^{\circ}8$. Stellar object 19.5 m at $09^{h}09^{m}25^{s}68-56^{\circ}24'33''.2$, 4" from the centroid and stellar object 21.0 m at $09^{h}09^{m}25^{s}60-56^{\circ}24'27''.8$, 2" from the centroid, see Hunstead et al. (1971). The ID is taken as the brighter object but both are possible or the ID could be neither if they are both just stars in the crowded field.

0915-543—Double source with unresolved components, plus a nearby weak unrelated point source. Crowded field, b = -3.7, hence no clear ID.

0916-605—Pair of unrelated point sources. Crowded field, b = -8%, hence no clear ID.

0918–383—Asymmetric double source with the stronger north-west component extended and the south-east component unresolved. The components may be unrelated but the presence of bridge emission and the alignment of the north-west lobe major axis with the component separation implies that they are lobes of a single source. Galaxy 19.5 m at 09^h18^m14^s81 –38°22'04".6, 9" from the centroid of the extended north-west component. Blank optical field for the south-east component and the centroid of the whole source.

0930-399—Complex source, an edge-brightened double but with little bridge emission (below the 2% level on the MOST image). Crowded field, b = 8.4, hence no clear ID.

0932-372—Single extended peak but with bent structure. Galaxy 17.0 m at $09^{h}32^{m}03^{s}24-37^{\circ}14'46''2$, 10'' from the centroid (z = 0.064, this paper). There is a close companion galaxy 19.5 m at $09^{h}32^{m}03^{s}85-37^{\circ}14'44''.7$.

0936-622—Double source with slightly-extended components. db galaxy 19.5 m, or two close galaxies, in a faint cluster at $09^{h}36^{m}18^{s}10$ $-62^{\circ}15'37''.6$, 3" from the centroid. Crowded field, $b = -7^{\circ}.6$.

0945-370—Double source with extended components and a bent ridge-line. Galaxy 16.5 m at $09^{h}45^{m}45^{s}07-37^{\circ}01'29''.2$, 42" south from the centroid (z=0.041, this paper). There is another possible ID, a galaxy, probably a face-on spiral, 17.0 m at $09^{h}45^{m}41^{s}24-37^{\circ}00'14''.7$, 58" north-west from the centroid. Neither is close to the centroid, but the bending of the radio structure indicates that there may be interaction in the cluster which could account for the offsets. There is another galaxy 17.0 m at $09^{h}45^{m}48^{s}13-36^{\circ}58'18''3$.

0952-306—Double source with slightly extended components. Galaxy 19.5 m, in a faint cluster, at 09^h52^m21^s02 -30°39'07".9, 4" from the centroid, see Shimmins & Bolton (1974).

1002-320—Single extended peak. Mapped by Ekers et al. (1989), who find double structure in a high-resolution VLA image. Galaxy 18.0 m at 10^h02^m26.58 -32°02'07".1, 6" from

the centroid, see Shimmins & Bolton (1974). In cluster AS 626 (ACO).

1010-647—Single extended peak. Diffuse object 21.0 m at $10^{h}10^{m}49.98 -64°43'01''2$, 8" from the centroid along the radio axis, see Hunstead et al. (1971). Crowded field, b = -7.1.

1011-316—Double source with extended components. Diffuse object 21.0 m at 10^h11^m32.64 -31°38′27″.6, 8″ from the centroid. There is also a nearby 21.0 m object at 10^h11^m33.79 -31°38′20″.2, 9″ from the centroid but further from the radio axis, plus several others in a faint cluster.

1011–320—Double source with extended components. (The MOST "cuts" image is affected by the strong nearby source 1011–316, above.) Diffuse object 20.5 m at 10^h11^m36:03 –32°04′57″.6, 14″ from the centroid along the major axis. If the two components are considered as separate extended sources then they may be identified with two 21.0 m diffuse objects at 10^h11^m30.55 –32°05′24″.5, 5″ from the south-west source and 10^h11^m40.52 –32°04′30″.4, 7″ from the north-east source.

1015-385—Pair of unrelated point sources. Blank optical field for the two components.

1025-612—Complex source, an edge-brightened double with weak bridge and core emission. Crowded field, b=-3.3. Search made at core component but no clear ID.

1034-659—Pair of unrelated sources, the north-east a point source, the weaker south-west source extended. Crowded field, b=-6.9, hence no clear ID.

1051-344—Pair of unrelated point sources. Stellar object 20.0 m at 10^h51^m01^s80 -34°30′34″.1, 3″ from the south-west source and stellar object 21.0 m at 10^h51^m15^s.24 -34°29′39″.3, 3″ from the north-east source.

1056-360—Giant complex source, two extended edgedarkened lobes bent into a C-shape plus a third smaller component at the north lobe. There is a weak extension to the south and a weak unrelated source at the west end. Model fitted by SSM. Mapped by Slee (1977) and Ekers et al. (1989). The latter shows compact structure in a high resolution VLA image, at the two strongest peaks of the MOST image, and a weak core between them. Galaxy 17.0 m at 10^h56^m34^s15 -36°03′17″2, in a cluster on the ridge-line between the two main peaks of the radio structure, with a close companion galaxy 18.5 m at 10^h56^m33*34 -36°03'14"6, see Bolton & Shimmins (1973) (z = 0.070, this paper). There is an unusual galaxy 16.5 m at $10^{\text{h}}56^{\text{m}}35^{\text{s}}40 - 36^{\circ}04'22''.6$, near the strongest peak of the radio structure and a stellar object 21.0 m at $10^{h}56^{m}29.66 - 36^{\circ}01'56.6$, 1" from the second strongest peak. No ID for the weak point source at the north-west end of the radio structure.

1112-545—Double source with extended components. Crowded field, b = 5.4, hence no clear ID.

1123–351—Double source with extended components or a halo. Models fitted by Ekers (1969) and SSM. Mapped by Slee (1977) and Ekers et al. (1989). The latter shows a core component in the VLA image. Galaxy 14.5 m, at $11^h23^m26^s40$ –35°07′10″8, 34″ from the centroid, see Bolton et al. (1965) (z = 0.0329, Tritton 1972). In cluster AS 665 (ACO).

1136–678—Single extended peak. Mapped by SM and WS. There are some nearby unrelated point sources, to the east. Diffuse object 20.0 m at $11^h36^m07^s94$ –67°53′49″9, 8″ from the centroid but in a crowded field, b = -6°3.

1136-320—Single extended peak. 21.5 m object at

11^h36^m47^s49 –32°06′00″.9, 3″ from the centroid. There are several more objects of 21.5 m nearby, possibly a faint cluster.

1137–463—Complex source, a head-tail source with a bend in the tail plus weaker diffuse structure to the south-east and a nearby weak unrelated point source. Galaxy 16.0 m, at $11^h37^m27^s45$ – $46^\circ21'12''.6$, 52" from the centroid but near the radio peak and consistent with the head-tail morphology (z=0.068, this paper). In cluster AS 673 (ACO). There is a 17.0 m galaxy at $11^h37^m12^s25$ – $46^\circ25'48''.5$ near the end of the radio tail which may be associated with the twist in the tail if it is in the cluster. There is a stellar object 19.0 m at $11^h37^m35^s24$ – $46^\circ24'25''.5$, 3" from the weak point source to the south.

1141-391—Double source with extended lobes and a bent ridge-line. Galaxy 16.0 m at $11^h41^m38^s58-39^\circ05'36''\!3$, 34'' from the centroid, see Bolton & Shimmins (1973) (z=0.056, this paper). There is a companion galaxy, probably an edge-on spiral, 16.0 m at $11^h41^m40^s06-39^\circ05'48''\!2$, 14'' from the centroid and another nearby galaxy 16.0 m at $11^h41^m43^s86-39^\circ07'04''\!4$.

1143-317/1143-316—Pair of unrelated sources, both sources extended. Mapped by SM and Slee (1977). Blank optical field for the two components. The area of the south-west source is obscured by the halo of a bright star on the SERC J survey.

1144-379/1145-379—Pair of unrelated sources, the north-west a point source, the weaker south-east source extended. Stellar object 19.0 m at 11^h44^m30^s81 -37°55′31″5, 1″ from the north-west source, a confirmed BL Lac object, see Nicholson et al. (1979). Blank optical field for the south-east source, but there is an extended source further to the southeast, which may be associated, and a galaxy 16.5 m between the two extended sources.

1148-353—Single extended peak. Galaxy 18.5 m at $11^{h}48^{m}43.06-35^{\circ}20'24.3, 9''$ from the centroid, see Bolton & Shimmins (1973).

1152-694—Double source with extended components, or a halo. Crowded field, b = -7.4, hence no clear ID.

1153-807—Pair of unrelated point sources. Diffuse object 21.0 m at 11^h53^m21^s82 -80°44′35″9, 5″ from the south-west source and stellar object 19.5 m at 11^h53^m53^s95 -80°42′06″0, 3″ from the north-east source.

1158-652—Double source with extended components. Since the major axes of the two components are along the line of separation, they are considered to be lobes of a single source, although they are not linked with bridge emission in the MOST image. Crowded field, b = -3.2, hence no clear ID.

1225-816/1226-816—Pair of unrelated sources, the west source extended (with major axis toward the east source), the east a point source, plus a nearby weaker point source to the south of the east source. Blank optical field. There is a galaxy 20.0 m at 12^h26^m24*77 -81°38′20″4, 10″ from the centroid, if the two strong sources are considered as one source, but it is more likely that the sources are unrelated.

1234–723—Complex source, a strong core plus two diffuse edge-darkened lobes. There are weak projections from the core at right angles to the major axis and a weak extended source near the south end of the south lobe. Mapped by SM and WS. Galaxy 15.5 m at $12^h34^m05^s52 - 72^\circ19'00''.1$, 3" south of the strong central peak and 35" from the centroid with z = 0.0234, Tritton & Schilizzi (1973).

1234–490—Pair of unrelated sources, both sources extended. Galaxy 20.0 m at 12^h34^m39^s71 –49°04′17″0, 1″ from the south-west source and blank optical field for the north-east source.

1241-663A*B—Complex source, an edge-brightened double with wide lobes, a bridge and a core. There is a weaker edge-brightened double nearby with nearly the same position angle. (Such alignment may be significant, but it is not known whether the two sources are at the same distance and hence physically related.) Crowded field, b = -3%. Search made at core component but no clear ID.

1256-331/1257-332—Pair of unrelated point sources. Blank optical field for the two components.

1259-445—Double source with extended components. 21.5 m object at 12^h59^m38^s38 -44°30′33″.5, 12″ from the centroid. The ID of Lü (1970b), given at 12^h59^m37^s.72 -44°29′55″.6, was found to be stellar and is rejected as too far from the centroid.

1259-367—Single extended peak. Galaxy 20.0 m at $12^{h}59^{m}53^{s}87 - 36^{\circ}43'30''.2$, 7" from the centroid.

1302–325A*B—Complex source, a double with extended lobes, the south lobe edge-brightened and the north lobe with a projection to the west. The weak source at the east of the south lobe is probably unrelated. db galaxy 18.0 m, in a cluster, with cores at 13h02m12*75 -32°33′08″8 and 13h02m13*07 -32°33′13″4, 63″ from the centroid along the major axis.

1302-491—Core-halo source with the halo elongated (the nucleus and disk of an edge-on spiral, see below). The MOST image is the average of two observations, to increase the dynamic range. Model fitted by Ekers (1969) and mapped by Cameron (1971), Harnett & Reynolds (1985), and Whiteoak & Bunton (1985). Edge-on spiral galaxy, NGC 4945, 9.3 m at $13^{\rm h}02^{\rm m}31^{\rm s}$ -49°12′12″ (Lauberts 1982), see Mills et al. (1960) (z=0.0018, Burbidge & Burbidge 1972).

1304-748—Double source with extended components. Diffuse object 20.5 m at 13^h04^m48^s45 -74°53′36″.1, 10″ from the centroid and probably in a cluster, with several more objects of 20.0 m or 20.5 nearby, close to the centroid. The stellar object of Anguita et al. (1979), given at 13^h04^m57^s.0 -74°54′08″, is rejected.

1308–441—Giant complex source; an asymmetric double with diffuse lobes, a strong slightly bent bridge and a core component plus another hotspot on the bridge to the south-east of the core. See Jones (1987). The structure is unusual for a relatively weak radio source. Galaxy 14.5 m at $13^h08^m30^s44$ –44°06′45″1, 13″ from the centroid and at the strong central radio peak (z = 0.051, Jones 1987). There is a galaxy 18.5 m at $13^h08^m39^s95$ –44°07′57″.6, 5″ north of the other strong hotspot on the ridge line, but the fainter galaxy is probably not associated with this hotspot.

1312-593—Three close unrelated sources, the north-west source extended. Crowded field, $b=3^{\circ}1.21.5$ m object at $13^{h}12^{m}33^{\circ}49-59^{\circ}20'55''.1, 2''$ from the central source and no good ID for the other two sources.

1318-434A*B—Complex source, an edge-darkened double with strong inner lobes, bent outer lobes and a core component. The MOST image is affected by spurious structure at the 2% level at position angle 45° from the nearby, very strong source 1322-427 (the inner components of Cen A, see below). Mapped by SM, WS, and Smith & Bicknell (1983,

1986). Galaxy 12.0 m, NGC 5090, at $13^h18^m17^s36$ $-43^\circ26'34''0$, 5" from the central peak and 38" from the centroid, plus nearby edge-on spiral galaxy 13.0 m, NGC 5091, at $13^h18^m23^s04$ $-43^\circ27'36''9$, see Bolton & Shimmins (1973) and Smith & Bicknell (1983) (z = 0.011, Schilizzi 1975).

1322-427—Inner components of Centaurus A, a complex source showing a core component plus two (inner) lobes with bent structure, particularly in the north-east lobe. The MOST observation does not detect the outer lobes since they extend over several degrees. Centaurus A is the closest and hence one of the most widely studied radio galaxies so only a few references are given here. The outer lobes can be seen best in the images of Cooper, Price, & Cole (1965) and Haynes, Cannon, & Ekers (1983). The inner lobes were mapped by Gardner & Whiteoak (1971), Cameron (1971), Slee (1977), Christiansen et al. (1977), Schreier, Burns, & Feigelson (1981), and Slee et al. (1983). Dust-lane galaxy, 7.7 m, NGC 5128, at 13^h22^m33^s -42°45′24″ (Lauberts 1982) at the radio core. This is a famous source, one of the first extragalactic radio sources identified (see Bolton et al. 1949) (z = 0.0018, Palumbo et al. 1983).

1324-300—Double source with slightly extended components. Galaxy 18.0 m at 13^h24^m56^s67 -30°02′45″1, 9″ from the centroid, see Shimmins & Bolton (1974).

1332–336*1333–337*1334–339—All merged in a complex source, showing a strong slightly bent bridge or jet between two diffuse lobes. The bridge shows double structure (inner lobes) near the center, but not a distinct core. The lobes are edge-brightened although it is an intrinsically weak radio source. Mapped by Gardner & Whiteoak (1971), SM, Goss et al. (1977), Slee (1977), Swarup (1984), Killeen, Bicknell, & Ekers (1986), and Ekers et al. (1989). Galaxy 11.0 m, IC 4296, at $13^h33^m47^s52 - 33^\circ42'42''.4$, between the two inner radio peaks and 45" from the centroid, see Mills et al. (1960) (z = 0.0124, Sandage 1978). In cluster A 3565 (ACO).

1343–377—Triple with extended components, the east outer component the strongest. This could be a core plus two lobes, or possibly a head-tail with two hotspots in the tail. Galaxy 15.0 m at $13^h43^m27^s24 - 37^\circ43'16''.6$, 84" from the centroid and 6" from the east peak. This galaxy is in cluster A 3570 (ACO) so that an ID at one end with the head-tail morphology is plausible (z = 0.037, cluster redshift from ACO. An alternative ID is a diffuse object 21.5 m at $13^h43^m20^s32 - 37^\circ43'23''.8$, 8" from the centroid and 13 arcsec from the central component.

1355–416—Double source with unresolved components. Model fitted by Ekers (1969). Stellar object 15.0 m at $13^h55^m57^s30$ –41°38′19″.5, 3″ from the centroid, see Lü (1970a). Confirmed QSO, z = 0.313, Tritton (1971).

1411-657—Double source with unresolved components. Crowded field, b = -4.5, hence no clear ID.

1413–364—Double source with extended components. Models fitted by Ekers (1969) and SSM. Mapped by Slee (1977) and Ekers et al. (1989). Galaxy 17.5 m at 14^h13^m31^s83 –36°27'01.5, 8" from the centroid, see Bolton et al. (1965).

1416-516/1416-517—Pair of unrelated point sources. Mapped by SM. Blank optical field for north-west source and stellar object 21.5 m at $14^{\rm h}16^{\rm m}29\,{}^{\rm s}69-51^{\rm o}44'46''.3$, 1" from the south-east source. Crowded field, b=8% so possibly the object is an unrelated faint star.

1418-557—Single extended peak or close double. Crowded field, b = 4.6, hence no clear ID.

1421-382—Double source with unresolved components. Stellar object 17.0 m at $14^{h}21^{m}11^{s}90-38^{\circ}13'13''.4$, 3" from the centroid, see Lü (1970a). Confirmed as QSO, z=0.41 but from only one line, Tritton (1971).

1425–479—Double source with extended components (plus a nearby point source). Galaxy 17.5 m at 14^h25^m38^s68 –47°58′45″2, 6″ from the centroid.

1437–368—Double source with extended components. Mapped by Slee (1977) and model fitted by SSM. Galaxy 20.0 m at 14^h37^m27^s32 –36°52′40″5, 5″ from the centroid, in a faint cluster with a nearby galaxy 20.0 m at 14^h37^m26^s69 –36°52′35″2, 13″ from the centroid.

1451–364—Double source with extended components. Mapped by Slee (1977) and model fitted by SSM. Galaxy 20.0 m, in a faint cluster, at $14^h51^m21^s96$ – $36^\circ28'09''.1$, 22'' from the centroid, along the major axis. There is also a galaxy 20.0 m at $14^h51^m21^s98$ – $36^\circ27'38''.9$, 20'' from the centroid and a diffuse object 21.0 m at $14^h51^m20^s44$ – $36^\circ27'55''.3$, 5'' from the centroid. The object at $14^h51^m20^s40$ – $36^\circ28'02''.0$, suggested by Lü (1970b) was found to be stellar 18.5 m, 10'' from the centroid and is rejected as less likely to be the ID than the other objects above.

1452–367—Single extended source with diffuse edges. (The MOST "cuts" image was affected by the strong nearby source 1451–364, above.) Galaxy 16.5 m at 14^h52^m01^s44 –36°42′59″7, 30″ from the centroid.

1452–517—Complex source, showing a strong core component with two broad diffuse lobes, the north lobe edge-brightened and the south lobe edge-darkened, and a bridge or jet. Overall, it is edge-brightened although it is an intrinsically weak source, see Jones (1986). Galaxy 16.5 m at $14^h52^m21^s49$ –51°48'39".7, 4" from the strong core component and 95" from the centroid, see Jones (1986) (z = 0.016, this paper).

1511-315—Double source with extended components. Diffuse object 21.0 m at 15^h11^m59^s96 -31°33′27″0, 7″ from the centroid.

1516–477—Complex source, an edge-brightened double with a weak extension from the end of the west lobe. Crowded field, b = 7.9, hence no clear ID.

1518-530—Double source with unresolved components. Crowded field, $b = 3^{\circ}2$, hence no clear ID.

1532-495—Pair of unrelated sources, both sources extended. Crowded field, b = 4.9, hence no clear ID.

1541–383—Double source with slightly-extended components. Blank optical field for the centroid and the two components. There is a galaxy 18.5 m at 15^h40^m57^s42 –38°18′22″.5 near the weaker north-west component, but not close enough to be considered the ID.

1545–321—Complex source, with four components, two outer lobes and two inner lobes, all extended. On the southeast side the inner lobe is the stronger, whereas on the northwest side the outer lobe is the stronger. Mapped by Slee (1977) and model fitted by SSM. Galaxy 17.5 m at 15^h45^m49.00 –32°07′48″0, 13″ from the centroid.

1600–445B/A—Pair of unrelated point sources. Blank optical field for the south-west source and a diffuse object 20.5 m at 16^h00^m59^s.65 –44°33′20″.1, 1″ from the north-east source.

The field is crowded, b = 5?8, so the object is possibly an unrelated faint star.

1601-633*1602-633—Complex source, an edge-brightened double with bent lobes and a core component. Model fitted by Ekers (1969). Mapped by SM, Christiansen et al. (1977), and WS. Galaxy 17.5 m at $16^{h}02^{m}09.99-63^{\circ}21'21''.9$, 27" from the centroid and 13" from the central peak, along the radio axis, see Ekers (1970) (z = 0.0591, Christiansen et al. 1977). The galaxy is confused by nearby stars in the crowded field, b = -8.5.

1607-454/1607-453—Pair of unrelated sources, the south-west source slightly extended, the north-east a point source. Blank optical field for the two components. Crowded field, b = 4.4.

1610-605—Head-tail source with a long, narrow tail of low surface brightness and with bends. Mapped by Christiansen et al. (1977). Galaxy 14.5 m at $16^{\rm h}11^{\rm m}13.07-60^{\circ}32'26''0$, at the south-east end of the radio structure, consistent with the head-tail morphology but 5''.5 from the centroid, see Christiansen et al. (1977), z = 0.0162. A member of the same cluster A 3627 (ACO) as 1610-608 following.

1610-608*1611-607—Complex source, an edge-darkened double with strong inner lobes but no MOST core component, with the outer lobes bent into a wide-angle tail. Model fitted by Ekers (1969). Mapped by SM, Christiansen et al. (1977), and WS. Galaxy 13.5 m at $16^h10^m43!12-60^\circ46'54''3$, between the two inner radio peaks and 77" from the centroid, see Ekers (1970) (z = 0.0167, Christiansen et al. 1977). In cluster A 3627 (ACO).

1619-634—Complex source with extended lobes with rotation-symmetry bending, to the north of the east lobe and south of the west lobe. Galaxy 17.5 m at $16^{h}19^{m}56.06-63^{\circ}28'35.7$, 13'' from the centroid. Crowded field, b = -9.9.

1623-434—Double source with extended edge-darkened lobes and slight bending. Crowded field, b=3.7, hence no clear ID.

1623-420A*1623-421/1623-420B—Pair of unrelated sources, the south-west merged source is a large edge-bright-ened double (with a weak source nearby) and the north-east source is extended. Crowded field, b = 4.7, hence no clear IDs.

1637–771—Complex source, an edge-brightened double but with a weak extension to the south-east past the hotspot, with core emission and a bend in the south lobe. Model fitted by Ekers (1969). Galaxy 16.0 m at $16^h37^m05^s24-77^o10'08''1$, 12" from the centroid, see Ekers (1970) (z = 0.0438, Burbidge & Burbidge 1972).

1717-620—Double source with unresolved components. Blank optical field for the centroid and the two components.

1720-476—Pair of unrelated sources, the west source slightly extended, the east a point source. Crowded field, b = -6.5, hence no clear ID.

1721-568—Complex source, a double with extended lobes and bridge emission with the ridge-line bent, plus a nearby unrelated point source. Crowded field, $b=-11^\circ$ 8, $l=334^\circ$ 3, hence no clear ID. There is a galaxy 19.0 m at $17^h21^m54^s69-56^\circ51'58''$ 2 but this is 51'' from the centroid and away from the bent ridge-line of the source.

1733-565B*A—Triple source with extended lobes, bridge and core emission. Model fitted by Ekers (1969). Mapped by Schwartz et al. (1974), SM, Christiansen et al. (1977), and

Hunstead et al. (1982). Galaxy 18.0 m at $17^{h}33^{m}21^{s}48 - 56^{\circ}32'16''.6$, 10" from the centroid and 5" from the central peak of the radio source, see Hunstead et al. (1982), z = 0.0985. The field is crowded, b = -3.0, and the galaxy image is confused by a star.

1733-712/1733-713—Pair of unrelated point sources (plus a third weak point source near the north source). Diffuse object 20.5 m at 17^h33^m28*57-71°17′13″7, 4″ from the northwest source and blank optical field for the south-east source.

1737-609—Double source with extended components. Model fitted by Ekers (1969). Diffuse object 20.0 m at $17^{h}37^{m}28^{s}82 -60^{\circ}53'51''.4, 5''$ from the centroid.

1744-630—Pair of unrelated sources, the north source extended, the south a point source. Blank optical field for the two components.

1749-508/1750-508—Pair of unrelated sources, the west a point source, the east source slightly extended. Crowded field, b = -12.4, l = 341.8, hence no clear ID.

1750-433/1750-434—Pair of unrelated sources, the west a point source, the south-east source extended (or a close double). Crowded field, $b = -8^{\circ}8$, hence no clear ID.

1756-348—Double source with extended components. Crowded field, b = -5.6, hence no clear ID.

1758–473—Triple with strong core and extended edge-darkened lobes. Stellar object 18.5 m at $17^h58^m21^s51$ –47°19′30″7, 7″ from the centroid and 3″ from the central peak plus close stellar object 18.5 m at $17^h58^m21^s39$ –47°19′34″7. Crowded field, $b = -11^s9$, $l = 345^s5$, so possibly these objects are unrelated stars.

1815-546—Single extended peak (or close double). Blank optical field. There is a stellar object 19.0 m at 18^h15^m59^s89 -54°36′22″.8, 6″ from the centroid, but this is likely to be a foreground star.

1820-774—Pair of unrelated sources, the south-west source slightly extended, the north-east a point source. Galaxy 20.0 m at 18^h20^m31^s58 -77°29'44".4, 2" from the south-west peak and blank optical field for the north-east peak. If the two components are considered as one source then the ID may be a diffuse object 20.5 m at 18^h20^m46*83 -77°29'15".3, 2" from the centroid. The ID of Anguita et al. (1979), a weak UV-excess stellar object, 18.5 m given at 18^h20^m42*5 -77°29'06", is rejected.

1821-583—Asymmetric double, or core-jet structure, with a strong unresolved peak and a weaker edge-brightened extended component. Mapped by SM. Diffuse object 20.0 m at 18^h21^m19^s.63 -58°19′19″3, 14″ west of the centroid. No good ID at the strong peak.

1829-778—Single extended peak. Diffuse object 20.5 m at $18^{h}28^{m}59.04-77^{\circ}50'24''.5$, 7" from the centroid.

1837-365/1838-365—Pair of unrelated sources, both sources extended. The west source is double. Crowded field, b = -13.9, l = 358.8, hence no clear ID.

1840-404—Single extended peak. Crowded field, b = -15.9, l = 355.3, hence no clear ID. There is a stellar object 21.0 m at $18^h40^m59.22 -40^\circ25'12''.8$, 11'' from the centroid but this is likely to be a foreground star. The ID of Lü (1970b), with a 19.2 m object given at $18^h40^m58.78 -40^\circ25'30''.6$, is rejected.

1846-631/1846-632—Three unrelated sources; the north and south are point sources; the slight extension of the middle source is uncertain, and it is not included in the confirmed

sample. Mapped by SM. Blank optical field for the three components. The ID of Tritton & Schilizzi (1973), a galaxy 16.0 m at 18^h46^m06^s.44 -63°07′59″.1, is 38″ east of the north point source and so is rejected.

1849–397—Double source with extended components. Galaxy 19.5 m at 18^h49^m57^s92 –39°45′10″2, 3″ from the centroid.

1902-578—Pair of unrelated sources, the west source extended, the east a point source. Blank optical field for the two components.

1908–623/1909–624—Pair of unrelated sources; the north-west is a point source; the south-east source appears extended, but this may be spurious and the source is not included in the confirmed sample. Galaxy 20.0 m at 19^h08^m40.803 –62°23′36″.5, 4″ from the north-west source and blank optical field for the south-east source.

1910–800—Complex source, a double with the north lobe edge-brightened and with weak bridge emission. Diffuse object 21.0 m at 19^h10^m40.903 –80°04′28″.6, 7″ from the centroid.

1919-551—Pair of unrelated point sources. Blank optical field for the two components.

1921–577—Complex source, an edge-darkened double with a bent ridge-line, particularly in the south lobe. The nearby point source may be linked with the double, but the reliability below the 2% level is doubtful. Galaxy 16.5 m, in a cluster, at 19^h21^m53*30 –57°46′16″1, 14″ from the centroid, see Wall & Cannon (1973). There is a nearby galaxy 19.0 m at 19^h21^m56*01 –57°46′03″2.

1922-627—Double source with unresolved components. Model fitted by Ekers (1969). Stellar object 17.5 m at 19^h22^m53^s55 -62°45′37″1, 4″ from the centroid.

1925-746/1926-747—Pair of unrelated sources, the north-west source slightly extended, the south-east a point source. Diffuse object 21.0 m at 19^h25^m38^s03 -74°40′38″5, 2″ from the north-west source and blank optical field for the south-east source.

1929–397—Double source with extended components. Model fitted by SSM. Mapped by Slee (1977) and Ekers et al. (1989). The latter shows a core component in the VLA image. Galaxy 15.5 m at 19^h30^m00.06 –39°46′52″1, 13″ from the centroid plus nearby galaxy 16.5 m at 19^h29^m58.32 –39°46′38″2, see Bolton & Shimmins (1973). In cluster AS 820 (ACO).

1936-357—Pair of unrelated point sources. Galaxy 17.0 m at 19^h36^m01^s93 -35°47′42″.9, 2″ from the west source and blank optical field for the east source.

1939–406/1940–406—Pair of unrelated sources, the west a point source, the east source a double with extended components (plus two weak point sources nearby). Models fitted by Ekers (1969) and SSM. Mapped by SM and Slee (1977). Blank optical field for the west source. Galaxy 20.0 m at 19^h40^m26^s30 –40°37′24″4, 9″ from the centroid of the east source. In cluster A 3646 (ACO). The ID of Schilizzi (1975) was found to be stellar, 19.0 m, at 19^h39^m48^s22 –40°36′42″9 and is rejected. The ID of Lü (1970b) was found to be stellar, 19.0 m, at 19^h40^m23^s66 –40°37′52″6 and is also rejected.

1942-316/1943-317—Pair of unrelated sources, the north-west source extended, the south-east a point source. Blank optical field for the two components.

1945-304—Double source with extended components. 21.5 m object at $19^{h}45^{m}12^{s}07 -30^{\circ}27'37''.2$, 4" from the cen-

troid plus a nearby object 21.5 m at $19^{\text{h}}45^{\text{m}}12^{\text{s}}10 - 30^{\circ}27'43''.5$, 7" from the centroid.

1951-310A/B—Pair of unrelated sources, the west a point source, the east source extended (or double) plus a third weaker point source to the south. Blank optical field for all the components.

1951–501A/B—Pair of unrelated sources, the north a point source, the south source a double with slightly extended components. Mapped by SM. Blank optical field for the north source. Galaxy 20.0 m at 19^h51^m23^s61 –50°10′21″7, 8″ from the centroid of the south source. The ID of Tritton & Schilizzi (1973) was found to be stellar, 20.0 m, at 19^h51^m21^s90 –50°05′43″7 and is rejected. The ID of Lü (1974) is also rejected. There is a galaxy 17.0 m at 19^h51^m28^s92 –50°07′47″7 between the two sources.

1954–552—Core-halo source with the weak halo elongated and bent. Model fitted by Ekers (1969) and mapped by Christiansen et al. (1977). Galaxy 15.0 m in a cluster, see Lü (1974) (z = 0.0600, Whiteoak 1972). There is a bright stellar object at $19^{\rm h}54^{\rm m}18^{\rm s}86$ –55°17'41".9, near the nucleus of the galaxy (with diffraction spikes), which is a G0 star (Westerlund & Smith 1966).

1954–356—Pair of extended sources, considered as the lobes of a double. (The MOST "cuts" image is badly affected by the nearby strong source 1955–357.) Galaxy 20.0 m at 19^h54^m34^s24 –35°39'11".1, 5" from the centroid.

1955-470—Double source with extended components. Blank optical field for the centroid and the two components.

1953-879/2007-879—Pair of unrelated sources, the west source a double with extended components, the east a point source. Diffuse object 21.5 m at 19^h53^m41.8 -87°55′52″3, 2″ from the centroid of the west source and diffuse object 21.0 m at 20^h07^m24.2 -87°58′29″4, 4″ from the east source.

2005–428/2005–429—Pair of unrelated point sources. Stellar object 21.0 m at 20\(^h05\)^m38\(^s23-42\)^o51'53".5, 2" from the north source and blank optical field for the south source.

2006-566—Giant, diffuse source of low surface-brightness with a twisted ridge-line (plus several weak unrelated sources). This is one of the largest source in the sample. Model fitted by Ekers (1969). Mapped by SM, WS, and Goss et al. (1982). The nearby MRC source 2007-568, to the south, has head-tail morphology. Galaxy 17.5 m at $20^{\text{h}}06^{\text{m}}22^{\text{s}}18-56^{\circ}36'49''.7, 58''$ from the centroid but near the center of the large bent radio structure, see Goss et al. (1982), z=0.0576. In clusters A 3667 and AS 854 (ACO). Within the radio contours are two nearby galaxies, 17.5 m at $20^{\text{h}}06^{\text{m}}15^{\text{s}}.13-56^{\circ}34'58''.8$ and S0 17.0 m at $20^{\text{h}}06^{\text{m}}19^{\text{s}}.78-56^{\circ}39'03''.1$. There is a galaxy 17.0 m at $20^{\text{h}}07^{\text{m}}27^{\text{s}}.48-56^{\circ}53'04''.4, 35''$ from the centroid of the nearby radio source 2007-568, consistent with the head-tail morphology (z=0.053, Goss et al. 1982).

2013-308/2013-307—Pair of unrelated sources, the south-west source an edge-brightened double, the north-east a point source. Mapped by Ekers et al. (1989). Galaxy 16.5 m at 20^h13^m07.67 -30°50′46″2, 8″ from the centroid of the south-west source, see Shimmins & Bolton (1974). Stellar object 19.5 m at 20^h13^m23.16 -30°44′34″5, 3″ from the north-east source, see Jauncey et al. (1982).

2013-557—Giant complex source, with a strong core and diffuse, edge-darkened lobes showing rotation symmetry. Model fitted by Ekers (1969). Mapped by SM and WS. Galaxy

16.5 m at $20^{\text{h}}14^{\text{m}}06\overset{\text{s}}{.}21 - 55^{\circ}48'51''.6$, 2" from the centroid and at the strong central peak of the radio structure, see Westerlund & Smith (1966) (z = 0.0608, Whiteoak 1972).

2014–312—Complex source consisting of four linked components, the west two a close double with extended components and the other two point sources. The structure is unusual for a single source so it may be three unrelated sources or a cluster. Diffuse object 21.0 m at 20^h13^m58^s86 –31°12′17″9, 6″ from the centroid of the west source, diffuse object 21.0 m at 20^h14^m09^s20 –31°13′10″5, 13″ from the central source and diffuse object 20.5 m at 20^h14^m16^s10 –31°11′38″3, 13″ from the east source.

2020-575—Single extended peak, which has been resolved into an edge-brightened double with strong core in a recent image by the Australia Telescope (R. W. Hunstead & A. M. Burgess 1991, private communication). The AT core is 8" south of the MOST centroid. Diffuse object 21.0 m at $20^{h}20^{m}21^{s}96 -57^{\circ}33'19''.1$, 4" from the MOST centroid was initially examined, but the identification is now clearly a 18.5 m compact, high-luminosity galaxy at $20^{h}20^{m}21^{s}60 -57^{\circ}33'26''.9$ within 2" of the AT core; z = 0.352 (Hunstead & Burgess 1991, private communication).

2022-537/2022-538—Pair of unrelated sources, the north-west source extended, the south-east a point source. Blank optical field for the two components.

2026–413/2026–414—Pair of unrelated sources, the north source extended, the south source a double with extended components. Blank optical field for the north source and diffuse object 21.5 m at 20^h26^m15.06 –41°28′51″6, 14″ from the centroid of the south source.

2028-732—Double source with unresolved components. Model fitted by Ekers (1969). Stellar object 18.0 m at $20^{\text{h}}28^{\text{m}}24^{\text{s}}95$ –73°14′13″2, 13″ from the centroid; confirmed as a QSO, z = 0.455 (R. W. Hunstead & A. M. Burgess 1991, private communication).

2030–378A/B—Pair of unrelated sources, the south-west a point source, the north-east source a double with unresolved components. Stellar object 21.5 m at 20^h30^m01^s13 –37°52′26″2, 3″ from the south-west source and nearby object 21.5 m at 20^h30^m01^s24 –37°52′19″1, 5″ from the south-west source. Diffuse object 21.0 m at 20^h30^m27^s65 –37°48′05″2, 8″ from the centroid of the north-east source. There is a galaxy 17.0 m at 20^h30^m28^s24 –37°48′58″1, at the south end of the north-east source but this is too far from the source centroid.

2036-612—Pair of unrelated point sources. Blank optical field for the two components.

2040-631/2041-631—Pair of unrelated point sources. Blank optical field for the west source, diffuse object 21.0 m at $20^{h}41^{m}09^{s}29-63^{\circ}11'21''9$, 2" from the east source.

2041–604—Single extended peak. The E flag in the MRC was possible only because the source is strong and the PA lies away from N and E. Blank optical field. There is a galaxy 17.5 m at 20^h41^m12^s88 –60°30′21″.9 but this is 46″ from the centroid and outside the radio structure. This galaxy was suggested by Westerlund & Smith (1966) but rejected by Véron (1977). The object suggested by Lü (1974) is also rejected as it is even further from the centroid.

2046-376—Double source with unresolved components. It was flagged E in MRC but the 843 MHz flux density is too weak for the confirmed sample. Comparison with the 408

MHz flux density suggests a steep spectrum or variable core. Blank optical field. There is a stellar object 19.0 m at $20^{h}46^{m}43.84 - 37^{\circ}40'49''.4$ but this is 12'' north of the centroid.

2048-572—Pair of unrelated sources, the east a point source. The west source has a weak projection linked to it extended at right angles to the separation. Mapped by Danziger et al. (1981). Galaxy 12.0 m, IC 5063, S0 with a dust-lane and in a cluster, at $20^{\rm h}48^{\rm m}12^{\rm s}78-57^{\circ}15'31''\!\!/8$, 19" south-east from the east peak and 76" from the centroid of the double, see Mills et al. (1961) and Danziger et al. (1981) (z=0.0113, Whiteoak 1972). The radio morphology is unusual for a radio galaxy double and the ID is probably associated with the east source only, with the west source unrelated. Blank optical field for the west source.

2052-736/2053-736—Pair of sources, the west source a double with slightly extended components and the east source extended. Considered to be a complex double with the west lobe edge-darkened and no bridge or core emission, but possibly two unrelated sources with centroids at 20^h52^m01^s5-73°39'45" and 20^h53^m11^s1-73°39'59". No good ID near the centroid of the double. Diffuse object 21.0 m at 20^h51^m59^s16-73°39'36".4, 10" from the centroid of the west source and blank optical field for the east source.

2055-650/2056-650—Pair of unrelated point sources. Blank optical field for the two components.

2122-660—Pair of unrelated point sources. Blank optical field for the two components.

2130–538—Complex source, consisting of four extended components plus bridge emission in a bent structure. Unusual structure for a single source so it may be two or more sources superposed. Model fitted by Ekers (1969) and mapped by SM. Two galaxies, both 15.5 m: at $21^h30^m38^s32 -53^\circ47'40''.5$, 96'' from the centroid and between the two northern peaks, and at $21^h30^m49^s18 -53^\circ51'33''.6$, 111'' from the centroid and between the two strong southern peaks, see Ekers (1970) (z = 0.0781 and 0.0763, respectively, Whiteoak 1972). In cluster A 3785 (ACO). The radio structure is attributed to both galaxies in the cluster and presumed to be bent by interaction between them. The stellar ID of Lü (1974) is rejected.

2132-554—Double source with extended components. Blank optical field for the centroid and the two components.

2140-568—Point source plus weak extended projection or an asymmetric double. Low 843 MHz flux density compared to the MRC 408 MHz value, hence steep spectrum or a variable core. Although flagged E in MRC and clearly extended, it is too weak for inclusion in our confirmed sample. Galaxy 16.0 m at 21^h40^m27^s79 -56°51′06″9, 2″ from the strong peak.

2143-556/2144-556—Pair of unrelated point sources. Stellar object 19.5 m at 21^h43^m53^s:10-55°37′04″.1, 4″ from the north-west source and stellar object 19.5 m at 21^h44^m17^s63-55°40′19″.4, 3″ from the south-east source.

2147–721—Three unrelated sources, the west source much stronger than the other two, the middle source slightly extended. Blank optical field for the three components.

2147-555*2148-555—Complex source, outer lobes edge-darkened, with strong inner lobes, a core component and slight rotation-symmetry bending of the ridge-line. Galaxy 14.5 m, at $21^{h}48^{m}03^{s}98-55^{\circ}34'18''.2$, 30" from the centroid and 6" from the central peak of the radio structure, see Savage et al. (1976). In cluster A 3816; z = 0.035 cluster redshift (ACO).

2151–461—Complex source similar to 2356–611 and 3C 234, with edge-brightened outer lobes, extended inner lobes, and a projection to the north-west. There is no bridge between the lobes. Alternatively, two unrelated sources. One is 0.93 Jy at centroid 21^h51^m05^s8 –46°07′37″, a double extending 1.′8 at PA 51°; the second is 0.36 Jy at 21^h51^m25^s3 –46°04′04″, 1.′7 at PA 48°. Galaxy 17.5 m at 21^h51^m12^s80 –46°06′43″, 17″ from the centroid of the whole source and near the inner end of the south-west component. This ID implies an unusual asymmetric source. There is no good ID for the north-east component as a separate source. There is a galaxy 19.5 m at 21^h51^m09^s24 –46°07′38″, 36″ from the centroid of the south-west component but this is off the axis of the component.

2152–325—Three unrelated point sources. Blank optical field for the three components.

2152-699/2153-699—Pair of strong sources. The west source is a double with slightly extended components. Model fitted by Ekers (1969). Mapped by Schwartz et al. (1974), SM, Christiansen et al. (1977), and Tadhunter et al. (1988). The east source is known to be extended in the same PA from a higher resolution (23") Fleurs observation at 1415 MHz. Galaxy 14.0 m at $21^h52^m58^s50-69^\circ55'41''.2$, 2'' from the centroid of the west source, see Westerlund & Smith (1966) (z=0.0266, Burbidge & Burbidge 1972). Galaxy 20.0 m at $21^h53^m40^s86-69^\circ56'11''.4$, 2'' from the east source.

2154–325A/B—Pair of unrelated point sources. Blank optical field for the west source. Stellar object 17.0 m at 21^h54^m42.08 –32°33′43″6, 5″ from the east source, see Peterson & Bolton (1973) and Jauncey et al. (1982) who claim optical variability.

2156-374—Double source with unresolved components. Blank optical field. There is a stellar object 15.0 m at 21^h56^m51^s83 -37°24'48".4, 13" from the centroid, confirmed as a star by AAT spectroscopy.

2158–380—Double source with unresolved components. Mapped by Fosbury et al. (1982) and Ekers et al. (1989). Galaxy 14.5 m at $21^h58^m17^s19-38^\circ00'52''.8,35''$ from the centroid but near the midpoint of the double, see Bolton & Shimmins (1973) (z=0.0333, Fosbury et al. 1982).

2215-508—Single point source. This source should not have been flagged as extended in the MRC. Stellar object 18.5 m at 22^h15^m09.65 -50°53'43".9, 2" from the centroid.

2217–505/2218–505—Pair of unrelated sources, the west source a double with extended components, the east a point source. Mapped by SM. Diffuse object 20.5 m at 22^h17^m57^s87 –50°33′32″3, 4″ from the centroid of the west source and blank optical field for the east source. Note that there is a faint cluster A 3868 (ACO) near both sources. The stellar object suggested by Lü (1970b) for the west source is rejected as too far from the centroid.

2225–308—Double source with slightly-extended components. A VLA image by Ekers et al. (1989) shows a compact south-east source in line with a head-tail source to the north-west, but apparently separate sources. Galaxy 16.5 m, at 22^h25^m01.08 –30°49′03″.1, 5″ from the centroid, see Shimmins & Bolton (1974). In cluster A 3880 (ACO). A second galaxy 14.5 m at 22^h25^m04.94 –30°49′50″.9 is 7″ south of the south-east peak and 68″ from the centroid.

2225-619—Double source with unresolved components. Blank optical field. There is a stellar object 16.0 m at

22^h25^m54^s08 -61°55′48″8, 13″ from the centroid, confirmed as a star by AAT spectroscopy.

2226-411/2226-410—Pair of unrelated sources, both sources extended. Stellar object 20.0 m at 22^h26^m22^s12 -41°06′55″1, 2″ from the south-west source, see Lü (1970b), optically variable. Blank optical field for the north-east source.

2227–665—Point source plus a weak extension, or an asymmetric double. Blank optical field. There is a stellar object 17.0 m at 22^h27^m34^s97 –66°34′21″.0, 10″ from the centroid.

2232–488/2232–489—Pair of unrelated point sources. Stellar object 17.0 m at 22^h32^m11^s40–48°51′31″2, 2″ from the north-west source, see Savage et al. (1976). Blank optical field for the south-east source.

2238-609/2239-609—Group of four close sources, the most southerly source extended and the other three point sources. The south-east two are linked. Possibly separate sources in a cluster. Mapped by SM. Blank optical field for the two north-west sources and a diffuse object 20.5 m at 22h39m15s93-60°59'44".5 between the two peaks of the southeast linked pair, in a faint cluster. The stellar ID of Lü (1974) is rejected as it is too far south outside the radio structure.

2243-529/2243-530—Pair of unrelated point sources. db galaxy with nuclei 14″.1 apart, or two close galaxies each 17.0 m, at $22^{h}43^{m}12.76-52^{\circ}59'03.4$ and $22^{h}43^{m}13.16-52^{\circ}59'17.0$, centered 5″ from the north-west source, and 21.5 m object at $22^{h}43^{m}47.00-53^{\circ}05'11.0$, 1″ from the south-east source.

2252-529/2252-530—Pair of unrelated point sources. Blank optical field for the two components. There is possibly an object, at the plate limit, at 22^h52^m51^s30 -53°01'45".4, 4" from the south-east source, see Lasker & Smith (1974). The ID suggested by Lü (1974) as a 17.5 m galaxy at 22^h52^m49^s96 -53°01'21".7 is found to be stellar and is rejected as too far from the components.

2302–713—Double source with unresolved components, plus a weak unrelated extended source on the same axis. Stellar object 17.0 m at $23^h02^m20^s28$ –71°19′23″.0, 11″ from the centroid, see Peterson & Bolton (1972a). Confirmed QSO, z=0.384, Peterson & Bolton (1972b). Blank optical field for the weak source to the north-east.

2316–423—Complex source, a strong extended peak with weak diffuse, edge-darkened structure to the north and east. A high-resolution VLA image (Hjellming & Bignell 1982) shows double structure in the head. Nearby there is a triple, low-brightness source 2315–425 of size 6′, plus several more weak sources. Galaxy 14.5 m, at 23^h16^m20^s94 –42°23′14″1, 74″ from the centroid but only 19″ from the strong radio peak and consistent with the head-double-tail morphology, see Wall & Cannon (1973). In cluster, AS 1111 (ACO). There is a 15.0 m galaxy at 23^h15^m11^s11 -42°29′57″3, 9″ from the centroid of the nearby extended source 2315–425.

2320-613—Double source with extended, edge-brightened lobes. Blank optical field. There is a stellar object 17.0 m at 23^h20^m37.03 -61°20′36″6, 13″ from the centroid, confirmed as a star by AAT spectroscopy.

2331-493/2331-492—Pair of unrelated sources, the north a point source, the south source extended with a weak source nearby. Blank optical field for the components.

2340-586—Double source with slightly extended components. Galaxy 18.5 m, in a cluster, at 23^h40^m46^s39 -58°40'31".7, 7" from the centroid, see Bolton & Savage

(1977). The ID of Wall & Cannon (1973) with the brightest galaxy in the cluster, to the north-east, is rejected.

2341-509—Double source with unresolved components. Stellar object 21.0 m at 23^h41^m57^s71-50°57′17″.0, 6″ from the centroid.

2356–611*2356–612A*B—Giant complex source, an edge-brightened double with two compact outer hotspots and two extended inner lobes, with a projection to the west. Model fitted by Ekers (1969). Mapped by Schwartz et al. (1974), SM, and Christiansen et al. (1977). Galaxy 17.0 m at $23^h56^m29^s44$ –61°11'41"8, 31" from the centroid and between the two inner radio lobes, see Westerlund & Smith (1966) (z = 0.0964, Whiteoak 1972).

2357–830—Pair of sources, the south a point source, the north source extended with a weak bent projection. Not related as lobes of a single source but may be two objects in the same cluster. Pair of galaxies, each 16.0 m, at 23^h56^m41^s63 –83°07′34″6, 16″ from the south source and 23^h58^m07^s73 –83°04′36″3, 24″ from the centroid of the north source.

2359–691—Four strong components, consisting of two doubles with all components unresolved (plus two weak sources nearby to the north). Considered to be two separate sources. No good ID at the four main components except for a stellar object 19.0 m at 23^h58^m59^s67 –69°05′52″.1, 5″ from the most westerly component. Considering the field as two doubles, there are two stellar objects: 19.0 m at 23^h59^m07^s.12 –69°05′54″.4, 7″ from the centroid of the north-west double source and 17.0 m at 23^h59^m33^s31 –69°08′44″.4, 10″ from the centroid of the south-east double source.

7. A CONFIRMED EXTENDED SAMPLE AND ITS

COMPLETENESS

In this section we consider a confirmed MRC extended sample which we define as having (1) angular size larger than 0.5, and (2) flux density greater than 0.4 Jy at 843 MHz (\S 3 and Table 1). The 193 sources in this sample are flagged in Table 1 with \P .

The new MOST data have clarified the morphology of MRC sources flagged as multiple (M) or extended (E, C, A) leading to some of these sources being excluded from the confirmed sample. Of the 138 sources with an M designation 103 are random associations, consistent with the number expected by chance from the MRC source density. However, the remaining M entries (and some groups of E sources) comprise genuine double and triple sources (marked with an asterisk in Table 1), which have components that are given separate listings in MRC. These entries will produce a spurious clustering signal in the two-point correlation analysis of the MRC (Shaver & Pierre 1989). Of the 201 MRC sources with an E, C, A, or T designation, 48 are found to be close alignments of unrelated sources in which blending has mimicked a single extended source. Of the total 339 MRC sources observed, only four have inappropriate extension flags: 0254-484 (E) and 2215-508 (E) are isolated point sources while 1846-631A (EM) and 2218-505 (AM) are point sources confused by close companions.

The confirmed MRC extended sample is not complete to the limits of our criteria (0.4 Jy and 0.5) because the flagging procedures in the MRC (Large et al. 1981) were conservative,

emphasizing reliability and requiring confirmation of extension. Uniform procedures of determining flux density and detecting extension were applied to the whole MRC survey, and in only a few cases (T flags) were results modified because additional information was available.

Figure 3 plots the flux density and angular size, as determined from the MOST observations, for the sources in the confirmed sample. For strong sources the distribution continues to smaller sizes without a sharp cutoff, but for weaker sources (less than 1 Jy) there is a sharp decrease in the number of sources below 1.5. This deficit of sources smaller than 1.5 is best seen in the histogram of angular sizes (Fig. 4) in which the counts peak well above the 0.5 limit of the sample.

The histogram of flux densities for sources in the confirmed sample (Fig. 5) exhibits a cutoff in flux density below ~ 0.6 Jy. This corresponds, in part, to the MRC limit of 1.0 Jy at 408 MHz which gives 0.6 Jy at 843 MHz for a spectral index of -0.7. However, it should be noted that the quoted limit of completeness in the MRC refers to the peak flux density not the total flux density of extended sources.

There is a deficit of sources of low surface brightness in Figure 3 at large angular size (>10') and low flux density (<1.5 Jy). The large diffuse sources were not included in the MRC if the fitted peak flux density was below the 0.7 Jy cutoff. A known example is 1401–33 (near NGC 5419) which has an integrated flux density of 6.5 Jy and a peak of 0.6 Jy at 408 MHz (McAdam & Schilizzi 1977; Goss et al. 1987) but the diffuse structure was missed by the MRC.

The distribution of position angles of the sources in the confirmed sample is given in Figure 6. There is an apparent deficit of sources with position angles near 0°, 90°, and (possibly) 180°. With the cross-type telescope used for the MRC, extension north-south or east-west was harder to detect than extension in the diagonal direction. The effect persists when the smaller sources of less than 1′.5 (many of which are A-type in

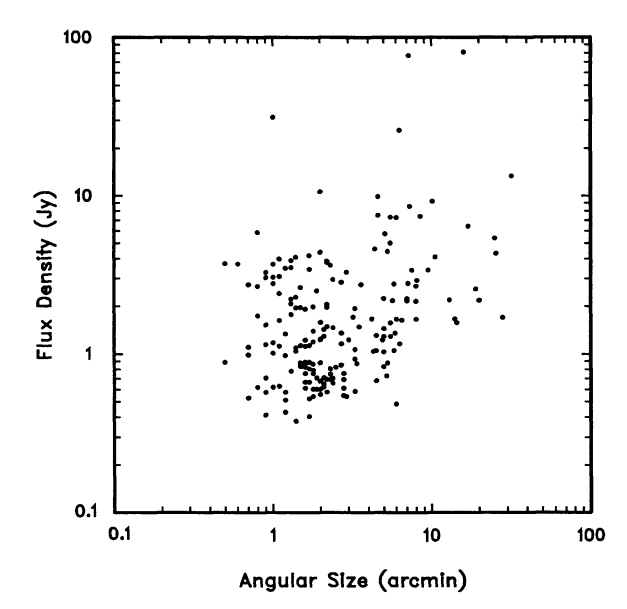


FIG. 3.—Plot of integrated flux density against angular size for the sources in the confirmed MRC extended sample. The parameters are obtained at 843 MHz from MOST observations.

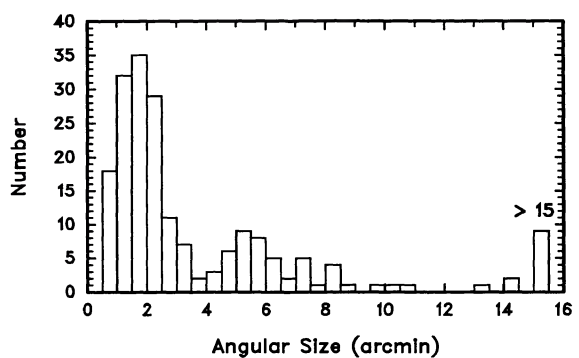


FIG. 4.—Distribution of angular size for sources in the confirmed sample. The last bin contains all sources larger than 15'.

the MRC) are excluded, showing that the confirmed sample is not complete even for these larger sources.

In summary, the confirmed MRC extended sample is known to be incomplete below angular size 1'.5 and flux density 1.0 Jy at 843 MHz. It may miss some sources that are larger and stronger than these limits because:

- 1. The E, C, and A flags in the MRC were conservative in that a source was not flagged unless there was confirmation of extension.
- 2. The MRC flux density is underestimated for extended sources. Some large, low surface brightness sources were excluded from the MRC even though their integrated flux densities are much larger than the 0.7 Jy limit.
- 3. The methods of detecting extension in the MRC tend to be biased against sources with position angles near 0° and 90° (Fig. 6).

8. RADIO SOURCE MORPHOLOGIES

Comments about the morphologies of individual sources are made in § 6, but as our sample represents a uniform selection from a quarter of the sky, it is also desirable to consider generalizations for the whole sample of extended sources and to highlight some trends.

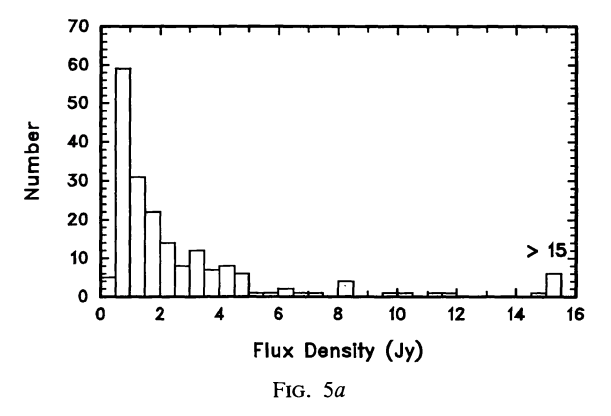
Multiple sources which are considered to be random associations of unrelated sources are identified in § 6. These sources, usually unresolved, comprise a large fraction (30%) of the original MRC extended and multiple-source list, but are excluded

so as not to bias our study of the single large angular size sources.

There are also some ambiguous cases where it is not clear whether the radio structure is associated with a single optical object or not. Some groups of separated radio sources may be physically related in that they arise from different galaxies within a single cluster. It is likely that the MRC source 2130–538 has superposed emission from two bright galaxies in the same cluster, so that the MOST radio structures overlap. MRC sources 0305–417 and 2014–312 have multiple peaks, linked together but identified with separate optical objects, and 2238–609/2239–609 have four close peaks. While a random association of two close sources is quite likely (§ 7), three or four close sources have negligible chance, so these groups may be sources that are physically related, perhaps in a distant cluster.

In the confirmed MRC extended sample of 193 sources, the simplest structure is a single radio peak of small angular size, only partially resolved with the MOST beam. There are 19 sources classified in this group: 0357-371, 0408-479, 0511-484B, 0719-553, 0909-564, 1002-320, 1010-647, 1136-320, 1136-678, 1148-353, 1259-367, 1312-593A, 1815-546, 1829-778, 1840-404, 2020-575, 2022-537, 2041-604, and 2357-830. These are generally sources smaller than 1'.5 which were flagged as extended sources in the MRC only because they are strong (and hence extension was easier to confirm). It is likely that most of these will show double structure at higher resolution and have sizes smaller than their deconvolved sizes (in Table 1) which are calculated assuming they have Gaussian profiles.

Most of the sources show double lobe structure, but for a typical source with lobe separation 2' the MOST observations (HPBW 0'.73) do not have sufficient resolution to distinguish structure within the lobes. There are 88 sources which are classified as simple doubles: 0003–833, 0020–747, 0030–485, 0032–738, 0043–424, 0103–453, 0110–692, 0111–385, 0118–501, 0130–620, 0150–480, 0153–826, 0251–677, 0258–520, 0336–355, 0357–506, 0423–687, 0450–387B, 0456–470, 0507–627, 0521–478, 0540–617, 0540–628, 0558–388, 0609–585, 0618–371, 0641–584, 0645–729, 0649–557, 0655–486, 0718–340, 0807–389, 0809–499, 0843–568, 0915–543A, 0918–383, 0936–622, 0952–306, 1011–316, 1011–320, 1112–545, 1123–351, 1152–694,



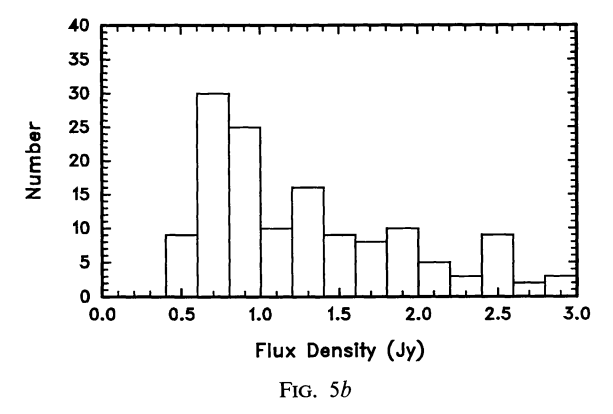
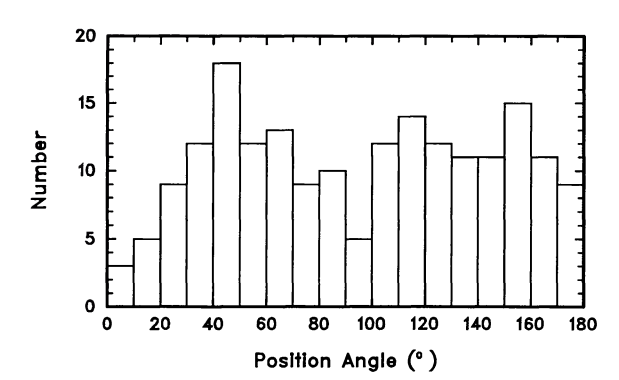


FIG. 5.—(a) Distribution of flux density for sources in the confirmed sample. The last bin contains all sources stronger than 15 Jy. (b) Same distribution with an expanded scale, showing the cutoff at 0.6 Jy.



1992ApJs...80..137J

Fig. 6.—Distribution of position angles, in 10° bins, of sources in the confirmed sample, showing the selection effect in position angle. Fewer sources than expected are found extended on NS or EW alignments.

1158-652, 1259-445, 1324-300, 1355-416, 1411-657, 1418-557, 1421-382, 1437-368, 1451-364, 1511-315, 1518-530, 1541-383, 1717-620, 1737-608, 1750-434, 1756-348, 1821-583, 1837-365, 1849-397, 1922-627, 1929-397, 1945-304, 1951-310B, 1951-501, 1953-879, 1954-356, 1955-470, 2013-312, 2028-732, 2030-378B, 2047-572, 2132-554, 2152-699, 2156-374, 2158-380, 2217-505, 2225-308, 2225-619, 2227-665, 2239-609, 2302-713, 2340-586, 2341-509, 2359-690, and 2359-691. Many of these sources have lobes which are extended, and their large range in the ratio of lobe flux densities indicates that there are several distinct morphologies within this group.

There are eight sources which show a single peak but have a large angular size. Five of these are identified with bright elliptical galaxies: 0651-603, 0843-336, 0932-372, 1452-367, and 1954-552. These are edge-darkened sources without obvious double structure, and are possibly seen end-on. One nearby, edge-on spiral galaxy 1302-492 (NGC 4945) has a strong core and weak disk emission. There is one large smooth source, without any small-scale structure in the MOST image, 0456-301, which is identified with a galaxy in a cluster (ACO 3297), where some of the emission may be associated with the whole cluster. At higher resolution there is distorted structure which may indicate a wide-angle-tail source (A. Unewisse 1991, private communication). The source 2006–566, which is also identified with a cluster, is of larger angular size and does show some structure within the broad diffuse emission but otherwise appears to be similar to 0456-301.

There are 11 sources which show "head-tail" or "twin-tail" morphology: 0058-507, 0427-539, 0616-487, 0620-526, 0809-492, 0816-704, 1137-463, 1343-377, 1610-605, 2007-568, and 2316-423. These consist of a strong extended peak, identified with a bright galaxy, and an edge-darkened single tail or a diffuse double tail which may be bent. It is thought that both "head-tail" and "twin-tail" sources are in the same class, but this assumes that all head-tail sources do have a double tail. The distinction is then due to the resolution and sensitivity of the observation as well as the angle between the two tails. (However, at no part of the long 25' tail for 1610-605 are two tails resolved.) The angles, lengths and knots in the tail all depend on projection of the three-dimensional structure onto the plane of the sky. These sources tend to be found in rich clusters (Robertson & Roach 1990).

For double sources larger than 3', distinctions based on structure within the lobes can be made. The most widely used classification is by Fanaroff & Riley (1974) which is based on the ratio of the spacing of the maxima in the two lobes to the total extent of the source at the lowest contour level. The diffuse-edged sources are FR I (edge-darkened), and sources with the hotspots near the end of the lobes are FR II (edge-brightened). This classification is used here with an additional distinction—whether or not a core component is detected in the MOST image of the source. There is, of course, a smooth transition between the extremes of edge-darkened and edge-brightened sources with many that are not readily classified. There is also a wide range in the strength of core components. Classification from the MOST images identifies sources with strong cores but misses many of the weak cores, since these may be blended into the bridge or inner lobes when observed at the relatively low frequency.

There are 11 edge-darkened, FR I sources without core components: 0214–480, 0332–391, 0523–327, 0625–545, 0715–362, 1056–360, 1141–391, 1425–479, 1610–608, 1623–434, and 1921–577. This group shows a large proportion of bent structures, both with reflection (C) and rotation (Z) symmetry (see below). There are five edge-darkened, FR I sources with core components: 1234–723, 1318–434, 1758–473, 2014–558, and 2148–555. There are similarities between 1234–723 and 2014–558, which show strong cores and broad diffuse lobes, and between 1318–434 and 2148–555, which show weak cores, strong inner lobes and weak outer lobes extended in a narrow ridge line.

There are 22 edge-brightened, FR II sources without core components: 0114–476, 0131–367, 0211–479, 0213–406, 0319–453, 0511–305, 0511–484, 0707–359, 0819–300, 0930–399, 0945–370, 1302–325, 1304–748, 1413–364, 1516–477, 1545–321, 1623–421, 1910–800, 2013–308, 2052–736, 2320–613, and 2356–611. There are nine edge-brightened, FR II sources with core components: 0424–728, 0518–458, 1025–612, 1241–663, 1602–633, 1637–771, 1733–565, 2151–461, and 2315–425.

There are many sources which do not fit well into the simplification of the edge-darkened or edge-brightened morphologies, either because their structure is truly intermediate or because the resolution of the observation is inadequate (although the sources are clearly not simple doubles). There are 11 of these intermediate source without core components: 0344-345, 0429-616, 0608-658, 0703-595, 0704-451, 0905-353, 1333-337, 1619-634, 1721-568, 1940-406, and 2026-414. There are eight intermediate sources with core components: 0101-649, 0218-452, 0320-373, 0336-356, 0546-329, 1308-441, 1322-427, and 1452-517. Some of these show one lobe edge-darkened and one side edge-brightened, e.g., 1452-517. Others, such as 0320-373 and 1322–427, have lobes with maximum brightness near the lobe center and diffuse edges. These are sometimes described as relaxed doubles. Note that the MOST image of 1322–427 = Cen A shows only the inner lobes; the total structure is taken from low-resolution Parkes data (Cooper et al. 1965). Some sources, such as 0546-329, 1308-441, and 1333-337, have strong ridge-lines characteristic of FR I sources but peaks of brightness near the end of the lobes.

In summary, of the 86 well-resolved sources in our con-

firmed sample, 66 are double (of which 22 have cores), eight are diffuse singles, 11 are head-tail or twin-tail, and one, 2130–568, is a complex superposition. For the doubles, the classification of Fanaroff & Riley (1974) is useful, particularly for observations where the lobes are only a few beamwidths in size, but is dependent on both the resolution and the sensitivity of the observation (Jones 1990). The complex morphologies of many sources cannot be described by such a simple scheme.

For their sample of 3CR sources, Fanaroff & Riley (1974) found a sharp division in power between the two morphology classes; FR I sources are weaker and FR II sources are stronger than a critical power log $P_{178} = 24.7$ (where power is in W Hz⁻¹ sr⁻¹ and a Hubble constant of $H_0 = 100$ km s⁻¹ Mpc⁻¹ is assumed as in this paper).

We examined this relationship for the large, identified sources in the confirmed MRC extended source sample (Jones 1990). There is a transition in morphology at $\log P_{843} = 24.15$ corresponding to the critical power of FR (assuming a typical spectral index -0.8), in that all of the sources above this power are edge-brightened. However, not all the sources below the critical power are edge-darkened. Our southern survey reveals that 8/22 = 36% of the large, weak sources are edge-brightened, whether determined by the FR classification or the more objective J classification (Jones 1990) based on moments of the brightness distribution. The usual claim that FR I are weak sources and FR II are strong sources is misleading and must be used only as a guide. Many anomalous sources exist like the intermediate ones discussed above.

That some sources below the critical power have class II morphology was noted by Gavazzi & Perola (1978), who also found that there are some class I sources above the critical power. More recent data on the 3CR sample also indicate that the division in power between FR classes I and II is not sharp. Using the 3CR subsample of Laing et al. (1983) with revised 178 MHz flux densities and redshifts the radio powers were calculated and compared to the FR classes. There is an overlap region between $\log P_{178}$ of 24.2 and 25.8 with both FR I and FR II sources. Of the 60 sources with z < 0.25, 6/26 of the sources below $\log P = 24.7$ are FR II and 9/34 of the sources above $\log P = 24.7$ are FR I. However, all sources with z > 0.25 have $\log P > 24.7$ (due principally to the well-known correlation of P and z from Malmquist bias) and all are FR II.

A different parameter, which is useful for classification of the structures, is the bending—from the head-tail sources, through the twin-tail, wide-angle-tail or reflection-symmetry (C-type) to straight sources. This trend is sometimes extended to the rotation-symmetry (Z-type) sources although these may be due to a different process. The degree of apparent bending of a source is modified by projection effects (Reynolds 1980) since only the two-dimensional projection of the three-dimensional structure is observed. The head-tail sources are believed to have double-lobe structure (e.g., 0058-507, 0427-539, and 1137-463), which is overlapping in projection although the longest head-tail source (1610-605) has many kinks but no sign of a double tail. The tails of 0427-539 and 1137-463 also have kinks. The twin-tail sources show a bending trend from 0816-705 to 2316-423 to 0620-526, where the double tail of the last source is very wide. Tracing the ridge-line to the lowest levels, 1921-577 and 1056-360 have large bending, followed by 0715-362, 0332-391, 1610-608, and 0703-595 while

1623-434, 1333-337, and 0945-370 have only slight bending.

There are many sources, mostly FR II morphology, which show little or no bending. Of the rotationally symmetric sources, 1318–434 and 2148–555 show slight bending, 0511–305 has bending of the diffuse structure in a FR II source, and 0214–480 and 0523–327 have sharp bending at the ends of a FR I source. The structure of 2014–558 with twisted, diffuse lobes could form by jets precessing over a very large angle. The ridge-line of 1619–634 shows extreme bending of more than 90°.

The reflection-symmetry bending is usually explained by orbital motion of the galaxy in the gravitational field of a cluster, or a companion. The lobes trail behind as they are entrained in the intergalactic medium (IGM). As mentioned above, the edge-darkened, FR I source class shows a large proportion of bent sources, particularly when the head-tail and twin-tail sources are included in this class. The correlation may arise if the key difference between the FR classes is the velocity of the jets and their interaction with the IGM (Bicknell 1985). The lower velocity FR I jets entrain and mix with the IGM, while the jets in FR II sources are less prominent and interact with the IGM at the hotspots near the ends of the lobes. An alternative interpretation of the reflection-symmetry bending is buoyancy of the radio-emitting region with respect to the IGM in the gravitational gradient within the cluster.

The rotation-symmetry bending can be explained, in the jet model, by the changing direction of the jet axis over the lifetime of the source. This could arise from precession of the central engine, presumed to be a massive black hole (Rees 1984).

9. CONCLUSION

The sources in the Molonglo Reference Catalogue that are south of declination -30° , and either flagged as extended or have a close neighbor (multiple flag) have been reobserved with the Molonglo Observatory Synthesis Telescope. The results include images with a resolution of 44" for a large sample of extended extragalactic radio sources.

The extension flags (E, C, or A) in the MRC are found to be 98% reliable, in that only four flagged sources are unresolved. However, 24% of these extended sources are resolved into groups of unrelated sources which had broadened the MRC beam. Most (75%) of the groups of neighboring sources (flagged M in the MRC) are found to be unrelated sources, as expected from the statistics of random associations, but some groups are components of larger sources.

We define a confirmed MRC extended sample of 193 sources larger than 0.5 and stronger than 0.4 Jy at 843 MHz. For this sample, 138 have identifications with galaxies, four with confirmed quasars and seven with stellar objects which are possible quasars. Only 44 sources have no optical identification; almost half of these are in crowded fields near the Galactic plane. Detection of core components using the higher resolution of the Australia Telescope should facilitate identification of many of these sources.

The confirmed sample is estimated as $\sim 80\%$ complete for sources larger than 1.5 and stronger than 1.0 Jy at 843 MHz. The incompleteness is due to the limits of the MRC flagging and peak-fitting routines. The missing sources are mostly those

with position angles near 0° and 90°, or extended sources of low surface-brightness.

Observations of the confirmed sample are continuing, with imaging at higher resolution using the Australia Telescope, with searches for core components using the Parkes-Tidbinbilla Interferometer, and with spectroscopy using the Anglo-Australian Telescope.

This work forms part of a Ph.D. thesis by P.A.J. at the Uni-

versity of Sydney. We would like to thank members of the Astrophysics Department, School of Physics, University of Sydney for help in all stages of this project. We also thank the staff of the Anglo-Australian Observatory and R. W. Hunstead for the optical spectra obtained with the AAT. The MOST is supported by the Australian Research Grants Scheme and the Science Foundation in the School of Physics. P.A.J. acknowledges the support of a Commonwealth Postgraduate Research Award.

REFERENCES

```
Abell, G. O., Corwin, H. G., & Olowin, R. 1989, ApJS, 70, 1 (ACO)
Anguita, C., Campusano, L. E., Torres, C., & Pedreros, M. 1979, AJ, 84,
Arp, H. C., & Madore, B. F. 1987, A Catalogue of Southern Peculiar
```

Galaxies & Associations (Cambridge: Cambridge Univ. Press)

Bajaja, E. 1970, AJ, 75, 667

Bennett, A. S. 1962, MmRAS, 68, 163

Bicknell, G. V. 1985, Proc. Astron. Soc. Australia, 6, 130

Bolton, J. G., Clarke, M. E., & Ekers, R. D. 1965, Australian J. Phys., 18,

Bolton, J. G., & Ekers, J. 1966, Australian J. Phys., 19, 275

Bolton, J. G., Gardner, F. F., & Mackey, M. B. 1964, Australian J. Phys.,

Bolton, J. G., & Savage, A. 1977, Australian J. Phys., Astrophys. Suppl., No. 41, 25

Bolton, J. G., Savage, A., & Wright, A. E. 1979, Australian J. Phys., Astrophys. Suppl., No. 46, 1

Bolton, J. G., & Shimmins, A. J. 1973, Australian J. Phys., Astrophys. Suppl., No. 30, 1

Bolton, J. G., Stanley, G. J., & Slee, O. B. 1949, Nature, 164, 101

Burbidge, E. M., & Burbidge, G. R. 1972, ApJ, 172, 37

Cameron, M. J. 1971, MNRAS, 152, 439

Carter, D. 1980, MNRAS, 190, 307

Christiansen, W. N., Frater, R. H., Watkinson, A., O'Sullivan, J. D., Lockhart, I. A., & Goss, W. M. 1977, MNRAS, 181, 183

Clarke, J. N., Little, A. G., & Mills, B. Y. 1976, Australian J. Phys., Astrophys. Suppl., No. 40, 1

Cooper, B. F. C., Price, R. M., & Cole, D. J. 1965, Australian J. Phys., 18,

Danziger, I. J., & Goss, W. M. 1983, MNRAS, 202, 703

Danziger, I. J., Goss, W. M., & Frater, R. H. 1978, MNRAS, 184, 341

Danziger, I. J., Goss, W. M., & Wellington, K. J. 1981, MNRAS, 196, 845

Dickens, R. J., Currie, M. J., & Lucey, J. R. 1986, MNRAS, 220, 679 Durdin, J. M., Large, M. I., & Little, A. G. 1984, in Proc. URSI/IAU

Symp. Indirect Imaging, ed. J. A. Roberts (Cambridge: Cambridge Univ. Press), 75

Edge, D. O., Shakeshaft, J. R., McAdam, W. B., Baldwin, J. E., & Archer, S., 1959, MmRAS, 68, 37

Ekers, R. D. 1969, Australian J. Phys., Astrophys. Suppl., No. 6, 1 1970, Australian J. Phys., 23, 217

Ekers, R. D., Goss, W. M., Kotanyi, C. G., & Skellern, D. J. 1978, A&A,

Ekers, R. D., Goss, W. M., Wellington, K. J., Bosma, A., Smith, R. M., & Schweizer, F. 1983, A&A, 127, 361

Ekers, R. D., et al. 1989, MNRAS, 236, 737

Fanaroff, B. L., & Riley, J. M. 1974, MNRAS, 167, 31P

Fosbury, R. A. E., et al. 1982, MNRAS, 201, 991

Gardner, F. F., & Whiteoak, J. B. 1971, Australian J. Phys., 24, 899

Gavazzi, G., & Perola, G. C. 1978, A&A, 66, 407

Goss, W. M., Ekers, R. D., Skellern, D. J., & Smith, R. M. 1982, MNRAS, 198, 259

Goss, W. M., McAdam, W. B., Wellington, K. J., & Ekers, R. D. 1987, MNRAS, 226, 979

Goss, W. M., Wellington, K. J., Christiansen, W. N., Lockhart, I. A., Watkinson, A., Frater, R. H., & Little, A. G. 1977, MNRAS, 178, 525

Harnett, J. I., & Reynolds, J. E. 1985, MNRAS, 215, 247

Hawkins, M. R. S. 1979, MNRAS, 188, 691

. 1981, MNRAS, 194, 1013

Haynes, R. F., Cannon, R. D., & Ekers, R. D. 1983, Proc. Astron. Soc. Australia, 5, 241

Hjellming, R. M., & Bignell, R. C. 1982, Science, 216, 1279

Högbom, J. A. 1974, A&AS, 15, 417

Hunstead, R. W. 1971, MNRAS, 152, 277

. 1972, MNRAS, 157, 367

Hunstead, R. W., Durdin, J. M., Little, A. G., Reynolds, J. E., & Kesteven, M. J. L. 1982, Proc. Astron. Soc. Australia, 4, 447

Hunstead, R. W., Lasker, B. M., Mintz, B., & Smith, M. G. 1971, Austra-

lian J. Phys., 24, 601 Jauncey, D. L., Batty, M. J., Gulkis, S., & Savage, A. 1982, AJ, 87, 763

Jones, P. A. 1986, Proc. Astron. Soc. Australia, 6, 329

. 1987, Proc. Astron. Soc. Australia, 7, 208

-. 1989, Proc. Astron. Soc. Australia, 8, 81 -. 1990, Proc. Astron. Soc. Australia, 8, 254

Killeen, N. E. B., Bicknell, G. V., & Ekers, R. D. 1986, ApJ, 302, 306

Laing, R. A., Riley, J. M., & Longair, M. S. 1983, MNRAS, 204, 151

Large, M. I., Cram, L. E., & Burgess, A. M. 1991, Observatory, 111, 72

Large, M. I., Mills, B. Y., Little, A. G., Crawford, D. F., & Sutton, J. M. 1981, MNRAS, 194, 693

Lasker, B. M., & Smith, M. G. 1974, Australian J. Phys., 27, 135

Lauberts, A. 1982, ESO/Upsalla Catalogue of the ESO (B) Sky Survey, (Munich: European Southern Observatory)

Lü, P. K. 1970a, AJ, 75, 1161 . 1970b, AJ, 75, 1164

. 1974, AJ, 79, 453

McAdam, W. B., & Schilizzi, R. T. 1977, A&A, 55, 67

McAdam, W. B., White, G. L., & Bunton, J. D. 1988, MNRAS, 235, 425 Macdonald, G. H., Kenderdine, S., & Neville, A. C. 1968, MNRAS, 138,

Mackay, C. D. 1969, MNRAS, 145, 31

Mills, B. Y. 1954, Observatory, 74, 248

-. 1981, Proc. Astron. Soc. Australia, 4, 156

. 1985, Proc. Astron. Soc. Australia, 6, 72

Mills, B. Y., Slee, O. B., & Hill, E. R. 1960, Australian J. Phys., 13, 676 . 1961, Australian J. Phys., 14, 497

Nicholson, G. D., Glass, I. S., Feast, M. W., & Andrews, P. J. 1979, MNRAŚ, 189, 29P

Palumbo, G. G. C., Tanzella-Nitti, G., & Vettolani, G. 1983, Catalogue of Radial Velocities of Galaxies (New York: Gordon & Breach)

Pawsey, J. L. 1955, ApJ, 121, 1

Pence, W. 1976, ApJ, 203, 39

Peterson, B. A., & Bolton, J. G. 1972a, Astrophys. Lett., 10, 105

. 1972b, ApJ, 173, L19

-. 1973, Astrophys. Lett., 13, 187

Peterson, B. A., Bolton, J. G., & Shimmins, A. J. 1973, Astrophys. Lett., 15, 109

Price, R. M., & Milne, D. K. 1965, Australian J. Phys., 18, 329

Rees, M. 1984, ARA&A, 22, 471

Reynolds, J. E. 1980, Proc. Astron. Soc. Australia, 4, 74

Robertson, J. G., & Roach, G. J. 1990, MNRAS, 247, 387

Robertson, J. G., & Smith, R. M. 1981, Proc. Astron. Soc. Australia, 4, 187 Sandage, A. 1978, AJ, 83, 904

Savage, A. 1976, MNRAS, 174, 259

Savage, A., Bolton, J. G., & Wright, A. E. 1976, MNRAS, 175, 517

. 1977, MNRAS, 179, 135

Schilizzi, R. T. 1975, MmRAS, 79, 75

Schilizzi, R. T., & McAdam, W. B. 1970, Proc. Astron. Soc. Australia, 1,

1975, MmRAS, 79, 1 (SM)

Schmidt, M. 1965, ApJ, 141, 1

Schreier, E. J., Burns, J. O., & Feigelson, E. D. 1981, ApJ, 251, 523

Schwartz, U. J., Whiteoak, J. B., & Cole, D. J. 1974, Australian J. Phys., 27, 563

Shanks, T., Stevenson, P. R. F., Fong, R., & MacGillvray, H. T. 1984, MNRAS, 206, 767

Shaver, P. A., & Pierre, M. 1989, A&A, 220, 35

Shimmins, A. J., & Bolton, J. G. 1974, Australian J. Phys., Astrophys. Suppl., No. 32, 1

Slee, O. B. 1977, Australian J. Phys., Astrophys. Suppl., No. 43, 1

Slee, O. B., Sheridan, K. V., Dulk, G. A., & Little, A. G. 1983, Proc. Astron. Soc. Australian, 5, 247

Slee, O. B., Siegman, B. C., & Mulhall, P. S. 1982, Proc. Astron. Soc. Australia, 4, 278 (SSM)

Smith, R. M. 1983, Ph.D. thesis, Australian National Univ.

Smith, R. M., & Bicknell, G. V. 1983, Proc. Astron. Soc. Australia, 5, 251 ——. 1986, ApJ, 308, 36

Spinrad, H., Kron, R. G., & Hunstead, R. W. 1979, ApJS, 41, 701

Swarup, G. 1984, J. Astrophys. Astron., 5, 139

Tadhunter, C. N., Fosbury, R. A. E., di Serego Alighieri, S., Bland, J., Danziger, I. J., Goss, W. M., McAdam, W. B., & Snijders, M. A. J. 1988, MNRAS, 235, 403 Tritton, K. P. 1971, MNRAS, 155, 1p
——. 1972, MNRAS, 158, 277

Tritton, K. P., & Schilizzi, R. T. 1973, MNRAS, 165, 245

Tritton, K. P., & Whitworth, D. P. D. 1973, MNRAS, 165, 253

Véron, M. P. 1977, AJ, 82, 937

Véron-Cetty, M. P., & Véron, P. 1983, A&AS, 53, 219

Wall, J. V., & Cannon, R. D. 1973, Australian J. Phys., Astrophys. Suppl., No. 31, 1

Wall, J. V., & Cole, D. J. 1973, Australian J. Phys., 26, 881

Wall, J. V., & Schilizzi, R. T. 1979, MNRAS, 189, 593 (WS)

Westerlund, B. E., & Smith, L. F. 1966, Australian J. Phys., 19, 181

Westerlund, B. E., & Wall, J. V. 1969, AJ, 74, 335

White, G. L., McAdam, W. B., & Jones, I. G. 1984, Proc. Astron. Soc. Australia, 5, 507

----. 1988, MNRAS, 233, 189

Whiteoak, J. B. 1972, Australian J. Phys., 25, 233

Whiteoak, J. B., & Bunton, J. D. 1985, Proc. Astron. Soc. Australia, 6, 171